

Alma Mater Studiorum – Università di Bologna

**DOTTORATO DI RICERCA IN
SCIENZE BIOMEDICHE**

Ciclo XXVI

Settore Concorsuale di afferenza: BIO/09

Settore Scientifico disciplinare: 05/D1

**PHARMACOLOGICAL RESCUE OF DENDRITIC
PATHOLOGY IN THE Ts65Dn MOUSE MODEL OF
DOWN SYNDROME**

D.ssa Fiorenza Stagni

Coordinatore Dottorato

Relatore

Prof. Lucio Cocco

Prof.ssa Renata Bartesaghi

Dipartimento di Scienze Biomediche e Neuromotorie
Esame finale anno 2014

INDEX OF CONTENTS

1.	RATIONALE AND GOAL OF THE STUDY	1
2.	INTRODUCTION.....	4
2.1	DOWN SYNDROME	4
2.1.1	Etiology.....	4
2.1.2	Epidemiology.....	5
2.1.3	The Human Chromosome 21 (HSA21)	7
2.1.4	The most studied triplicated genes.....	9
2.1.5	Genes expression profiling in Down Syndrome	11
2.1.6	Phenotype features of DS individuals.....	12
2.1.7	Other medical problems associated with DS	13
2.1.8	Neurological defects	15
2.2	MOUSE DS MODELS: TOOLS FOR THE UNDERSTANDING OF DS PATHOLOGY AND THERAPY DESIGN.....	17
2.2.1	Model with triplication of the whole Mmu16.....	18
2.2.2	Segmental trisomic mice.....	18
2.2.3	Models with triplication of Mmu17 or Mmu10/16/17.....	21
2.2.4	Models with insertion of Hsa21	22
2.2.5	Models with triplication of individual genes	23
2.2.6	Trisomic mice with removal of triplicated genes.....	23
2.3	NEUROANATOMY OF DS	24
2.3.1	Gross anatomy	24
2.3.2	Cytoarchitecture, cell density, cell number.....	25
2.4	CAUSES OF BRAIN HYPOTROPHY IN DS	27
2.4.1	Neurogenesis alterations	28
2.4.2	Dendritic hypotrophy	30
2.5	ALTERATIONS OF SYNAPTIC FUNCTION IN THE DS BRAIN AND TRISOMIC GENES INVOLVED.....	34
2.5.1	Synaptic density, excitatory vs. inhibitory synapses.....	35
2.5.2	Synaptic proteins.....	35
2.5.3	Electrophysiology	37
2.5.4	Trisomic genes and dendritic/synaptic alterations	38
2.6	THERAPEUTIC APPROACHES IN THE DS MOUSE MODEL	39
2.7	RESTORATION OF THE SEROTONERGIC SYSTEM: A TOOL FOR IMPROVING BRAIN DEVELOPMENT IN DS?.....	44
2.7.1	Serotonergic system in normal brain development.....	44
2.7.2	Serotonergic system in DS.....	46
2.8	PHARMACOTHERAPY WITH SELECTIVE SEROTONIN RE-UPTAKE INHIBITORS.....	47
2.8.1	Fluoxetine modulates neurogenesis and dendritogenesis.....	47
3.	MATERIALS AND METODS	51
3.1	Colony	51
3.2	Experimental protocol.....	51

3.3	Histological procedures	53
3.4	Western blotting.....	55
3.5	High-performance liquid chromatography (HPLC).....	55
3.6	Real-time reverse transcriptase quantitative PCR (RT-qPCR).....	56
3.7	Patch-clamp experiments: preparation of slices	57
3.8	Patch-clamp experiments: voltage-clamp recordings, drugs, and data analysis.....	57
3.9	Measurements	60
4.	RESULTS	65
4.1	Effect of fluoxetine on the dendritic tree of newborn granule cells in euploid and Ts65Dn mice	65
4.2	Effect of fluoxetine on the dendritic tree of the oldest granule cell in euploid and Ts65Dn mice.....	70
4.3	Effect of fluoxetine on granule cell spine density in euploid and Ts65Dn mice.....	76
4.4	Effect of fluoxetine on hippocampal SYN levels in euploid and Ts65Dn mice	76
4.5	Effect of fluoxetine on the glutamatergic innervation of the granule cells in euploid and Ts65Dn mice ...	78
4.6	Effect of fluoxetine on DSCAM levels in the DG of euploid and Ts65Dn mice	80
4.7	Effect of fluoxetine on the hippocampal serotonergic system in euploid and Ts65Dn mice.....	81
4.8	Effect of fluoxetine on spine density on the proximal shaft of CA3 pyramidal neurons in euploid and Ts65Dn mice	82
4.9	Effect of fluoxetine on the size of the mossy fiber bundle in euploid and Ts65Dn mice	85
4.10	Effect of fluoxetine on overall innervation in the stratum lucidum of euploid and Ts65Dn mice	85
4.11	Effect of fluoxetine on glutamatergic innervation in the stratum lucidum of euploid and Ts65Dn mice ...	88
4.12	Effect of fluoxetine on basal synaptic input in CA3 neurons	90
4.13	Effect of fluoxetine on BDNF expression	95
5.	DISCUSSION	98
5.1	Fluoxetine rescues connectivity of trisomic granule cells	99
5.2	Fluoxetine normalizes DSCAM levels in the DG of Ts65Dn mice	100
5.3	Restoration of granule cell dendritic development parallels restoration of the serotonergic system	101
5.4	Impaired connectivity in the stratum lucidum of field CA3 of Ts65Dn mice.....	102
5.5	Fluoxetine restores the mossy fiber projections and functional connectivity in the stratum lucidum of Ts65Dn mice	103
5.6	BDNF may contribute to synaptic remodeling in field CA3 of Ts65Dn mice treated with fluoxetine.....	105

5.7	Fluoxetine has moderate or no effects in euploid mice	105
5.8	Conclusions.....	106
6.	REFERENCES.....	109

1. RATIONALE AND GOAL OF THE STUDY

Down syndrome (DS) is a genetic condition due to triplication of human chromosome 21. Cognitive disability, that is already present in infants with DS and worsens with age, is the most invalidating feature of DS. The trisomic brain is characteristically small starting from early developmental stages and produces fewer neurons than the normal brain, suggesting that neurogenesis impairment may be a determinant of cognitive disability.

Dendritic pathology is a consistent feature and represents a possible substrate for mental retardation in different conditions. In DS, the pathogenesis of dendritic abnormalities is distinctive and appears to correlate to some extent with the cognitive profile. In children and adults with DS, there is a marked reduction in dendritic branching and spine density (see(18)). Mouse models that mimic human pathologies as closely as possible are becoming invaluable tools because they can be exploited to identify the mechanisms underpinning a given pathology and to examine the outcome of targeted therapies. The Ts65Dn mouse is a widely used model of DS because it recapitulates numerous features of the human condition. Similarly to individuals with DS, the granule cells of dentate gyrus and CA3 pyramidal neurons of Ts65Dn mice have less branched and less spinous dendrites. Moreover, in the hippocampal field CA3 of Ts65Dn mice the frequency of miniature EPSCs is reduced, indicating an overall impoverishment of afferent synaptic input from the dentate gyrus, which is in agreement with the reduced number of granule neurons in these trisomic mice.

Though defective neurogenesis most likely represents a crucial determinant of mental retardation, **dendritic abnormalities** with consequent **connectivity alterations** are likely to be equally important actors in the neurological phenotype of DS.

DS has long been associated with a loss of serotonin (5-HT) in postmortem brains and there is evidence for a reduction in 5-HT levels and dysregulation of the 5-HT_{1A} receptor in the fetal DS brain. It is well established that lack of serotonin during early stages of brain development impairs

neurogenesis and dendritogenesis. Consequently, in view of the role played by 5-HT in neurogenesis and dendritic maturation, dysregulation of this transmitter system may contribute to alterations in neurogenesis as well as dendritic pathology in DS. Fluoxetine is a selective serotonin reuptake inhibitor that increases serotonin bioavailability in the brain. Previous evidence showed that administration of fluoxetine during early phases of brain development fully restored neurogenesis of granule cell precursors in the dentate gyrus and total number of granule cells and that this effect was accompanied by recovery of hippocampus-dependent memory performance (28).

Restoration of neurogenesis in the trisomic brain is an essential but not sufficient prerequisite for the rescue of brain functions. It is equally important that neurons are endowed with a well-developed dendritic arbor, a property that is fundamental for the establishment of proper synaptic connections. Several lines of evidence show that fluoxetine has a positive impact on dendritic maturation in the normal brain, which is in line with the key effects of serotonin on dendritic development and suggests that this drug may improve the typical dendritic pathology that characterizes trisomic neurons. Thus, the rescue of cognitive functions observed in trisomic mice neonatally treated with fluoxetine may to be underpinned by an improvement/restoration of dendritic development that accompanies restoration of neurogenesis.

Since currently there is no evidence that the defective dendritic development of individuals with DS can be pharmacologically rescued, **the overall goal of this project was to establish whether treatment with fluoxetine restores dendritic pathology and connectivity in addition to neurogenesis in the Ts65Dn mouse model of DS.**

The fact that in the DS brain neurons are morphologically normal at birth, but the number of dendrites and spines decreases steadily in postnatal life compared to the normal brain, suggests that the early postnatal period may represent a critical time window in which an attempt may be made to improve dendritic architecture. Thus, to establish whether it is possible to improve dendritic

maturation and synaptic function in DS, we treated animals with fluoxetine during the first phases of postnatal life. We focused on the effect of pharmacotherapy on the dendritic pattern in the hippocampal dentate gyrus and on the functional synaptic connectivity between the dentate gyrus and CA3, two hippocampal regions essential for long-term declarative memory.

2. INTRODUCTION

2.1 DOWN SYNDROME

Down syndrome (DS) is a genetic pathology due to the triplication of human chromosome 21. Its most severe aspect is the mental disability linked to the pathology.

Trisomy of chromosome 21 can be total or partial, and in most cases DS is not familial. The extra chromosome 21 copy usually arises during the formation of the parental germ cell when two 21 chromosomes stick together in one cell, instead of moving apart and taking a place individually in separate cells. This is called non-disjunction. Non-disjunction is more likely in mothers (88%), especially older ones, than in fathers (9%), because all of a mother's eggs are present in an immature form before her birth. In contrast, new sperms are continually being produced by fathers across their reproductive lifespan. The small remainder of cases of DS are familial ones and reflect either traslocation of an extra piece of the long arm of 21 to another chromosome or mosaicism (135).

2.1.1 Etiology

Genomic aneuploidy, defined as an abnormal number of copies of a genomic region, is a common cause of human genetic disorders.

Classically, the term aneuploidy was restricted to the presence of supernumerary copies of whole chromosomes (trisomy), or absence of chromosomes (monosomy), but now we can extend this definition to include deletions or duplications of subchromosomal regions. Trisomy 21 is a model of all human disorders that are the result of supernumerary copies of a genomic region (11). In DS, the extra copy of genes presents on HSA21 (134) is caused by three types of genetic rearrangements: (i)

the presence of a third whole 21st chromosome, (ii) Robertsonian translocation of chromosome 21, (iii) mosaicism.

Full/free trisomy 21(Ts21). This is the most common cause of DS, caused by the presence of a third whole 21st chromosome, which is usually of maternal origin. This kind of trisomy is caused by a chromosomal non-disjunction: if an egg or a sperm with two 21st chromosomes instead of one merges with a normal mate, the fertilized egg has three 21st chromosomes. The net result is that the total number of chromosomes in every somatic cell is 47 instead of the normal 46 (71).

Robertsonian translocation. Robertsonian translocation is a special type of genetic rearrangements where the smaller arms of chromosome break away and the larger arms become fused to those of one of a different chromosome pair. This is the second type of cause in DS, much less prevalent than full Ts21, leading to attachment of chromosome 21 to chromosome 14, 21, or 22. So, while the number of chromosomes remains normal, there is a triplication of the 21st chromosome material. This abnormality may be carried by both parents and can increase the probability of DS in offspring (71).

Mosaicism. This is the third and very rare cause of DS. It is caused by an error in mitotic cell division soon after conception (71). Because of this, people with mosaic DS have two cell lines: one with the normal number of chromosomes, and one with an extra number 21. This can occur in one of two ways: a non-disjunction event during early embryogenesis in a normal embryo or a DS embryo undergoes non-disjunction and some of the cells revert to a normal chromosomal arrangement.

2.1.2 Epidemiology

DS occurs in 1 every 700–800 live births and epidemiologic data give an estimated incidence of more than 200000 cases per year worldwide (44), data that lead to an estimation of 5-6 million of case in the world.

The birth prevalence of DS increases with maternal age from about 1 in 1500 under age 25 to about 1 in 100 at age 40 (Fig. 1).

Over 5700 cases of DS were registered with the UK National Down Syndrome Cytogenetic Register from 1989 to 1993 and, of these, 95% were regular trisomy 21 and 1% were mosaic. The remaining 4% were due to chromosomal translocations (almost all Robertsonian) (see (127)).

In the last decades, the number of DS pregnancies has increased, probably due to the old age of mothers (94). According to a study published on “American Journal of Public Health” (101), two factors which could affect the incidence of DS individuals live birth, through the accessibility to prenatal testing (maternal serum screening, nuchal translucency screening, amniocentesis and chorionic villus biopsy), are geographic origin and mother occupation.

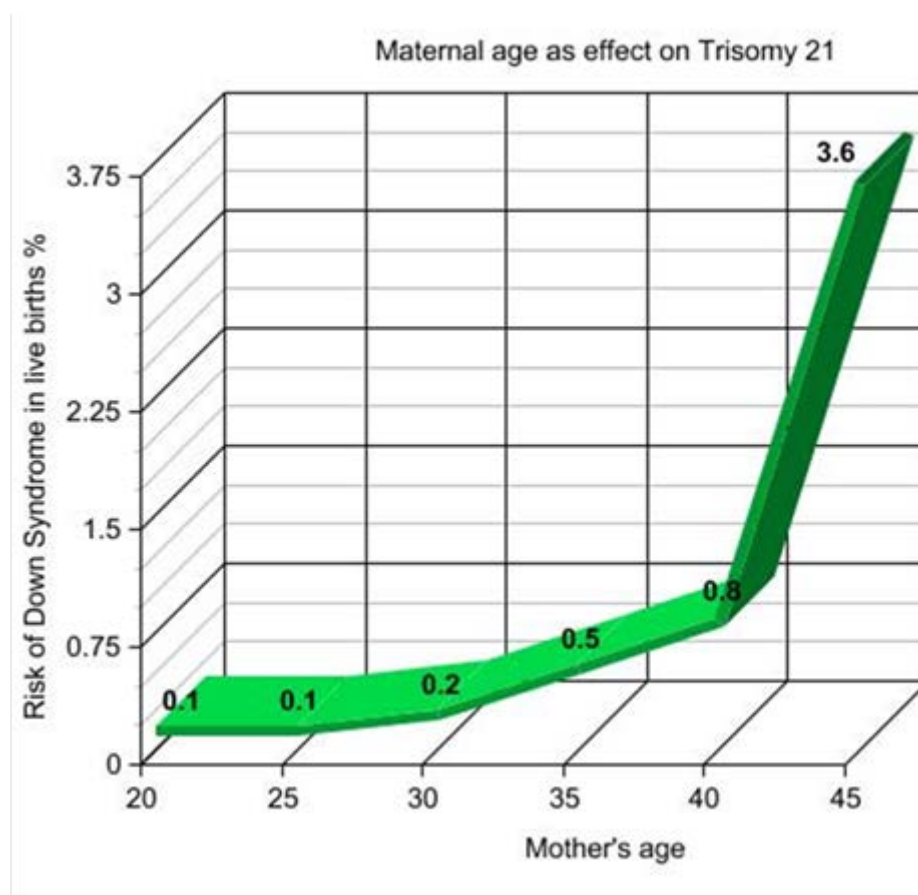


Figure 1 - Graph (*American Family Physician, 2000*) shows links between maternal age and percent chance for Down syndrome.

The data reveal that socioeconomic differences in use of prenatal testing have created disparities in the live-birth prevalence of DS.

Life expectancy of DS individuals is generally shorter than that of the normal population and varies with the severity of the phenotype. However, at least in occident, in the last years the life expectancy of people affected by DS is increased, thanks the care of life, from forties to sixties.

2.1.3 The Human Chromosome 21 (HSA21)

Chromosome 21 is the smallest human chromosome representing about 1.5 percent of the total DNA (Fig. 2). Since the discovery in 1959 that DS occurs when there are three copies of chromosome 21, about twenty disease loci have been mapped to its long arm (87).

The short arm of chromosome 21, 21p, is largely made up of ribosomal RNA genes and other repeat sequences that are probably involved in other chromosomal abnormalities.

The long arm, 21q, instead, was estimated to be around 38Mb and approximately 3% of its sequence encodes for proteins of different functional categories like transcription factors, regulators and modulators; proteases and protease inhibitors; ubiquitin pathway; interferons and immune response; kinases; RNA processing; adhesion molecules; channels; receptors; and energy metabolism (180).

There are rich- and poor- genes regions on 21q, which is correlated with the G+C content (87): the distal one third of 21q is the most gene-rich while the proximal two thirds are uniformly AT-rich (74). But the total number of genes (protein-coding and non coding RNAs) on the long arm has not been conclusively determined.

Currently, about 500 genes and gene models exist on HSA21q and an additional 4 have been assigned to HSA21p. Of these, we have information about the function of about 145 (134). An additional, unexpected finding is that the actual fraction of chromosome 21 that is transcribed into RNA might be an order of magnitude higher than the fraction occupied by gene coding sequences

(158). This could lead to additional unidentified genes, RNA transcripts without protein-coding capacity, alternative RNA isoforms or “illegitimate” non functional transcription.

HSA21 is a chromosome with a low content of G-negative bands (that is light band of a chromosome after treatment with GIEMSA dye), and thanks the literature, we know that genomic regions with G-negative bands are rich of structural genes. The distal half of the HSA21q (21q22) is the major G-negative region of the chromosome, and for this reason the band has been associated with the syndrome (173) and with development of cognitive disabilities (see(44)). This region of ~5.4 Mb, between the carbonyl reductase (CBR) and transcriptional regulator ets-related gene (ERG), was called “Down Syndrome Critical Region” (DSCR), in turn divided into several “critical region”, two of which are called DSCR1 and DSCR2.

There are two hypotheses to explain the pathogenesis of Down syndrome caused by the genetic overdosage. The first one is called “gene dosage effect hypothesis”: it holds that the phenotype is a direct result of cumulative effect of the imbalance of the individual gene located on the triplicated chromosome or chromosomal region (148). Because of the triplication of a particular subset of genes, this is responsible for particular pathological traits associated with trisomy 21. The second hypothesis called “amplified developmental instability hypothesis” in contrast claims the imbalance of the hundreds of genes on HSA21 determines a non specific disturbance of genomic regulation and expression. This global disruption of the correct balance of gene expression in development pathways alters the normal developmental homeostasis and determines most manifestation of DS. The discussion about validity of one of the two hypotheses is still open. Moreover, the two different hypotheses could coexist. Indeed, a recent study provided evidence that trisomy for the DSCR is necessary but not sufficient for the brain phenotypes observed in trisomic mice (132), and that individual genes on HSA21 act in concert to enhance or ameliorate the deleterious effects of the extra copies of genes.

2.1.4 The most studied triplicated genes

Among the over-expressed genes of the HSA21, pursuant to Roizen et al. (158), the principal of them involved in brain DS phenotype are SIM2, DYRK1A, DSCAM, APP, S100B, SOD1. They possibly affect normal brain development and could provoke neuronal loss and Alzheimer's like pathology, when they are in trisomic condition.

SIM2. Single-minded homolog 2. SIM2 is a basic helix loop helix transcription factor involved in normal neuronal development. SIM2 can heterodimerize with aryl hydrocarbon receptor nuclear translocator (ARNT) and translocate to the nucleus to transcriptionally regulate gene expression (41). His over expression could directly or indirectly induce the neuroanatomic and neurochemical abnormalities that often occur in DS (209).

DYRK1A. Dual-specific tyrosine-(Y)-phosphorylation regulated kinase 1A. DYRK1A is a proline-directed serine/threonine kinase, which phosphorylates several transcription factors, including calcineurin, CREB, NFAT, Synj1, GSK3B, dynamin and FKHR (133). It seems to play a significant role during brain development by regulating neurogenesis and neuronal differentiation (59). It is considered a strong candidate gene for learning defects in DS. Moreover it contributes to AD-like neuropathological features in DS by modulating the formation of intracellular Tau inclusions and the production of β -amyloid (133).

DSCAM. Down syndrome cell adhesion molecule. It is an adhesion protein, mainly expressed in the brain, which has conserved functions in developing nervous system across invertebrates and vertebrates, including axon guidance, axonal and dendritic branching and targeting, and synapse maturation (50). In DSCAM deficient mice, retinal ganglion cells have defects in neuronal spacing and dendritic arborization patterns, exhibiting neuronal self-avoidance phenotypes (145).

APP. Amyloid beta (A4) precursor protein. APP is a trans-membrane protein expressed mainly in the synapses of neurons. It participates at synapses formation (143) and neural plasticity (190). APP can be processed by the secretases, a family of proteases that include three isoforms: α , β , γ . In turn

activity of β and γ secretases bring to the formation of A β -42 fragment, a fibrillar peptide which can form amyloid plaques. Amyloid plaques are molecular markers of Alzheimer's disease, but they are also present in adult DS individuals.

S100 β . S100 calcium binding protein beta. S100 β is a protein produced and released by astroglial cells, with particularly high levels during development and aging. In some cases, S100 β is trophic and promotes differentiation, growth, recovery, and survival of neurons, otherwise it can be toxic and lead to cell loss and apoptosis (26). The overexpression of S100 β in DS promotes β -amyloid plaque formation and progression.

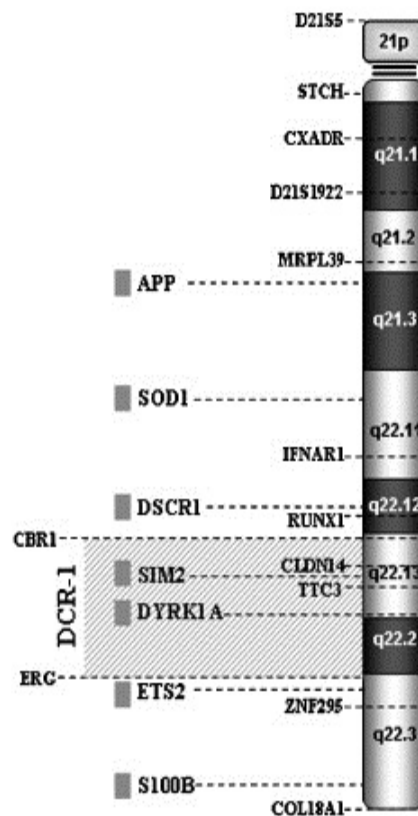


Figure 2 - Rachidi and Lopes, 2008, European Journal of Paediatric Neurology - The human chromosome 21 (HSA21). The principal genes located on HSA21, the regions 21p (short arm) and 21q (long arm) and their sub-regions, including the Down syndrome critical region (DSCR) are represented.

SOD1. Superoxide dismutase 1. This enzyme attaches (binds) to molecules of copper and zinc to break down toxic, charged oxygen molecules called superoxide radicals. Superoxide radicals can damage cells if too many accumulate within cells. SOD1 converts them in hydrogen peroxide, a

much less reactive molecule than superoxide. Superoxide radicals are byproducts of normal cell processes, particularly energy-producing reactions, and must be broken down regularly. In DS brains, SOD1 is known to be 50% over-expressed and so hydrogen peroxide is over-produced.

2.1.5 Genes expression profiling in Down Syndrome

Trisomy 21 was the first discovery of a genetic substrate for intellectual disability. Understanding the link between the genes carried by chromosome 21 and brain and cognitive disorders stands as a challenge for public health (161). To this purpose, gene expression studies have crucial importance (147). Analysis of gene transcription provides two kinds of information to understand mental retardation pathogenesis in DS. On one hand, these studies allowed identification of genes specifically expressed in the brain and, on the other hand, to select them as candidate genes for cognitive impairment ((149); (150); (52); (155)). Nowadays, transcriptome studies are evidencing a complex transcriptional environment characterized by transcriptional variability of a given gene in the different tissues and in the different individuals that complexes the interpretation of the overexpression analyses in DS and evaluation of their effects in phenotype determination. The results of these works showed different transcriptional changes that could be grouped in three classes. The majority of trisomic genes showed transcript levels increased of about 1.5-fold in human trisomic tissues ((68) ; (119)). Other HSA21 trisomic genes showed different transcriptional changes being overexpressed at different ratios than 1.5 or, for a few of them, a decreased expression was found (147). These studies are leading to the identification of potential targets in the altered pathways involved in cognitive disability pathogenesis that may be potentially corrected, in the perspective of new therapeutic approaches.

2.1.6 Phenotype features of DS individuals

Individuals with DS may have some or all of the following physical characteristics: microgenia (abnormally small chin), oblique eye fissures with epicanthic (epicanthus: a skin fold of the upper eyelid) skin folds on the inner corner of the eyes (formerly known as a mongoloid fold), muscle hypotonia (poor muscle tone), a flat nasal bridge, a protruding tongue (due to small oral cavity, and an enlarged tongue near the tonsils) or macroglossia, a short neck (127). Although Down's syndrome is usually linked to intellectual disability, the morbidity from other associated congenital abnormalities is considerable. Overall, about one in five liveborn children with DS die before the age of 5 years, and about two in five survivors have major health problems in addition to intellectual disability in early childhood. (90).

Congenital heart defects. About half of children with DS are born with congenital heart disease. The most frequent lesions are atrioventricular septal defect (45% of newborns with DS) and ventricular septal defect (35%); isolated secundum atrial septal defects (8%), isolated persistent patent ductus arteriosus (7%), isolated tetralogy of Fallot (4%), and other lesions (1%) can also arise. Assessment of all newborns with DS with an echocardiogram is the standard recommendation (American Academy of Pediatrics Committee on Genetics).

- **Atrioventricular septal defects (AVSDs).** Of all the heart defects, AVSDs are the most serious and the only ones, which have an adverse impact on survival. AVSDs are a grave heart malformation with particular clinical features. In the normal formation of the heart the endocardial cushions grow toward each other and leave openings between the atria and the ventricles. The mitral and tricuspid valves form in the openings. The AVSDs are caused by the formation of a single valve structure with a septal defect above and below it. Depending on the location of this valve structure it can also present as an inlet ventricular septal defect (resulting in blood flow only between the ventricles) or an ostium primum atrial septal defect (leaving only a hole between the atria) (see(127)). AVSDs are genetically linked to

HSA21 and are about 420 times more common in those affected with DS than in the general population (see (127)).

- **Ventricular septal disease (VSD).** VSD is a defect characterized by a hole between the top chambers (receiving chambers or atria) which provoke a backwash from the right hearth side (pulmonary) to the left (arterial). The holes can be located in the middle of the central heart wall (most common), in the top septum (sinus venosus defects) or in the lower part of septum (partial atrioventricular septum disease).

Other rare congenital hearth problems are: patent ductus arteriosus, tetralogy of Fallot, atrial septal defects, defects due the pulmonary hypertension.

Gastrointestinal defects. The second most common malformations in DS individuals are those of the gastrointestinal tract. The principal defects are Hirschsprung's disease (HD), duodenal atresia and tracheo-esophageal fistula (see (127)).

- **Hirschsprung's disease.** HD is a relatively rare condition that hits approximately 2% of children with DS. It involves a long segment of lower part of the large bowel wall, in which there is a loss of nerve cells. This encourages chronic constipation, poor weight gain, vomiting and swollen abdomen. There is a form of pathology in which only a short part of bowel participates and the symptoms are less severe.

In addition to the hearth and gastrointestinal deficits, DS individuals could present congenital problems like urinary tract malformations (6%), limb defects (9%) and congenital cataract (1%).

2.1.7 Other medical problems associated with DS

There are several serious medical problems associated with DS and some of these are leukaemia, epilepsy, hypertension, thyroid disorders and Alzheimer's disease (AD).

Leukaemia. DS increases the risk of developing acute megakaryoblastic Leukaemia (AMKL) and acute lymphoblastic leukaemia (ALL) in comparison with the normal people. Hayes and colleagues

reported in their study that 1.65% of the DS children developed leukaemia (see (127)). Usually DS patients develop leukaemia before 4 years of age and probably this is due to the trisomy of HSA21, which perturbs hematopoiesis, making megakaryocyte-erythroid progenitors susceptible to the effects of GATA1 (transcription factor) (205).

Thyroid disorders. Hypothyroidism develops in one third of patients with DS before the age of 25 years. Because symptoms of hypothyroidism might be mistaken for symptoms related to the natural course of DS, it is important to monitor annually for thyroid function (98) in view of the fact that neuro-endocrine changes, occurring with aging, have been demonstrated to play a main role, not only in homeostasis but also in the occurrence and/or in the progression of metabolic, functional and cognitive alterations (66).

Epilepsy. In a study reported by Noble J, about 15% of DS patients (16-18 years old) were affected by epilepsy. The frequency of this disorder is related to the age of the patients, probably because epilepsy is a clinical sign of dementia.

Alzheimer's disease. A connection between Alzheimer's disease (AD) and DS has long been suspected and in 1987 a gene that codes for a protein (amyloid precursor protein), subsequently shown to be involved in the pathogenesis of AD, was located on chromosome 21 (see (127)). By the age of 40, 50-70% of DS patients develop dementia. Trisomy of APP is likely to make a significant contribution to the greatly increased risk of early-onset AD (205). HSA21 genes other than APP may also contribute to the early onset of AD in people with DS. DYRK1A, for example, can phosphorylate tau at a key priming site that permits its hyperphosphorylation, followed by depolymerization of actin microfilaments, dendritic hypotrophy and neurofibrillary tangles formation, A β -42 fragment and tau actions affect several brain regions in DS, including prefrontal cortex, hippocampus, basal ganglia, thalamus, hypothalamus and midbrain (207).

2.1.8 Neurological defects

The most salient feature present in all cases of DS, even in the early infancy (147), is mental retardation and it is the most invalidating pathological aspect. Mental retardation is evident as lower verbal and mental performance in the mild-to-moderate range, with an IQ varying from 50 to 70 for mild disability and from 40 to 50 for moderate disability.

Generally, individuals with DS have normal performance in simple tasks like associative learning, but they have difficulties with spatial memory, and long- and short-term memory performance. Most indications suggest that the impairment is not spread across all learning and memory systems equally, but instead selectively impacts only some systems (see (126)), like verbal short-term memory and explicit long-term memory, with poor information encoding, impaired retrieval abilities and attention deficits (see (18)). Usually, for the rest, children with DS have normal learning ability for tasks requiring implicit memory, like visual–spatial short-term memory and implicit long-term memory, which are relatively preserved. In general, infants with DS show relatively normal abilities in learning and memory (see (126)), but in childhood specific deficits in verbal short-term memory become apparent (longer period of phonological errors, comprehension, cognition); in adolescence, the specific deficits in verbal short-term memory continue, and specific working memory deficits become evident (40). DS children perform worse than normal children on explicit memory tasks, while they show normal learning ability for tasks requiring implicit memory processing. To understand better this point, we have to explain the two types of memory: while explicit memory deals with intentional conscious learning and requires information coding and a high degree of attention, implicit memory is sustained by automatic processes requiring low attention. All these defects are probably due to the impaired brain structure typical of DS: the medial temporal lobe, and particularly the hippocampus, as well as parts of the cerebellum, are included in this category, but there are also strong evidences about an implication of the prefrontal cortex. Patients with DS also show a higher incidence of febrile and non febrile seizures than non-

DS individuals. Seizures occur in a bimodal distribution in DS, with 40% of individuals first developing seizures before 1 year of age and another 40% having an onset in their thirties or later (144).

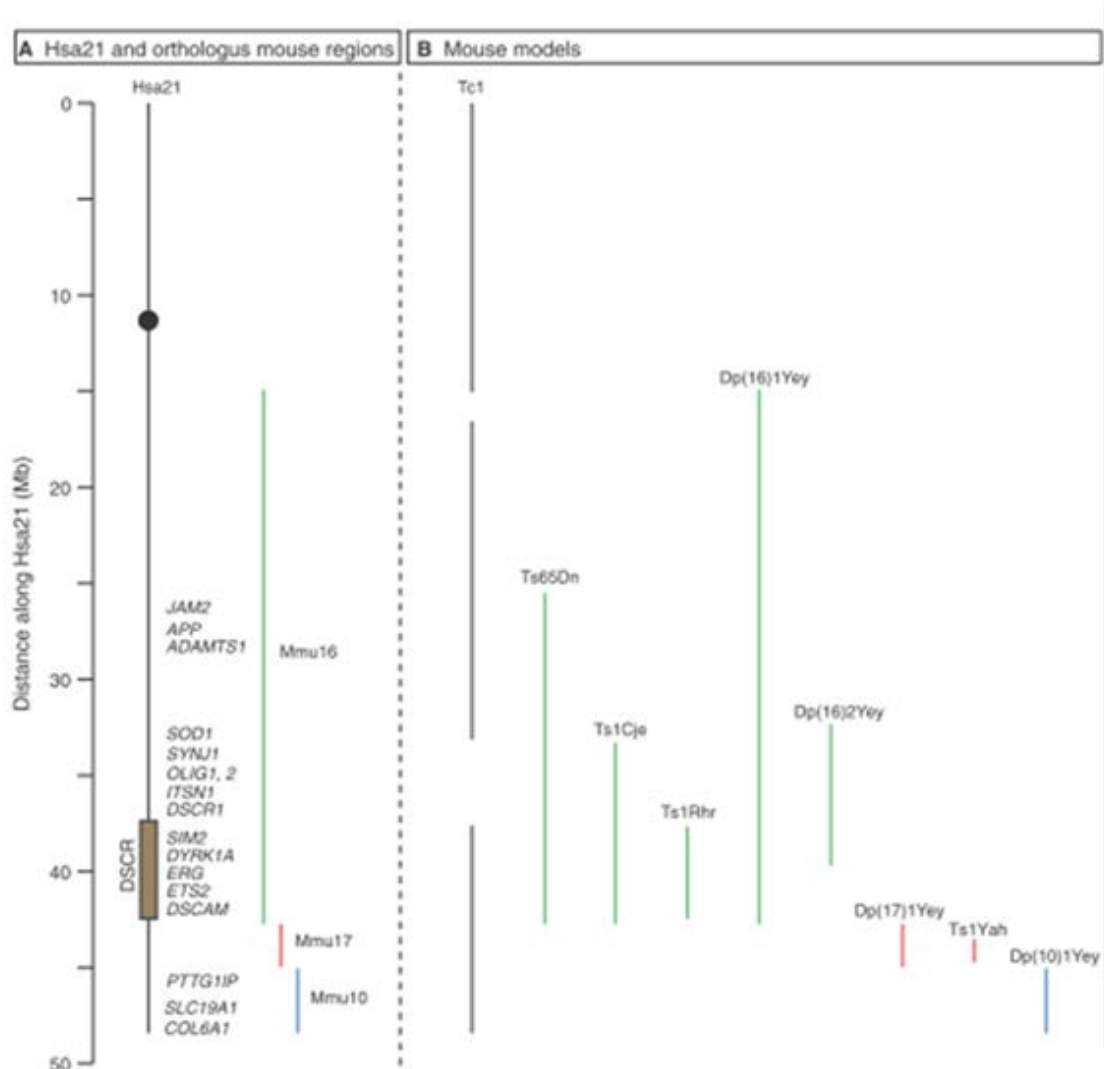


Figure 3 - Elola et al., 2011, Commentary in Disease Model & Mechanism - Syntenic regions of MMU17/MMU16/MMU10 and HSA21 (A) and their location on the modified chromosomes of DS mouse models (B)

Boys tend to have an earlier age onset, regardless of seizure type, although this may reflect the general male predominance in the infantile spasm group aged less than 1 year at onset. The prevalence of epilepsy increases with age and reaches 46% in those over 50. The mechanisms underlying the increased seizure susceptibility in DS have not yet been completely elucidated. Seizures in infancy have been linked to inherent structural brain abnormalities, such as fewer

inhibitory neurons, abnormal cortical lamination, persistent fetal dendritic morphology, and underdeveloped synaptic profiles (100).

Motor and non motor corticocerebellar and cerebellar-limbic circuits that are involved in attention, executive control, language learning, working memory and emotion, might contribute to DS cognitive phenotypes. Additionally, cerebellar hypoplasia in DS and motor dysfunction may have an important role in the development of learning skills. Impairment in perceptual-motor coupling seems to be associated with difficulties in regulating temporal aspects of actions: this problem could also affect visuospatial abilities of patients with Down syndrome (192).

2.2 MOUSE DS MODELS: TOOLS FOR THE UNDERSTANDING OF DS PATHOLOGY AND THERAPY DESIGN

To overcome the difficulties related to the study of the dosage-sensitive genes underlying DS in human subjects, several mouse models have been developed.

At the genomic level, the long arm of Hsa21 is approximately 33.7 Mb in length and contains about 430 protein-coding genes of which 293 have a homolog in the mouse genome.

These genes are divided in three syntenic regions localized in three different mouse chromosomes: Mmu16 (about 23,4 Mb in length with 115 orthologous genes), Mmu17 (1,1 Mb in length with 24 orthologous genes) and Mmu10 (2.3 Mb in length with 47 orthologous genes) (18). In these three syntenic regions, relative order and orientation of the genes are preserved between the two species.

Mouse models that mimic human pathologies as closely as possible are becoming invaluable tools because they can be exploited to identify the mechanisms underpinning a given pathology and to examine the outcome of targeted therapies.

In Fig. 3 are summarized the syntenic region between HSA21 and chromosomes of DS mouse models.

2.2.1 Model with triplication of the whole Mmu16

The first mouse model of trisomy 21, generated by spontaneous Robertsonian translocations of Mmu16 by Gropp et al (78), is labeled **Ts16** and is trisomic for the whole chromosome 16 (MMU16). Although it is a potential animal model for human trisomy 21, due to the substantial homology between the long arm of the human chromosome 21 and the distal portion of mouse chromosome 16 ((63) ; (107) ; (153)), its relevance is limited due to its embryonic lethality, given that MMU16 also contains hundred of genes located on HSA3, 8, 16. In order to overcome the viability problems associated with murine Ts16, three segmental Ts16 mouse lines have been generated: Ts65Dn, TsCje and MsTs65 mice, with Ts65Dn mice showing most similarities to the DS phenotype.

2.2.2 Segmental trisomic mice

The best studied model is that of a partial (segmental) trisomy 16, named **Ts65Dn** (Fig. 4) and was created by Davisson et al. in 1990 (54), who provoked a Robertsonian translocation with experimental exposure to radiation. The Ts65Dn strains carries an extra chromosome that has a region of Mmu16 translocated onto a short segment of Mmu17, and is thus trisomic for ~104 genes on Mmu16 that are orthologous to Hsa21 genes. However, it should be noted that it also has three copies of 19 genes on Mmu17 that are not orthologues of genes on Hsa21, and thus some phenotypes in this strain might not be related to human DS (see (108)).

Unlike Ts16 mice, Ts65Dn mice live until adulthood and show many clinical phenotypes similar to those seen in DS patients.

The phenotypic abnormalities in the Ts65Dn mouse model are: reduced birth weight, postnatal developmental delay, muscular trembling and male sterility, skeletal malformation corresponding to the cranio-facial dysmorphogenesis in DS (72). Also brain abnormalities have been found: reduced cerebellar volume and neuronal density in the dentate gyrus, reduced thickness of the internal

granule and molecular layers and reduced granule cell numbers compared to euploid mice (106). Both APP mRNA and APP protein from cerebral cortex are elevated at embryonic day 15 (E15): 2,5 and 2 fold respectively. Moreover in the Ts65Dn mouse there is an abnormal cholinergic function and degeneration of cholinergic basal forebrain neurons. These characteristics are also found in DS individuals and are considered the initial signs of the onset of Alzheimer's disease (72).

Adult Ts65Dn mice exhibit hyperactivity under certain experimental condition, impairment of memory and learning. Two studies have shown that long-term potentiation (LTP) and depression (LTD), electrophysiological correlates for learning and memory, are abnormal in young adult Ts65Dn mice. It has been demonstrated that pyramidal cells of the CA1 subfield from Ts65Dn mice have a reduced LTP and an enhanced LTD compared to control animals.

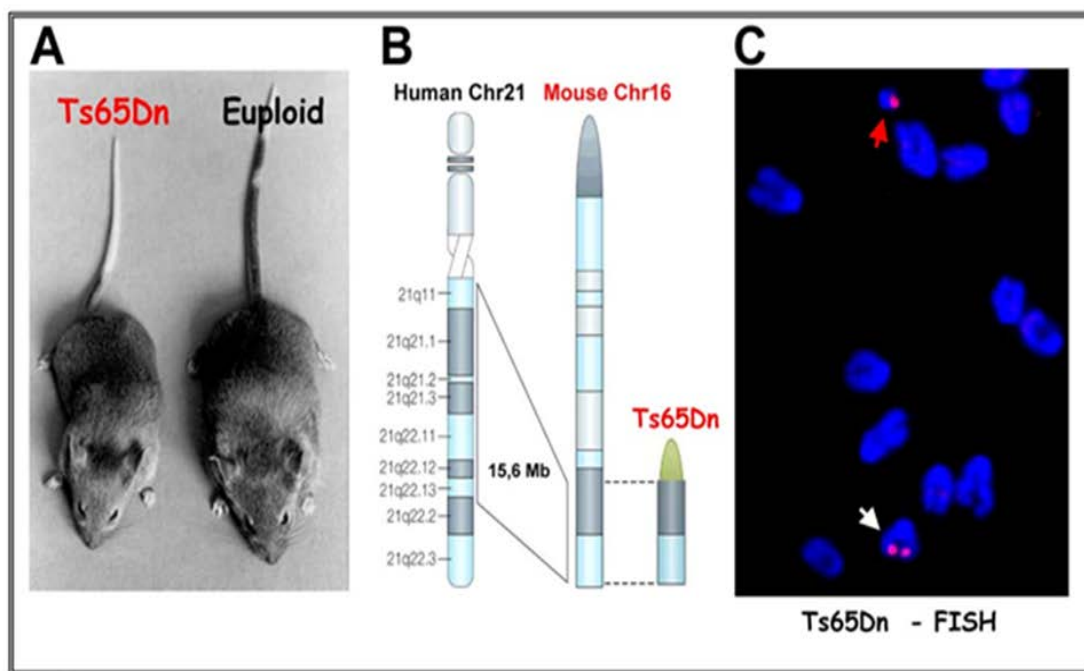


Figure 4 - <http://www.jax.org/cyto/mice.html#HHSN275201000006> - The Ts65Dn mouse model. A: Example of a Ts65Dn and a control mouse. B: The Ts65Dn mouse model shows segmental trisomy for a distal region of chromosome 16, a region that shows perfectly conserved linkage with human chromosome 21. C: Fluorescent in situ hybridization (FISH) in the Ts65Dn mouse.

The fact that there is a significant reduction in the number of neurons in the granule cell layer of the dentate gyrus in Ts65Dn (93), may lead to a concomitant decrease in the number of synaptic sites available in the dentate gyrus for receiving information through the perforant path. In adult Ts65Dn mice, neocortical pyramidal neurons have shorter and less branched dendrites with significantly reduced spine numbers as compared to controls. Moreover, synaptic structures of trisomic mice are less responsive to stimuli. Cerebellar granule neuron precursors have been isolated and cultured in vitro to demonstrate the reduced proliferation in response to mitogenic factors. This aspect may affect any trisomic cell and may represent the primary cause of reduced body size, developmental defects and premature aging of DS individuals.

The **Ts1Cje** mouse model, created by Sago et al, has a duplication of a shorter region of Mmu16, encompassing ~81 genes (from Sod1 to Znf295) with orthologues on Hsa21. Ts1Cje mice show reduced cerebellar volume and abnormalities in craniofacial development similarly to Ts65Dn mice, but generally less severe.

The **Ms1Ts65** mouse model has a partial trisomy that starts from APP to SOD1 and includes about 33 genes, the region of difference between Ts65Dn and TsCje. This allows comparisons among the trisomies and permits to assess the contributions of the phenotype of Ts65Dn mice of genes proximal to App up to Sod1 regarding the learning and behavioral phenotype (162). These segmental trisomic mice have fewer similarities to DS than do Ts65Dn and Ts1Cje mice.

A comparison of Ms1Ts65 and Ts65Dn demonstrates that the deficits of Ms1Ts65 mice in the Morris water maze are significantly less severe than those of Ts65Dn, as triplication of the region from Sod1 to Mx1 plays a major role in the abnormalities of Ts65Dn in the Morris water maze, (162).

In Ms1Ts65 mice, a neurological alteration has been identified at the cerebellar level: the granule cell density is moderately reduced, similarly to Ts1Cje, compared to Ts65Dn mice.

Olson et al. (130) addressed the hypothesis that the DS critical region (DSCR) contains all the major genes involved in generating DS phenotypes. Using chromosomal engineering they generated a new mouse, named **Ts1Rhr** (131), which was trisomic for the *Cbr1-Orf9* genetic interval (DSCR) including 33 genes. Somehow, the DSCR was not sufficient to induce the cranio-facial defects in mice. Similarly, impairment in learning and memory tasks involving the hippocampus found in Ts65Dn mice is not reproduced in Ts1Rhr mice, confirming that the DSCR was not sufficient to induce the brain phenotype observed in Ts65Dn models. Interestingly, mice combining the deletion of the *Cbr1-Orf9* region (**Ms1Rhr**) with the Ts65Dn trisomy achieve normal performance in the Morris water maze (132), indicating that the DSCR is not sufficient but contributes to learning and memory.

Additionally, the **Ts2Cje** mouse has been recently established after a fortuitous translocation of the Ts65Dn marker chromosome to chromosome 12 (193). Both Ts65Dn and Ts2Cje mice, carrying the same trisomic segment, showed enlargement of the brain ventricles and impaired neurogenesis (95).

2.2.3 Models with triplication of Mmu17 or Mmu10/16/17

Two models have recently been created, Ts1Yah and Ts43H ((136) ; (191)), which are not trisomic for Mmu16 genes, but rather for a segmental region of Mmu17. The **Ts1Yah** mouse, which is trisomic for 12 genes in the Mmu17 region, syntenic to the sub-telomeric region of Hsa21, displays deficits in novel object recognition, similarly to other DS models. Conversely, it displays enhanced learning in the hippocampus-dependent spatial memory, revealing the complexity of the genetic code that modulates different aspects of behavior in DS patients. To distinguish between the specific effects of dosage-sensitive genes and non specific effects of a large number of arbitrary genes, the Ts(1617)43H (Ts43H) mouse, which is trisomic for 30 Mb of proximal Mmu17, was created (191). The **Ts43H** model exhibited spatial learning deficits analogous to those observed in Ts65Dn mice. This is in accordance with the hypothesis that the over-expression of a large number

of triplicated genes causes a disruption in genetic homeostasis that impairs gene regulation of developmental processes (see (18)).

Recently a new mouse DS model that carries duplications spanning the entire Hsa21 syntenic regions on all Mmu10, Mmu16 and Mmu17 mouse chromosomes has been created (**Dp(10)1Yey/+;Dp(16)1Yey/+;Dp(17)1Yey/+**). This mouse mutant exhibits DS-related neurological defects, including impaired learning/memory and decreased hippocampal LTP (212), very similarly to the Ts65Dn mouse. These results suggest that the critical genes associated with the DS brain phenotypes may reside within the *Mrpl39–Zfp295* genomic segment of the Mmu16 and support the use of the Ts65Dn mouse as the best genetic murine DS model.

2.2.4 Models with insertion of Hsa21

The **Tc1** mouse model, created by O’Doherty et al, has a triplication of the entire human Hsa21. This model exhibits several key phenotypes of DS like alterations in synaptic plasticity and cerebellar neuronal number ((70); (128); (125)).

However, the random loss of this human chromosomal fragment during mouse development resulted in variable levels of mosaicism of the extra chromosome in different tissues, confounding the analysis of phenotypic consequences. Four mouse strains were generated with a trisomy for a selected short fragment of Hsa21, to produce polytransgenic mice with partial trisomies for the DSCR ((179); (178)). Two of the four polytransgenic mice had learning and memory defects, in particular the one containing the *Dyrk1a* gene.

2.2.5 Models with triplication of individual genes

Several transgenic mouse models with one orthologous HSA21 gene were created like **TgSod1**, **TgApp**, **TgEts2**, **TgS100 β** , **TgDyrk1A**, **TgDSCR1**, **TgSim2**, **TgBACE2**, **TgSynj1** and **TgPfk1** in order to evaluate the contribution of triplicated individual genes to the mouse phenotype.

Recent work focused on the role of *Dyrk1a* triplication in the cognitive deficit of DS, showing that transgenic mice (TgDyrk1a) exhibit various but not all learning defects of Ts65Dn mice (6). Extracellular hippocampal recordings in these transgenic mice demonstrated altered induction of LTP and LTD during the learning and memory process, although the changes in both processes were in the opposite direction to that seen in other more complete trisomic mouse models, namely Ts65Dn and Ts1Cje ((103) ; (3)). The transgenic mice for *App* exhibited over-expression of App in the neocortex and hippocampal region, mimicking features of DS. These amyloid precursor protein transgenic models with Alzheimer disease-like pathology showed dystrophic neuritis associated with plaques and mild learning defects. Learning deficits were shown in transgenic mice overexpressing synaptojanin 1 (*Synj1*) (194), but the learning deficits of Ts65Dn mice was more severe. All this data are consistent with the general concept that neurological defects in DS and genetic models are the result of contributions of multiple genes.

2.2.6 Trisomic mice with removal of triplicated genes

A last group of DS mouse models was obtained by selectively manipulating the dosage of candidate genes. These models were obtained by removing one copy of a specific gene from a mouse model of DS and used to examine the behavioral outcome ((35); (58); (194); (37)). For instance, when Ts65Dn mice are crossed with a knockout of the *App* gene, thus reducing *App* to disomy, the development of some cellular abnormalities, including degeneration of basal forebrain cholinergic neurons (BFCNs), was prevented (35).

2.3 *NEUROANATOMY OF DS*

The DS brain is characterized by numerous structural alterations that start to be present from early developmental stages and are retained in adulthood.

2.3.1 **Gross anatomy**

HUMANS

The DS brain is characterized by shape changes that include an anteroposteriorly shorter cerebrum, reduced frontal lobes, flattening of occipital poles and narrowing of the superior temporal gyri ((167); (206); (198); (152); (139)). Individuals with DS have a typically reduced brain volume. The volume is disproportionately small in frontal, temporal and cerebellar regions and relatively preserved in the occipital and parietal cortical gray matter (139). The reduced size of the DS brain can be traced back to early developmental stages as hypotrophy of the hippocampus, parahippocampal gyrus and cerebellum is already present during gestation ((204); (80)). Magnetic resonance images of the corpus callosum in adolescents with DS reveal that callosa are decreased in widths throughout their rostral fifth, which serves frontal lobe projections. This correlates with the hypocellularity and hypofrontality of neocortex in subjects with DS and with their neuropsychological profile of frontal lobe dysfunction (197). Atrophy of the corpus callosum has been also seen in non-demented adults with DS (188). In addition, DS patients have an area of the anterior commissure smaller compared with that of control subjects (184) and a decrease in white matter throughout the inferior brainstem (202). The reduced volume of the white matter and fiber tracts is consistent with the reduced number of neurons forming the DS brain (see below). Defective biochemical composition of myelin and delay in myelin formation ((208); (20); (104)) are likely to contribute to decrease the size of the white matter and fiber tracts.

MOUSE MODELS

In **Ts65Dn** mice, brain volume is reduced during the embryonic period, though at birth and at further life stages it is similar to that of euploid mice ((37); (5); (92)). The shape of the hemispheres

is characterized by an increase in the height of the posterior cerebrum and a reduction in the rostrocaudal length and mediolateral width (5). The overall hippocampal volume and the volume of the pyramidal layer are not reduced in Ts65Dn mice ((92); (112); (93)), though the granule cell layer and hilus have a reduced volume ((28) ; (46) ; (112)). Unlike the cerebrum, the cerebellum of Ts65Dn mice has a notably reduced volume (5). In **Ts1Cje and Ts2Cje** mice at embryonic day 14.5 brains are smaller when compared with diploid littermates, which is consistent with the reduced neurogenesis (95). At one, three and six months of age the ventricles of Ts1Cje and Ts2Cje mice are enlarged, but there are no differences in total brain volume, though the brain has a shorter anteroposterior length (95). Another study shows that there are no differences in brain weight in Ts1Cje mice aged 6-6.5, 7-7.5 and 9-10 months. (22). Likewise, the area of the hippocampus shows no difference between Ts1Cje aged 18 months and the euploid counterpart (22). Similarly to Ts65Dn mice, Ts1Cje mice have a reduced cerebellar volume (131). **Ms1Rhr** mice have a cerebrum with reduced volume, height, width and length and a cerebellum with reduced volume (5). The cerebrum of **Ts1Rhr** mice (aged four months) shows a few differences in linear distances vs. controls. These include a reduced rostrocaudal and mediolateral length of the anterior portion of the cerebrum but an increased rostrocaudal length of the posterior portion of the cerebrum (5). While at 4 months of age Ts1Rhr mice have a reduced volume of the cerebrum and cerebellum, at 7.5 months they have a brain weight and volume of the posterior hippocampus that are larger than euploid mice (21).

2.3.2 Cytoarchitecture, cell density, cell number

HUMANS

In the DS brain cell density appears normal in early gestation, but there are fewer neurons than normal in late gestation (after weeks 19-23), and this paucity continues throughout early life ((199); (75); (80)). In fetuses with DS, total neuron number is reduced in the hippocampal dentate gyrus

(DG), hippocampus and parahippocampal gyrus (80) and the cellular layers of the cerebellum are characterized by prominent hypocellularity and reduced thickness (81). Morphometric studies in DS cases from birth show fewer neurons, lower neuronal densities and cortical dysgenesis (206). Children and adults with DS retain a reduced granule cell density in the cerebellum (19) and have a greatly reduced number of neurons in the ventral cochlear nucleus, a small nuclear volume, low cell packing density (73). Architectonic abnormalities and a significant poverty of granular cells are present in the DS brain, particularly in granular fields such as areas 3, 17, and 41 (160). Accompanying neuronal alterations are alterations of other cell types: astrocytes, oligodendroglia and microglia. Fetuses with DS show an increased astrocyte-neuron ratio in all hippocampal structures compared with controls (80). Astrocytic hypertrophy and an increase in astrocyte number are present in both the developing and adult DS brain ((77); (123)). Microglia appears more prominent in DS and oligodendroglia dysfunction is reflected in delayed myelination in pathways of frontal and temporal lobes (20).

MOUSE MODELS

Development of the neocortex of the **Ts16** mouse model is characterized by a transient delay in the radial expansion of the cortical wall and a persistent reduction in cortical volume (88). Similarly to Ts16 mice, **Ts65Dn** mice exhibit delayed expansion of the neocortex during the embryonic period, though this difference disappears by E18.5 (37). At E18.5, however, despite the cortical growth to normal thickness, there is a reduction in cell density. Reduced cell density is present also postnatally at P8, specifically in layers IV, V, and VI with no change in the density of layers II–III, suggesting a selective deficit in the early born neurons of the deeper cortical layers (37). Similarly to the neocortex, the hippocampal wall of Ts65Dn mice has a reduced thickness but this difference, which is present from E13.5, persists up to E18.5. The pyramidal cell layer has a very reduced thickness and the DG is smaller in size (46). In the hippocampal region of Ts65Dn mice (Fig. 5), the granule cell layer of the DG has a reduced number of granule cells across all postnatal life

stages ((46); (28); (112); (93)). In contrast, the number of hippocampal pyramidal cells is not reduced (112) and in aged Ts65Dn mice the number of cells in hippocampal field CA3 appears to be larger vs. controls (93).

In the hippocampus of Ts65Dn mice the astrocytes exhibit a significant hypertrophy and are more numerous, though this difference is not statistically significant (92). The cerebellum of Ts65Dn mice has a reduced layer thickness, a reduced granule cells density and number starting from P2 to adulthood ((159); (19); (45)). In addition, Purkinje cells density is also reduced (19).

In **Ts1Cje** mice aged 18 months, the thickness of the granule cell layer and molecular layer of the DG is similar to that of controls (22). Ts1Cje mice show a moderate decrease in cerebellar granule cell density and no changes in Purkinje cell density (130). In **Ts1Rhr** mice aged 7.5 months the thickness of the motor cortex has been found to be larger than in euploid mice (21).

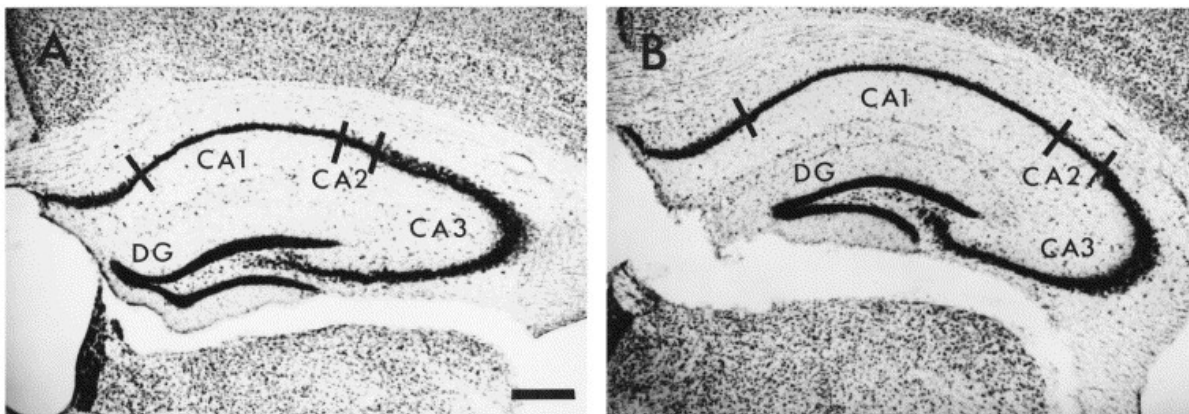


Figure 5 - Insausti et al., 1998 Neuroscienceletters - 50 μ m thick slices of the hippocampus, stained with thionin, of a control case (A) and a Ts65Dn case (B).

2.4 CAUSES OF BRAIN HYPOTROPHY IN DS

The widespread hypoplasia of the DS brain is considered to be the main cause of mental retardation. Several lines of evidence show that neurogenesis reduction and dendritic hypotrophy are the two major determinants of brain hypotrophy in DS: An increase in cell death does not seem to play a

role at early life stages, but at more advanced life stages it may contribute to further reduce neuron number.

2.4.1 Neurogenesis alterations

The fact that brain and cerebellar volume reduction and cortical hypocellularity are already present in children and fetuses with DS ((75); (204); (139)) strongly suggests that defective *neuronogenesis* during critical phases of brain development may be a major determinant of microencephaly. Neurons and glial cells destined to form the cortical mantle derive from the embryonic ventricular zone (VZ). At advanced stages of embryogenesis the VZ decreases in size and is gradually replaced by the subventricular zone (SVZ). The SVZ plays a pivotal role in corticogenesis during the embryonic/early postnatal period. At further life stages it produces granule cells that migrate to the olfactory bulb (31). Neurons forming the DG derive, initially, from the dentate neuroepithelium, which will give rise to the postnatal subgranular zone (SGZ) (8). In rodents, the bulk of DG neurogenesis takes place in the early postnatal period and continues at a slower rate into adulthood. Neurons forming the cerebellum are mainly formed prenatally, with the exception of the granule cells of the inner granule cell layer that are formed both prenatally and in the early postnatal period from precursors in the external granular layer (EGL) ((1); (182)). Neurogenesis alterations in the VZ, SVZ, SGZ and EGL have been documented in the DS brain.

HUMANS

Due to the obvious difficulties in obtained fetal material, very little information is available concerning neurogenesis in the fetal DS brain. We recently obtained evidence that in fetuses with DS cell proliferation is severely impaired in the DG (most likely due to alteration of the cell cycle), in the germinal matrix of the inferior horn of the lateral ventricle and in the germinal zones of the hippocampus proper and parahippocampal gyrus ((46); (80)). Quantification of the number of mature neurons and astrocytes in the hippocampus and parahippocampal gyrus showed that in all

these regions fetuses with DS had proportionally fewer neurons and a larger number of astrocytes compared with normal fetuses (80). In trisomic fetuses, we also found a defective neurogenesis in the EGL of the cerebellum, and in a region of the fifth lobe that is the remnant of the cerebellar VZ (81). This evidence clearly shows proliferation impairment in numerous regions of the fetal DS brain. Importantly, these defects are shared by trisomic mice which validates the use of mouse models for DS and renders evidence obtained in mouse model transferable to the human condition.

MOUSE MODELS

Neurogenesis in the VZ/SVZ. In Ts16 mice the number of precursors of the future somatosensory cortex just before neuronogenesis begins, is notably reduced. At each cell cycle during neuronogenesis, a smaller proportion of Ts16 progenitors exit the cell cycle and the cell cycle duration is longer in Ts16 than in euploid progenitors (89). In the Ts65Dn mouse a reduced proliferation has been detected at all examined life stages. Reduced neural precursor proliferation, due to elongation of the cell cycle, is already present during embryonic development in the cortical and hippocampal VZ, with a reduction in the number of neocortical and hippocampal neurons (37). In a subsequent study, Chakrabarty et al. found that in Ts65Dn mice, unlike the cortical and hippocampal VZ, the embryonic medial ganglionic eminence (MGE), which is the source of inhibitory neurons, undergoes divisions at a normal rate but gives a higher neuronal output, due to a large progenitor population (36). Interestingly, there is an imbalance between production of excitatory and inhibitory neurons, with an increase in the number of inhibitory neurons. The large output from the MGE explains the observation that in the neocortex and hippocampus of neonate and young Ts65Dn mice there are fewer excitatory but more inhibitory neurons. This excessive production of inhibitory interneurons is due to over-expression of the triplicated genes *Olig1* and *Olig2*, as normalization of their expression rescues the Ts65Dn phenotype (36). In Ts65Dn mice, the postnatal SVZ of the lateral ventricle, which is the largest neurogenic area of the adult brain, presents a remarkably reduced proliferation rate that starts in the perinatal period and continues up

to senescence ((189); (28)). A severe neurogenesis reduction has also been documented in the embryonic neocortex and VZ and in the SVZ of adult Ts1Cje and Ts2Cje mice (95). In the adult Ts1Cje SVZ trisomy does not appear to affect the number of neural stem cells but results in reduced numbers of neural progenitors and neuroblasts (91). Analysis of differentiating Ts1Cje neural progenitors shows a severe reduction in number of produced neurons and an increase in the number of astrocytes (91).

Neurogenesis in the SGZ. A severe neurogenesis impairment characterizes the DG of the **Ts65Dn** mouse at all examined life stages ((93); (46); (112) ; (28)). The study of the phenotype acquired by differentiating neural progenitor shows a reduction in the number of new neurons with an increase in the number of astrocytes ((46); (28)). A severe neurogenesis reduction has been documented also in the SGZ of adult (3 months) **Ts1Cje** and **Ts2Cje** mice (95).

Neurogenesis in the EGL of the cerebellum. A reduced proliferation of cerebellar granule cell precursors in the EGL of Ts65Dn mice has been documented at P0 and P6 (159). This reduction has been confirmed in P2 Ts65Dn mice and is due to elongation of the cell cycle (45). Also in the cerebellum, an altered differentiation leads to a proportionally smaller percentage of cells that acquire a neuronal phenotype and a larger percentage that acquire an astrocytic phenotype (45).

2.4.2 Dendritic hypotrophy

Dendritic pathology is a typical feature of the DS brain and appears to correlate to some extent with cognitive profile.

HUMANS

Dendrites. It has been argued that DS persons start their lives with an apparently normal neuronal architecture that progressively degenerates. Thus, normal or even increased branching in the DS foetus and newborn contrasts with reduced dendrites and degenerative changes in older children

with DS. Becker et al. (1986) showed that in infants with DS younger than 6 months, dendritic branching and length in both apical and basilar dendrites were greater than in normal infants. During the peak period of dendritic growth and differentiation, quantitative analysis of dendrites in layer IIIc pyramidal neurons of prefrontal cortex of the brains of 2.5-month-old infants revealed no significant differences in dendritic differentiation between euploid and DS cases (195). In contrast, the pyramidal neurons of the visual cortex of newborns older than 4 months have shorter basilar dendrites (185). These findings suggest that children with DS begin their lives with morphologically normal layer III pyramidal neurons and that pathologic changes in key prefrontal input–output neuronal elements occur after 2.5 months of postnatal age. Subsequent to this age, there is a steady decrease so that in subjects with DS older than 2 years, these parameters are reduced relative to controls especially in apical dendrites. Dendritic hypotrophy is also present in pyramidal neurons of the parietal cortex of children with DS (176). The dendritic hypotrophy seen in childhood continues into adulthood, with a marked decrease in dendritic branching and dendritic length in elderly adults with DS (186). This evidence shows that unlike in normal brains, where accomplishment of dendritic maturation is attained in early childhood, in DS brains the dendritic tree begins to be atrophic in early infancy without a recovery at subsequent life stages.

In agreement with the deteriorated dendritic development, various proteins forming neuron cytoskeleton or associated with the endoplasmic reticulum are down-regulated in the DS brain. These proteins include the microtubule-associated protein MAP2 (129), beta-tubulin and neurofilament proteins of medium (NF-M) and high (NF-H) molecular-weight, ((140); (62)); actin-related protein complex 2/3 (Arp2/3) (200), actin-related protein 3beta (ARP3beta) (175), cencentractin alpha and F-actin capping protein alpha-1, alpha-2 and beta subunits (82), the neuroendocrine-specific protein C (NSP-C) (102) and moesin, which is involved in plasma membrane-actin cytoskeleton cross-linking (113). Moreover, the ratios of beta-tubulin and NFs in relation to beta

actin are notably decreased (140). All these changes may be involved in the deteriorated neuritic outgrowth and arborization of DS neurons.

Spines. While in the visual cortex of fetuses with DS spine counts (basilar dendrites) are similar to those of control fetuses, newborns and older infants with DS have a decreased number of spines and spines exhibit an altered morphology (185). In normal subjects, spine density on the basal dendrites of cortical pyramidal neurons increases from neonate to 15 years of age and gradually decrease after 20 years. In contrast, spine density poorly increases in children and rapidly decreases in adults with DS ((183); (186); (187)). A reduced spine density has been found in the apical dendrites of pyramidal neurons of the hippocampus and cingulate cortex and in both the apical and basilar dendritic arbors of CA1 and CA2-3 pyramidal neurons in patients with DS when compared to age-matched control ((183); (186); (187)). An additional decrease in spine density occurs in DS patients with associated AD, when compared to age-matched controls with no AD ((186); (67)). The dendritic spines of the DS brain exhibit, in addition to reduced density, also aberrant morphology. Spines are small, have short stalks and are intermingled with unusually long spines starting from infancy ((120); (146)). Drebrin A, one of the most abundant neuron-specific F-actin binding proteins, regulates dendritic spine morphology, size and density, presumably via regulation of actin cytoskeleton remodeling. Consistent with the reduced spine density, drebrin, is manifold decreased in brains of fetuses and adults with DS ((174); (199)). Over-expression of drebrin A results in the alteration of the normal excitatory-inhibitory ratio in favor of excitation in mature hippocampal neurons (96). Considering that drebrin expression is reduced in DS individuals (174), a reduced excitatory-inhibitory ratio is expected in DS individuals, which may lead to neuron hypoexcitation. It is expected that all these dendritic alterations lead to impairment of synaptic function. The most obvious mechanism by which dendritic pathology in general and reductions in dendritic arborizations in particular, could lead to neurologic impairment is a decrease in the cortical

postsynaptic surface. Dendritic hypotrophy should correlate with a reductions in synaptic density, while spine dysgenesis may represent a preferential reduction in excitatory synapses (99).

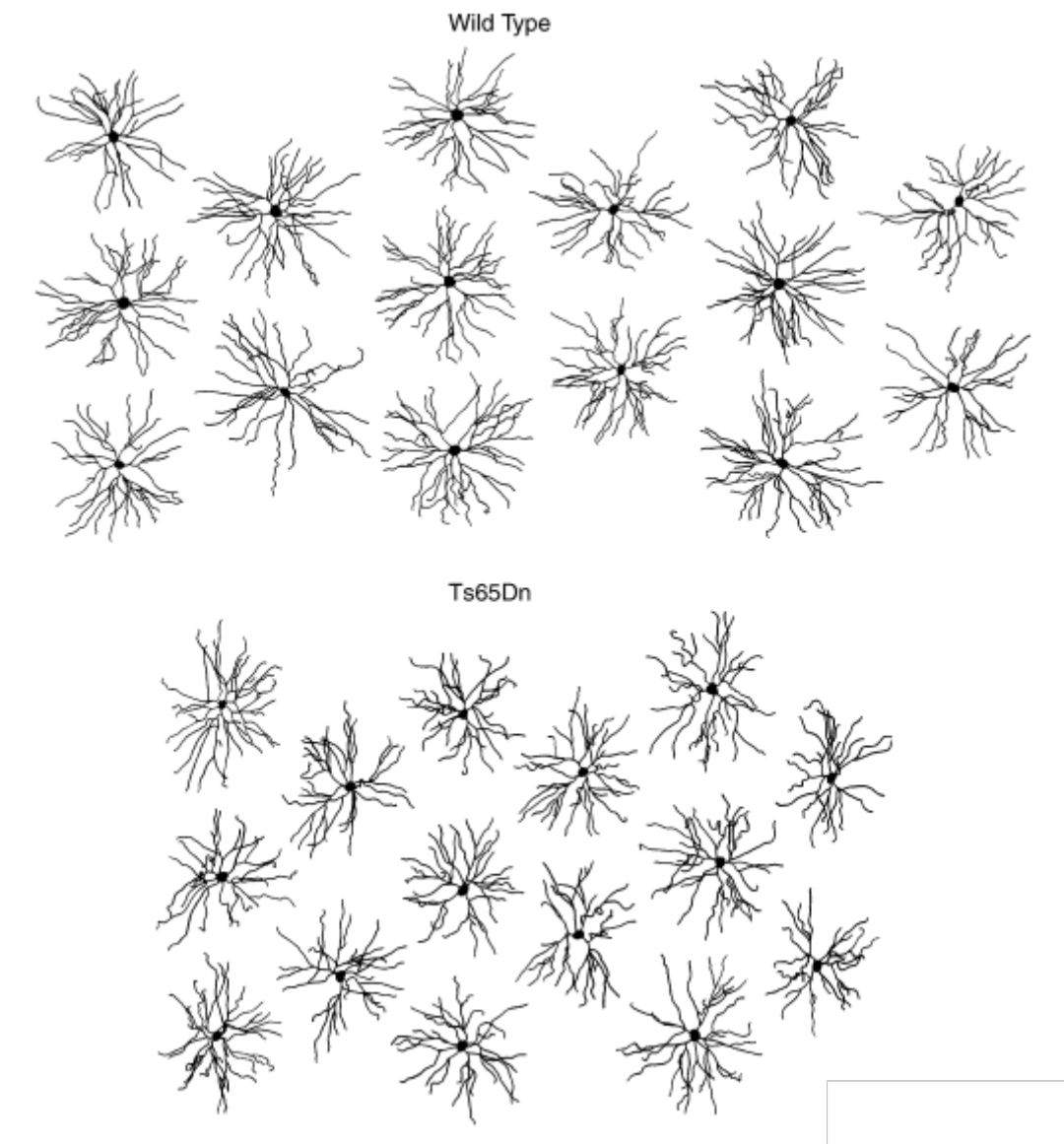


Figure 6 - Benavides-Piccione et al., 2004, Review in Progress in Neurobiology - Camera lucida drawings of basal dendritic arbours of layer III pyramidal neurons from wild type and Ts65Dn mice. Scale bar = 150 μ m.

MOUSE MODELS

Dendrites. In **Ts65Dn** mice aged 10 weeks the pyramidal cells of the neocortex are smaller and have fewer and shorter basal dendritic branches than controls (24) (Fig. 6). While in the brain of neonate Ts65Dn mice the levels of the dendritic marker MAP2 are significantly increased compared to littermate controls (141), in hippocampal extracts of adult (4 months) Ts65Dn mice MAP2 is

expressed at levels similar to those of littermate controls, However, in the hippocampal formation of middle-aged Ts65Dn mice (9-15 months old) MAP2 undergoes a decrease vs. controls (76), suggesting an age-related dendritic deterioration.

Spines. In **Ts65Dn** mice the basal dendrites of neocortical pyramidal cells exhibit a reduced spine density (57). A spine density reduction is also present in the granule cells of the DG, accompanied by a reorganization of inhibitory inputs, with a relative decrease in inputs to dendrite shafts and an increase in inputs to the necks of spines ((23); (142)). The thorny excrescences of CA3 pyramidal neurons (the site of termination of the axons of the granule cells) also exhibit a large decrease in the number of thorns (142). In addition to density reduction, spines of Ts65Dn mice exhibit an aberrant morphology; spines in the DG, field CA1, motor, somatosensory and entorhinal cortices, and medial septum of young (21 days) and adult Ts65Dn mice have a larger volume when compared to euploid mice (23). A decrease in spine density, an increase in the size of spine heads, a decrease in the length of spine necks and a reorganization of inhibitory inputs also appear in the granule cells of **Ts1Cje** mice, though these changes are less severe than in Ts65Dn mice (22). Likewise, the granule cells of **Ts2Cje** mice have enlarged spines with decreased density (193). Similarly to other mouse models, the granule cells of **Ts1Rhr** mice exhibit a reduced spine density. In contrast, spine density is not reduced in dendritic trees of pyramidal neurons in the motor cortex (21). Dendritic spines of Ts1Rhr mice show a significant increase in the size of spine heads without changes in the spine neck, both in the cortex and DG (21).

2.5 ALTERATIONS OF SYNAPTIC FUNCTION IN THE DS BRAIN AND TRISOMIC GENES INVOLVED

The proper neuronal function is related to the machinery involved in the release of neurotransmitters, the relative weight of excitatory and inhibitory inputs, the balance among different neurotransmitter systems and density and function of the corresponding receptors. The DS

brain is characterized by numerous defects at the synaptic levels that span from subtle synaptic alterations to patent alterations of various transmitter systems.

2.5.1 Synaptic density, excitatory vs. inhibitory synapses

HUMANS

To our knowledge, no data are available on synaptic density and relative abundance of excitatory/inhibitory synapses in the DS brain.

MOUSE MODELS

In the neocortex and hippocampal field CA1 of **Ts65Dn** mice a reduction in synaptic density has been detected as early as P8 (37). The synaptic density and the synapse-to-neuron ratio are reduced in the DG and hippocampal fields CA3 and CA1 of adult Ts65Dn mice (106), with a reduced ratio that is specific for asymmetric synapses (presumably excitatory), while symmetric synapses (presumably inhibitory) are unchanged. In aged Ts65Dn mice the temporal cortex has a lower number (30%) of asymmetric synapses while the number of symmetric synapses is not different vs. controls (105). The reduced number of excitatory synapses in Ts65Dn mice seems in agreement with the reduced levels of excitatory aminoacids found in the parahippocampal gyrus of patients with DS (157). The increase in the number of GABAergic interneurons found in the primary somatosensory cortex of 4-5 month old Ts65Dn mice (137) suggests that in some brain region excessive inhibition may be due to an absolute increase in the number of inhibitory synapses.

2.5.2 Synaptic proteins

HUMANS

Synapses in DS brain exhibit various alterations in the expression of synaptic proteins. Synapsin I (a pre-synaptic protein which binds synaptic vesicles to the cytoskeleton and regulates synaptic

vesicle release) is expressed at lower levels in neurospheres from human embryonic tissue ((14)). Moreover, in various brain areas of DS individuals there are significantly lower levels of synaptophysin (a pre-synaptic vesicle membrane glycoprotein known to mediate vesicle release) and SNAP-25 (soluble N-ethylmaleimide-sensitive fusion attachment protein) compared with controls ((60); (199)). Since all these protein play a role in the regulation of transmitter release, their down regulation may compromise synaptic function. Synaptojanin, a synaptic protein thought to be involved in clathrin-mediated synaptic vesicle endocytosis, is mapped on Hsa21q22.2. Consistent with Hsa21 triplication, excessive expression of synaptojanin has been demonstrated in the cerebrum of individuals with DS from fetus to adult period (12). In addition to changes in the expression of synaptic proteins, synapses of individuals with DS show abnormalities in synaptic length and contact zones (206).

MOUSE MODELS

In **Ts65Dn** neonate brains, the levels of synaptophysin, synapsin, spinophilin (a scaffold protein that is involved in spine morphology and density regulation) are similar to those of littermate controls (141). In 3 month-old Ts65Dn mice, synapses show relatively few changes outside of those expected from gene triplication (e.g., synaptojanin). For example synaptosomes prepared from the cerebrum of wild type and Ts65Dn mice exhibit no differences in their content of VGLUT1 or VGAT, presynaptic transporters necessary for the vesicular uptake of glutamate and gamma-aminobutyric acid (GABA), respectively, suggesting that the total number of excitatory and inhibitory vesicles is conserved (65). Moreover, there are no differences in the levels of other presynaptic proteins, such as synapsin, synaptotagmin (a putative calcium sensor in the presynaptic terminal) and synaptophysin (65). In the somatosensory cortex of 4-5 month-old Ts65Dn mice there is an increment of synaptophysin vs. euploid littermates (137). In the hippocampus of adult (4 months) Ts65Dn mice, whereas synapsin, spinophilin and gephyrin are expressed at levels similar to those of controls, the expression levels of synaptophysin are significantly decreased (141). The

inconsistent results of different studies suggest that the expression of synaptic proteins in trisomic mice may differ according to age and brain regions.

2.5.3 Electrophysiology

HUMANS

In view of the obvious obstacles, there is no electrophysiological evidence of synaptic function in individual regions of the DS brain. Electroencephalogram (EEG) recordings, however, can provide information on the overall cortical activity. A study of EEG coherence in subjects with DS (from 6 months to 30 years) shows some coherence differences vs. controls that became more prominent with increasing age (169). Da Nobrega et al. (51) showed that though a typical EEG pattern for DS could not be established, 20.7% of the examined patients had EEG abnormalities and 31.3% of these were epileptic. The high incidence of epilepsy in individuals with DS is difficult to reconcile with the over-inhibition found in mouse models for DS (see below). Recent evidence, however, shows that GABA_B receptor agonists have convulsant properties in rodents (47). Given that an enhanced GABA_B receptor function occurs in DS patients, similarly to Ts65Dn mice (25), this may be one of the mechanisms that contributes to the high incidence of epilepsy in children with DS. Devinsky et al. reported a relatively preserved EEG alpha activity in young individuals with DS but an abnormal activity in older patients with dementia (56).

MOUSE MODELS

In **Ts65Dn**, **Ts1Cje**, **Ts1Rhr** and **Tc1** mice, while basal synaptic transmission in the DG is normal, LTP is impaired as a result of reduced activation of NMDA receptors ((103); (22); (21); (128)). After suppression of inhibition with picrotoxin, a GABA_A receptor antagonist, NMDA receptor-mediated currents are normalized and induction of LTP is restored, indicating that an excess of GABA_A receptor-mediated inhibition underlies impairment of LTP. Ts65Dn mice exhibit increased

G-protein-activated inwardly rectifying potassium channel 2 (*Girk2*), a protein that is encoded by a triplicated gene, in various cortical regions and hippocampus (86). In hippocampal neurons, *Girk* channels generate a GABA_B receptor-dependent slow inhibitory postsynaptic potential (114). Several lines of evidence suggest that an increase in *Girk2* gene-dosage may have a functional effect on the balance of excitatory and inhibitory neuronal transmission perturbed in DS models ((177); (36)). An excessive GABA_B receptor-mediated inhibition due to *Girk2* over-expression (25) may contribute to impair the induction of LTP in trisomic mice. In addition, since the formation of synapses is activity-dependent, an exaggerated inhibition through the GABA_A and GABA_B -GIRK signaling may contribute to disrupt spine formation. Seizures have never been reported in Ts65Dn mice. Based on the convulsant properties of GABA_B receptor agonists, Cortez and colleagues sought to establish whether these drugs might induce seizures (47). They found that such treatments produce clusters of extensor spasms in the Ts65Dn mouse that were associated with burst discharges in EEG recordings. Unlike the other mouse models, **Ts1Yah** mice exhibit enhancement of LTP, which is consistent with their better performance in the Morris water maze test (136).

2.5.4 Trisomic genes and dendritic/synaptic alterations

Dyrk1a, has been reported not only to influence neurogenesis but also dendritic development ((211); (84)). *Dyrk1A* regulates development of the dendritic trees of neurones and modulates the activity of the c-AMP response element-binding protein (CREB), which participates in signal transduction pathways involved in synaptic plasticity and neuronal differentiation. Moreover, *Dyrk1a* may modulate dendrite development by regulating vesicle trafficking which is dependent on *Dynamin1* (84), a GTPase putative substrate of *Dyrk1a* that plays a fundamental role in neurite outgrowth (42). Interestingly, mice with one functional copy of *Dyrk1a* (*Dyrk1a*^{+/-} mutants) display a brain size 30% smaller than that of wild-type mice, considerably smaller and less branched cortical pyramidal cells and behavioral defects (24). In humans, *DYRK1A* has been proposed to be

associated with microcephaly and mental retardation, given its localization to the minimal overlapping region observed in patients with partial monosomy 21 ((121); (124)). Transgenic mice over-expressing *Dyrk1a* exhibit altered synaptic plasticity associated to learning and memory defects (4). These studies with human and animal models, which are monoallelic or triallelic for *DYRK1A/Dyrk1a*, indicate that this gene is important in neural plasticity and necessary for the normal size and development of the brain in a dosage-sensitive way.

DSCR1 (Down syndrome critical region gene 1), also called myocyte-enriched calcineurin-interacting protein 1 (MCIP1) or calcipressin 1 (CSP1), acts as a negative regulator of calcineurin-mediated signaling. Calcineurin, that acts mainly by activation of the NFAT (nuclear factor of activated T-cells) transcription factor, plays several important roles in the brain, in particular modulates synaptic formation and function and memory development ((170); (118); (214)). Over-expression of DSCR1 in the brain of individuals with DS (69), and the learning defects in *Drosophila* due to over-expression of the *DSCR1* homologue (*nebula*) (38), suggest that DSCR1, through calcineurin-mediated signaling inhibition, may be involved in DS neurological defects. Notably, inhibition of calcineurin activity leads to increased NMDAR mean open time and opening probability (110), supporting the view that altered excitatory neurotransmission may arise from DSCR1 over-expression in the DS brain. Recently, it has been demonstrated that *DYRK1A* and DSCR1, both located in the critical DCR-1 region of human chromosome 21, act synergistically to block NFAT dependent transcription, suggesting a cooperation of two trisomic genes in the DS developmental phenotypes.

2.6 THERAPEUTIC APPROACHES IN THE DS MOUSE MODEL

The preceding sections showed that the cognitive impairment in individuals with DS is underpinned by a constellation of brain defects. Ideally, identification of the mechanisms underlying the abnormalities of brain development that characterize DS will provide a rational basis to devise

therapies that, by targeting specific cellular pathway/s, may correct the developmental defects of the DS brain. Though various laboratories are trying to unravel the causes of brain malfunctioning in DS, the molecular mechanisms underlying the DS neurological phenotype remain still obscure. Yet, various attempts have done to specifically rescue different facets of brain alterations in DS, by exploiting drugs and/or neurobiological factors that are known to have a positive impact on the brain of normal individuals.

Mouse models are the principal tool exploited for therapeutic approaches aimed at finding an effective treatment for DS. Historically, the choice of potential therapeutic agents in preclinical research involving mouse models for DS has followed four different strategies: 1) compensation for the putatively enhanced function of a trisomic gene product; 2) modulation the molecular target of a trisomic gene product; 3) compensation of an observed phenotype; and 4) modulation of a molecular target associated with a pathway thought to be perturbed by the overexpression of trisomic gene products. A recent review describes the therapeutic approaches attempted so far (48).

Target	Treatment (Mechanism of action)	Assessment	Outcome	Reference
Compensation for the putatively enhanced function of a trisomic gene				
Sod1/↑ ROS	Vitamin E (Antioxidant)	Water-escape radial arm maze	Rescued	Lockrow et al.
Sod1/↑ ROS	Vitamin E (Antioxidant)	Elevated-plus maze and Morris water maze	Rescued	Shichiri et al.
App	DAPT (γ- secretase inhibitor)	Morris water maze	Rescued	Netzer et al.
Dyrk1a	EGCG (polyphenol, found in large concentration in	Object recognition test	Rescued	Guedj et al.

	green and fairly specific DYRK1A inhibitor activity)			
Dyrk1a	EGCG (polyphenol, found in large concentration in green and fairly specific DYRK1A inhibitor activity)	LTP	Rescued	Xie et al.
Dyrk1a	Harmine (selective DYRK1A activity inhibitor)	Level of plasma homocysteine	Rescued	Noll et al.
Dyrk1a	Harmine (selective DYRK1A activity inhibitor)	Premature neuronal differentiation in cell culture	Rescued	Mazur-Kolecka et al.
Girk2 (?) / 5-HT1A / ↓ Serotonin Level (?)	Fluoxetine (selective serotonin reuptake inhibitor, Girk2-containing channel antagonist?)	Hippocampal neurogenesis	Rescued	Clark et al.
Girk2 (?) / 5-HT1A / ↓ Serotonin Level (?)	Fluoxetine (selective serotonin reuptake inhibitor, Girk2-containing channel antagonist?)	Contextual fear conditioning	Rescued	Bianchi et al.
Girk2 (?) / 5-HT1A / ↓ Serotonin Level (?)	Fluoxetine (selective serotonin reuptake inhibitor, Girk2-containing channel antagonist?)	Morris water maze	Failed	Heinin et al.
Girk2 (?) / 5-HT1A / ↓ Serotonin	Fluoxetine (selective serotonin reuptake inhibitor, Girk2-containing	Granule cells morphology	Rescued	Guidi et al.

	channel antagonist?)			
Girk2 (?)	Ethosuximide and Gabapentin (antiepileptic drugs with and without Girk2-containing channel antagonistic properties)	Morris water maze, and cued – or context – fear conditioning	Failed	Vidal et al.
Modulation the molecular target of a trisomic gene				
GABA _B receptors / Girk2	CGP55845 (GABA _B receptor antagonist)	Novel place recognition, novel object recognition, contextual fear, and LTP	Rescued	Kleschevnikov et al.
Noradrenergic receptors / App	I-DOPS and carbidopa	Contextual fear conditioning	Rescued	Salehi et al.
Brain-derived neurotrophic factor (BDNF)	Neurotropin (analgesic widely used in Japan for treatment of disorders associated with chronic pain, and show to stimulate the expression of BDNF)	Radial-arm water maze and BDNF expression levels	Rescued	Fukuda et al.
Reduced astrocytic release of Activity Dependent Neuroprotective Protein (ADNP) and Activity Dependent Neurotrophic Factor (ADNF).	NAPVSIPQ and SALLRSIPA (active fragments of ADNP and ADNF)	NR2A and NR2B Levels	Rescued	Vink et al.
Reduced astrocytic release of Activity Dependent Neuroprotective Protein (ADNP) and Activity	NAPVSIPQ and SALLRSIPA (active fragments of ADNP and ADNF)	Motor and sensory milestones	Rescued	Toso et al.

Dependent Neurotrophic Factor (ADNF).				
Increased GABA _A receptor-mediated neuronal inhibition	Picrotoxin (GABA _A receptor antagonist)	LTP	Rescued	Kleschevnikov et al.
Increased GABA _A receptor-mediated neuronal inhibition	Picrotoxin (GABA _A receptor antagonist)	LTP	Rescued	Costa and Grybko
Increased GABA _A receptor-mediated neuronal inhibition	PZT (GABA _A receptor antagonist)	Novel object recognition and LTP	Rescued	Fernandez et al.
Increased GABA _A receptor-mediated neuronal inhibition	PZT (GABA _A receptor antagonist)	Morris water maze	Rescued	Rueda et al.
Increased GABA _A receptor-mediated neuronal inhibition	Compound $\alpha 5$ IA (Inverse Agonist of $\alpha 5$ -containing GABA _A receptors)	Morris water maze and Expression of IEGs	Rescued	Braudeau et al.
Increased GABA _A receptor-mediated neuronal inhibition	Compound $\alpha 5$ IA (Inverse Agonist of $\alpha 5$ -containing GABA _A receptors)	Novel-object recognition and Morris water maze	Rescued	Braudeau et al.
Modulation of a molecular target through to be involved in a pathway perturbed by trisomic genes				
NMDA receptor (altered gating properties?)	Memantine (NMDA receptor antagonist)	Contextual fear conditioning	Rescued	Costa et al.
NMDA receptor (altered gating properties?)	Memantine (NMDA receptor antagonist)	LTD	Rescued	Scott-McKean and Costa
NMDA receptor (altered gating properties?)	Memantine (NMDA receptor antagonist)	Novel object recognition	Rescued	Lockrow et al.

NMDA receptor (altered gating properties?)	Memantine (NMDA receptor antagonist)	Morris water maze	Rescued	Rueda et al.
--	--------------------------------------	-------------------	---------	--------------

Table 1 - Summary of the preclinical studies in DS.

Table 1 clearly shows that it is possible to pharmacologically improve some of the morphofunctional defects of the trisomic brain and related behavior in mouse models of DS. Most of these studies have been carried out in adult animals with a certain degree of success. This achievement is of obvious relevance because it gives the demonstration that something can be done for adults with DS. It must be noted, however, that in spite of a certain degree of plasticity retained in adulthood, the overall organization of the brain mainly depends on events taking place during embryonic and perinatal life stages. Considering that one of the most severe defects of trisomy is early neurogenesis impairment, therapies to improve this defect should be started as soon as possible, otherwise the brain will have a permanently reduced asset of neurons. Likewise, the severe dendritic pathology due to trisomy should be restored as early as possible, in order to consent the establishment of appropriate neuronal connections.

2.7 RESTORATION OF THE SEROTONERGIC SYSTEM: A TOOL FOR IMPROVING BRAIN DEVELOPMENT IN DS?

2.7.1 Serotonergic system in normal brain development

Serotonin named also **5-hydroxytryptamine (5-HT)**, is a monoamine neurotransmitter initially found in the gastrointestinal tract and then, in the central nervous system of humans and animals. This was the first evidence that serotonin has a role in the maintenance of normal and abnormal brain function. The serotonergic system derives from the Raphe nuclei of the brainstem.

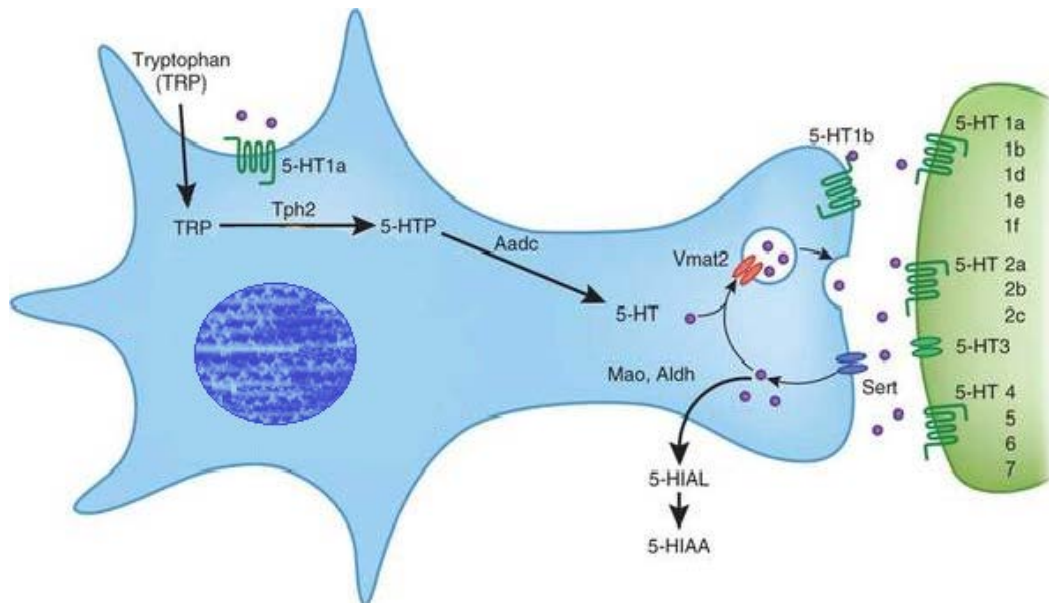


Figure 7- Modified from <http://dmangus.blogspot.it/2012/06/damsio-on-complexity-of-mind-and.html> - Release and reuptake of 5-HT. Serotonin activates the 5-HTRs on the post-synaptic cell membrane. It is recycled by SERT in the presynaptic terminal.

It innervates the entire brain, including the hippocampus, substantia nigra, striatum, nucleus accumbens, cerebellum and spinal cord. For this reason 5-HT has several functions in the CNS, such as the regulation of mood, appetite, circadian rhythms, learning and memory. The serotonin receptors belong to the 5-HT receptors family. They are both inhibitory and excitatory and are able to modulate the release of many neurotransmitters, including glutamate, GABA, dopamine, noradrenaline and acetylcholine. 5-HT receptors are classified in seven families: six are G protein-coupled receptors, and one is a ligand-gated ion channel. Another important protein which interacts with 5-HT is the serotonin transporter (SERT) that mediates the serotonin reuptake from the synaptic space to the presynaptic terminal in a sodium-dependent manner, thereby interrupting the action of the neurotransmitter (Fig. 7).

Serotonin can increase cell proliferation in the two major neurogenic regions of the telencephalon, the subventricular zone (SVZ) of the lateral ventricle and subgranular zone (SGZ) of the hippocampal dentate gyrus. Following either acute or chronic 5-HT depletion, a significant decrease in the number of newborn cells in the SVZ and SGZ has been evidenced (32). Administration of

agonists of serotonin receptors increases neurogenesis both in the SVZ and SGZ. Serotonin might increase cell proliferation by directly acting on receptors expressed by progenitor cells; this is consistent with evidence that serotonin receptor 1A (5-HT1A) might be expressed by neural stem cells (16).

In the developing fetal brain, neurotransmitters like amino acids and monoamines (serotonin, noradrenaline and dopamine) appear at a time before they assume their roles as neurotransmitters and have an established role in maturation of the central nervous system. All of the monoamine neurotransmitter systems are present relatively early, but in particular serotonin is likely present the earliest (201). In the human brain, serotonergic neurons are evident by 5 weeks of gestation and increase rapidly through the 10th week of gestation. The molecules serotonin, dopamine, γ -aminobutyric acid and taurine are critical for brain development because they promote the detailed wiring within the developing fetal brain. Serotonin appears to influence neurogenesis also in the adult brain, since depletion of serotonin decreases neurogenesis in the hippocampal dentate gyrus (32). During brain development serotonin plays also a role in dendritic development, including overall dendritic length, spine formation and branching in the hippocampus and cortex. In adult animals, removal of serotonin causes loss of dendrites, which may be reversed by treatment with 5-HT1A receptor agonists ((13); (201)).

2.7.2 Serotonergic system in DS

DS has long been associated with a loss of serotonin (5-HT) in postmortem brain (117). Whittle et al. (203) provide evidence for a reduction in serotonin, dopamine, γ -aminobutyric acid and taurine levels in the fetal DS brain. In vitro studies have demonstrated that decreases in the concentration of these compounds result in dysfunctional brain developmental events, such as generation, migration, and differentiation of neurons and glial cells (203). The trisomic gene S100 β appears to negatively regulate the outgrowth of serotonin terminals which may contribute to the reduced serotonin levels

in DS (201). Moreover, 5-HT_{1A} receptor peaks earlier in developing DS brains and decreases to below normal levels by birth (17). Similarly to individuals with DS, Ts65Dn mice exhibit a reduced expression of the 5-HT_{1A} receptor at neonatal life stages (28). The reduced expression of the 5-HT_{1A} receptor, in conjunction with the reduced 5-HT levels in fetuses and adults with DS (157), indicates a generalized impairment of the serotonergic transmission. Thus, in view of the role of 5-HT in neurogenesis, neuronal differentiation, dendritic development, axon myelination and synaptogenesis (201), the impairment of this transmitter system in DS, during the most critical time window of brain development, may be a key determinant of neurogenesis and neuron maturation impairment. If so, treatments that increase serotonin availability may prove useful in compensating for these defects.

2.8 PHARMACOTHERAPY WITH SELECTIVE SEROTONIN RE-UPTAKE INHIBITORS

Selective serotonin re-uptake inhibitors (SSRIs) increase the level of 5-HT in the synaptic cleft by inhibiting its reuptake. There is growing interest in antidepressant drugs because it has been found that multiple classes of antidepressant drugs, including selective serotonin reuptake inhibitors, increase neurogenesis in the DG and SVZ ((116); (172)) and can reverse or prevent the decrease in hippocampal volume of depressed subjects (115). This raises the possibility of pharmacologically improving neurogenesis with drugs that are usable by humans in order to correct brain pathologies characterized by reduced neuron production/neurodegeneration.

2.8.1 Fluoxetine modulates neurogenesis and dendritogenesis

Fluoxetine is an [antidepressant](#) of the [selective serotonin reuptake inhibitor](#) (SSRI) class widely used by adults and increasingly prescribed in children and adolescents (30) to treat a wide spectrum of mood disorders. It has no patent aversive effects on somatic development ((15); (61)). It was first

used more than ten years ago, and soon after its introduction it became the most prescribed agent for depression in many countries.

Fluoxetine was shown to be effective for depression in 6-week long double-blind controlled trials, where it also alleviated anxiety and improved sleep. The peculiar pharmacokinetics of fluoxetine with its brain levels rising extremely slowly over at least the first 5 weeks of treatment makes it unclear whether the 20-mg/day optimal dose established in the short term (6-8 weeks) trials is applicable for the longer term supportive treatment.

Fluoxetine and neurogenesis

A first study in adult (2-5 months old) Ts65Dn mice examined the effect of chronic treatment (28 days) with fluoxetine (5 mg/kg). They found that trisomic mice had a reduced neurogenesis in the DG and that treatment with fluoxetine restored neurogenesis (43). Since this study did not examine the effect of treatment on behavior it was not possible to establish whether the neurogenesis increase was followed by an improvement of hippocampus-dependent memory functions.

More recently, Bianchi et al. (28) treated neonate Ts65Dn mice with fluoxetine for 13 days, from P2 to P15. This strategy was adopted because in mice more than 80% of the hippocampal granule cells are born in the first two postnatal weeks. Treatment with fluoxetine completely restored proliferation in both the DG and SVZ, the source of cortical cells during the prenatal and perinatal period. This proliferative effects of fluoxetine in the SGZ and SVZ were not accompanied by a higher death rate. Moreover, the short-term effects of fluoxetine on cell proliferation were followed by a positive and enduring effect on cell survival, with an expansion of the pool of cycling cells. Importantly, in Ts65Dn mice not only did fluoxetine increase cell proliferation and survival but it also affected the differentiation program, increasing the percentage of cells that acquired a neuronal phenotype, thereby fully restoring neuronogenesis. All this evidence indicates that treatment with fluoxetine is able to fully restore neurogenesis in Ts65Dn mice by increasing the number of actively dividing cells, increasing their survival rate, and favoring acquisition of a neuronal phenotype. In

agreement with this concept, also the number and the density of granule cells were restored by fluoxetine (28). Increases in neurogenesis after fluoxetine administration require the activation of 5-HT1A receptors (166), which is in agreement with evidence that 5-HT1A receptor antagonists decrease cell proliferation in the dentate gyrus (151). Thus, the 5-HT1A receptor plays a key role in the regulation of neurogenesis. Defective 5-HT1A receptor expression in precursor cells of Ts65Dn mice may underlie proliferation impairment: this is supported by the finding that in Ts65Dn mice treatment with fluoxetine restored the expression of the 5-HT1A receptor and this effect was accompanied by rescue of proliferation. Brain-derived neurotrophic factor (BDNF) plays a key role in hippocampal neurogenesis by increasing cell survival and neuronal differentiation (163) and chronic treatment with antidepressants increases its expression (115). In Ts65Dn mice fluoxetine restored BDNF expression, suggesting that this may be the mechanism whereby treatment increased the survival of newborn cells and restored the differentiation program. Consistently with previous evidence (164), contextual fear conditioning, a task that is considered to involve in addition to the amygdala also hippocampus-dependent memory functions (138), was impaired in trisomic mice. After treatment with fluoxetine the performance of trisomic mice became similar to that of euploid mice, showing that the neurogenesis increase was functionally effective (28).

Fluoxetine and dendritic architecture

In view of the role played by serotonin in neuron maturation, it is likely that serotonin reuptake inhibitors, such as fluoxetine, exert their positive effects on the DS brain by improving/restoring dendritic maturation and connectivity in addition to increasing neurogenesis. This possibility is strengthened by evidence that, in the rat hippocampus, fluoxetine modulates the cytoskeletal microtubular systems, which plays a fundamental role in dendritic and axon remodeling (27). In addition, treatment with fluoxetine triggers pyramidal dendritic spine synapse formation in rat hippocampus (83) and renormalizes dendrite atrophy of hippocampal neurons. Finally, chronic

treatment with fluoxetine in normal mice accelerates the maturation of immature granule neurons, with an increase in dendritic length (196).

3. MATERIALS AND METODS

3.1 *Colony*

Female Ts65Dn mice carrying a partial trisomy of chromosome 16 (154) were obtained from Jackson Laboratories (Bar Harbour, ME, USA) and maintained on the original genetic background by mating them with C57BL/6JEi x C3SnHeSnJ (B6EiC3) F1 males. Animals were karyotyped using real-time quantitative PCR (RTqPCR) as previously described (111). Genotyping was validated with fluorescent in situ hybridization (FISH) (181).

The day of birth was designed as postnatal day (P) 0. A total of 132 mice were used. The animals' health and comfort were controlled by the veterinary service. The animals had access to water and food ad libitum and lived in a room with a 12:12 hour dark/light cycle. Experiments were performed in accordance with the Italian and European Community law for the use of experimental animals and were approved by Bologna University Bioethical Committee. In this study all efforts were made to minimize animal suffering and to keep the number of animals used to a minimum.

3.2 *Experimental protocol*

Euploid (n = 34) and Ts65Dn (n = 29) mice received a daily subcutaneous injection (at 09:00–10:00 h) of fluoxetine (Sigma-Aldrich, St. Louis, MO, USA) in 0.9% NaCl solution from P3 to P15 (dose: 5 mg/kg from P3 to P7; 10 mg/kg from P8 to P15). We chose a maximum 10 mg/kg dose because, as a result of the extremely short half-life of fluoxetine in rodents compared with humans, a daily 10 mg/kg dose is thought to produce a brain concentration of a magnitude similar to that of 20–60 mg taken daily by humans ((33); (55)). Age-matched euploid (n = 34) and Ts65Dn (n = 35) mice were injected with the vehicle (Fig. 8). Each treatment group had approximately the same composition of males and females. On P45, animals were deeply anesthetized with ether and killed. A first group of

animals (n = 8 for each experimental condition) was transcardially perfused with ice-cold phosphate-buffered saline (PBS) followed by a 4% solution of paraformaldehyde in PBS. Brains were stored in the fixative for 24 h, cut along the midline and placed in a 20% sucrose in phosphate buffer solution for an additional 24 h.

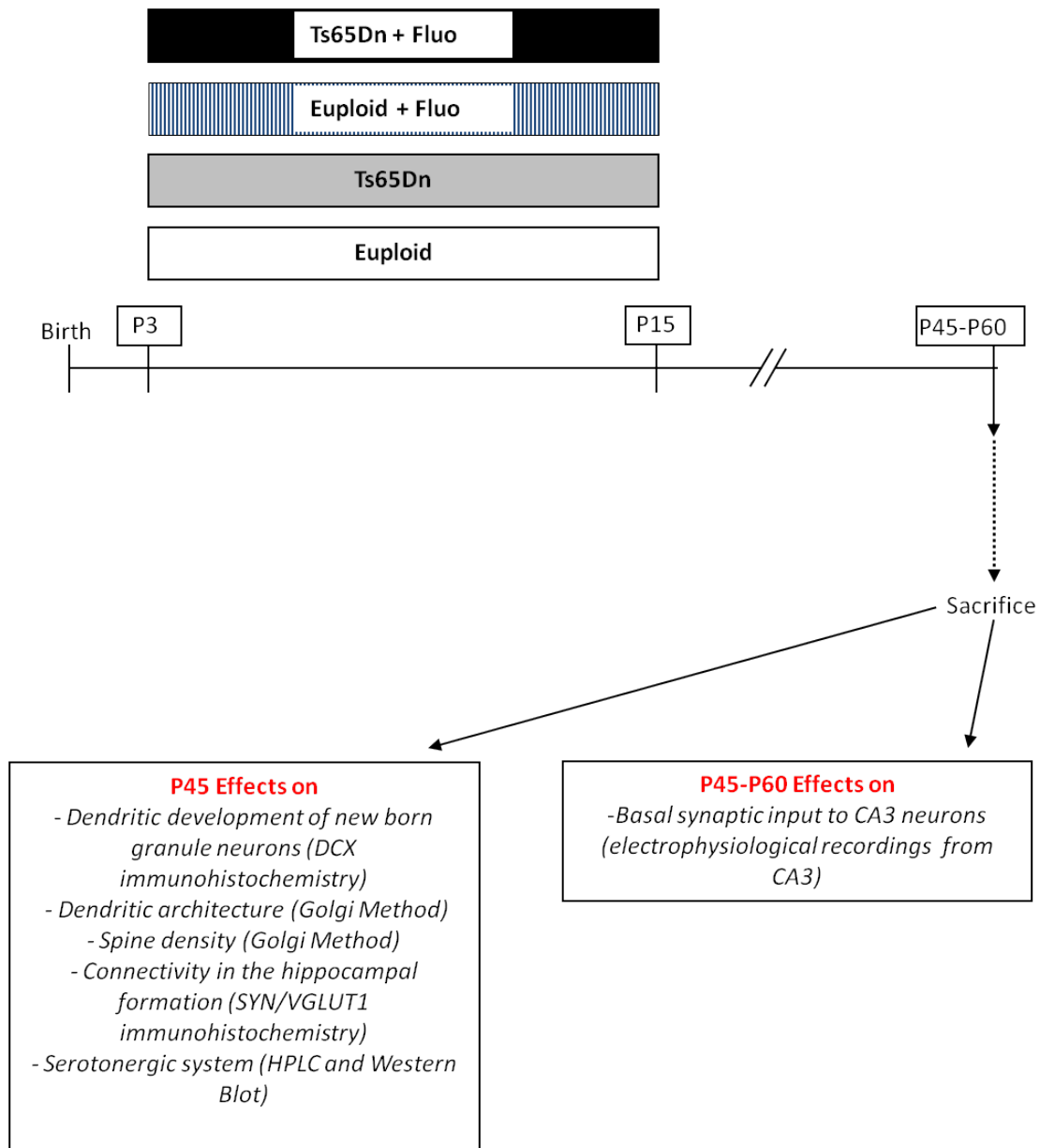


Figure 8 - Outline of the experimental protocol

Hemispheres were frozen and stored at -80°C. The left and right hemispheres were cut with a freezing microtome in 30- μ m-thick coronal sections that were serially collected in antifreeze

solution containing sodium azide. Sections from the right hemisphere were used for doublecortin (DCX) immunohistochemistry and polysialylated neural cell adhesion molecule (PSA-NCAM), sections from the left hemisphere were used for synaptophysin (SYN) and vesicular glutamate transporter 1 (VGLUT1) immunohistochemistry and for Down syndrome cell adhesion molecule (DSCAM) immunohistochemistry.

A second group of animals (n = 6–9 for each experimental condition) was not perfused, the brain was quickly removed, cut along the midline, rinsed in PBS and Golgi stained, as described below. A third group of animals (n = 10 for each experimental condition) was not perfused, the brain was quickly removed, the hippocampal region of each hemisphere was dissected and kept at -80°C. The hippocampus of one side was used for either Western blotting (n = 5 for each experimental condition) or RT-qPCR analysis (n = 5 for each experimental condition) and the hippocampus of the other side was used for analysis of serotonin levels (n = 5 for each experimental condition). Two additional groups of untreated animals aged 2 days (four euploid and five Ts65Dn mice) and 15 days (6 euploid and 5 Ts65Dn mice) were used to examine the expression of the 5-HT1A receptor in the hippocampal region. Animals belonging to a fourth group of animals (n = 4–8 for each experimental condition) were used for electrophysiological recordings from field CA3.

3.3 *Histological procedures*

DCX immunohistochemistry. One out of six free-floating sections from the DG was processed for DCX immunohistochemistry. Sections were permeabilized with 0.1% Triton X-100 in PBS for 30 minutes and subsequently endogenous peroxidase activity was inhibited using a methanol/H₂O₂ 0.3% solution for 30 minutes. Sections were incubated overnight at 4°C with a primary antibody anti-DCX (goat polyclonal, Santa Cruz Biotechnology, Santa Cruz, CA, USA) diluted 1:100. Sections were then incubated for 1 h at room temperature with a biotinylated anti-goat IgG secondary antibody (dilution 1:200, Vector Laboratories Inc., Burlingame, CA, USA) and thereafter

incubated for 1 h with VECTASTAIN® ABC kit (Vector Laboratories). Detection was performed using DAB kit (Vector Laboratories).

Golgi method. Brains were Golgi stained using the FD Rapid Golgi Stain™ Kit (FD NeuroTechnologies, Inc., Columbia, MD, USA). Brains were immersed in the impregnation solution containing mercuric chloride, potassium dichromate, and potassium chromate, and stored at room temperature in darkness for 3 weeks. Hemispheres were cut with a microtome in 90-µm-thick coronal sections that were mounted on gelatin-coated slides and were air dried at room temperature in the dark for 1 day. After drying, sections were rinsed with distilled water and subsequently stained in a developing solution (FD Rapid Golgi Stain Kit).

SYN, VGLUT1 DSCAM immunohistochemistry. Free-floating sections (n = 3–4 per animal) from the hippocampal formation were submitted to double fluorescence immunohistochemistry for SYN and VGLUT1 or DSCAM immunohistochemistry. For SYN and VGLUT1 immunohistochemistry, sections were incubated for 48 h at 4°C with mouse monoclonal anti-SYN (SY38) antibody (Millipore Bioscience Research Reagents, Merck Millipore, Billerica, MA, USA) and rabbit polyclonal anti-VGLUT1 (Abcam, Cambridge, UK, Europe) antibody both diluted 1:1000. Sections were then incubated overnight at 4°C with a DyLight-conjugated goat anti-mouse IgG (Thermo Scientific, Rockford, IL, USA) and a RRX-conjugated donkey anti-rabbit IgG (Jackson Laboratory, Bar Harbor, ME, USA) both diluted 1:100. For DSCAM immunohistochemistry, sections were incubated overnight at 4°C with a primary antibody anti-DSCAM (generous gift from Dr Maria Luz Montesinos) (9) diluted 1:50. Sections were then incubated for 1 h at room temperature with a CY3-conjugated donkey anti-rabbit (Jackson Laboratory) diluted 1:200.

PSA-NCAM immunohistochemistry. Free-floating sections (n =3–4 per animal) were permeabilized with 0.1% Triton X-100 in PBS, blocked for 1 h in 1.5% Goat Serum in 0.1% Triton X-100 and PBS, incubated overnight at 4°C with an anti-Polysialic Acid-NCAM mouse monoclonal antibody (Chemicon), diluted 1:100. Sections were then incubated for 2 h with a peroxidase-conjugated AffiniPure goat anti-Mouse IgM secondary antibody (Jackson ImmunoResearch), diluted 1:200, reacted with diaminobenzidine and rinsed in water, mounted on glass slides and dehydrated with a gradient of alcohols, cleared and cover slipped.

3.4 Western blotting

Total proteins from the hippocampal formation were obtained by homogenization and protein concentration was estimated by the Lowry method. Proteins (20 µg) were subjected to electrophoresis on a 4%–20% Mini-PROTEAN® TGX™ Precast Gel (Bio-Rad) and transferred to a Hybond ECL nitrocellulose membrane (Amersham Life Science, Arlington Heights, IL, USA). The following primary antibodies were used: anti-SYN (1:1000, Millipore Bioscience Research Reagents); anti-DSCAM (1:500, a gift from Dr Maria Luz Montesinos); anti-VGLUT1 (1:1000, Abcam) and anti- GAPDH (1:5000, Sigma, St Louis, MO, USA) antibodies. Densitometric analysis of digitized images was performed with Scion Image software (Scion Corporation, Frederick, MD, USA), and intensity for each band was normalized to the intensity of the corresponding GAPDH band.

3.5 High-performance liquid chromatography (HPLC)

The left hippocampus was homogenized with ultrasonic cell disruptor in Acapulco buffer solution (methanol-acetonitrile-50 mM phosphate buffer, pH 2.8, 15:8:77, containing 200 mg/L of sodium dodecylsulphate). One volume of homogenate was diluted in 3 vol. of water and 50-mL portions of

clear supernatants were directly injected into a HPLC system, as described by Grossi et al (79). Protein levels in the sampled tissue were evaluated by Lowry method. The measured amounts of 5-HT and 5-hydroxyindoleacetic acid (HIAA) were expressed as pg/ng protein.

3.6 Real-time reverse transcriptase quantitative PCR (RT-qPCR)

Total RNA was extracted from the hippocampus of the right hemisphere with TriReagent (Sigma-Aldrich) according to the manufacturer's instructions. Complementary DNA (cDNA) synthesis was achieved with 1.0 mg of total RNA using the iScript cDNA synthesis kit (Bio-Rad, Hercules, CA, USA) according to the manufacturer's instructions. The used primer sequences are as follows: (i) brain-derived neurotrophic factor (BDNF) (NM_007540.4), forward 5'-GTGACAGTATTAGCGAGTG-39 and reverse 5'-GCCTTCCTTCGTGTAACC-39; (ii) 5-hydroxytryptamine (serotonin) receptor 1A (5-HT1A) (NM_008308), forward 5'-ACAGGGCGGTGGGGACTC-3' and reverse 5'-CAAGCAGGCGGGGACATAGG-3'; (iii) solute carrier family 6 (neurotransmitter transporter serotonin alias SERT) (NM_010484.2), forward 5'-GATCCCTGCTCACACTGACATC-3' and reverse 5'-CCATAGAACCAAGACACGACGAC-3'; (iiii) glyceraldehyde-3-phosphate dehydrogenase (GAPDH) (NM_008084.2), forward 5'-GAACATCATCCCTGCATCCA-3' and reverse 5'-CCAGTGAGCTTCCCGTTCA-3'.

Real-time PCR was performed using a SYBR *Premix Ex Taq kit* (Takara, Shiga, Japan) according to the manufacturer's instructions in an iQ5 real-time PCR detection system (Bio-Rad). Fluorescence was determined at the last step of every cycle. Real-time PCR assay was done under the following universal conditions: 2 minutes at 50°C, 10 minutes at 95°C, 50 cycles of denaturation at 95°C for 15 s, and annealing/extension at 60°C for 1 minute. Quantifications were normalized using endogenous control GAPDH. Relative quantification was performed using the $\Delta\Delta C_t$ method.

3.7 *Patch-clamp experiments: preparation of slices*

Mice were anaesthetised by inhalation of isoflurane (Merial Italia, Milan, Italy) and decapitated. The brain was quickly extracted under hypothermic conditions and submerged in an ice-cold artificial cerebro-spinal fluid (ACSF) composed of (in mmol l⁻¹): 125 NaCl, 3 KCl, 24 NaHCO₃, 1.25 KH₂PO₄, 1.2 MgSO₄, 2 CaCl₂, 10 D-glucose (pH 7.4 by saturation with 95% O₂, 5% CO₂). Two coronal cuts were made, in order to remove the anterior half and the occipital pole of the brain, and the piece thus obtained was laid on the posterior section plane. The tissue was blocked on the stage of a Microslicer DTK-1000 vibratome (Dosaka, Kyoto, Japan) using cyanoacrylate glue. During the sectioning procedure the tissue was submerged in an ice-cold (~ 1°C) cutting solution containing (in mmol l⁻¹): 130 K-gluconate, 15 KCl, 20 N-2-hydroxyethyl piperazine-N-2-ethanesulphonic acid (HEPES), 0.2 EGTA, 11 D-glucose (pH 7.4 with KOH). The use of this high-K⁺ solution was found to improve neuron viability (Stéphane Dieudonné, unpublished results). 350 micron-thick sagittal sections across the dorsal hippocampus were cut, then rinsed in ACSF and transferred to an incubation chamber filled with the same solution (continuously bubbled with 95% O₂, 5% CO₂). The slices were kept submerged in the incubation chamber at room temperature for at least one hour before the recording was started.

3.8 *Patch-clamp experiments: voltage-clamp recordings, drugs, and data analysis*

Whole-cell, patch-clamp recordings from CA3 pyramidal neurons were carried out on acute slices of the dorsal hippocampus obtained as described above (Figure 9A). The experimental set-up employed and the basic procedures followed were the same as described by Castelli et al (34). Briefly, cells were visualized by means of an upright microscope (Axioskop 2 FS; Zeiss, Oberkochen, FRG) equipped with a 660 water-immersion objective lens, differential contrast optics, and a near-infrared charge-coupled device (CCD) camera. Slices were perfused with ACSF (continuously bubbled with 95% O₂, 5% CO₂) at a rate of about 1.5 ml/min. Patch pipettes were

fabricated from thick-wall borosilicate glass capillaries (CEI GC 150–7.5; Harvard Apparatus, Edenbridge, UK) by means of a Sutter P-87 horizontal puller (Sutter Instruments, Novato, CA, USA).

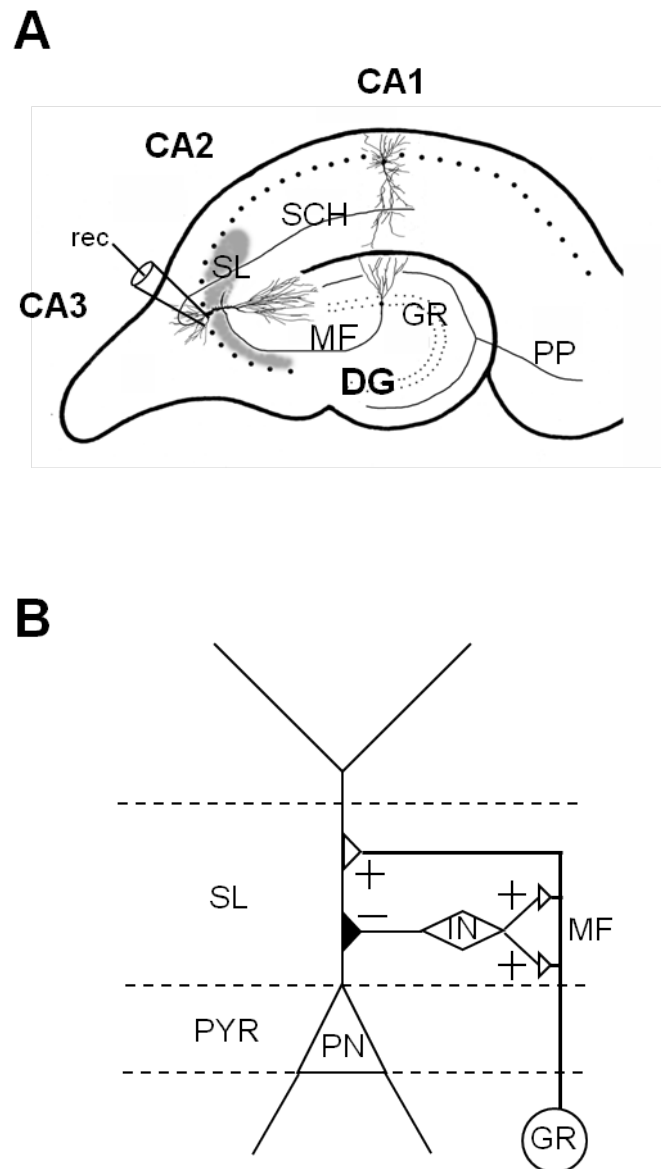


Figure 9 - A: Schematic drawing of a section across the hippocampal formation showing the major intrinsic connections. Patch clamp recording (rec) of miniature synaptic potentials were carried out from pyramidal neurons of field CA3. The area occupied by the mossy fiber terminals in the stratum lucidum of field CA3 is indicated in gray. B: Mossy fiber circuitry in CA3. Mossy fibers establish excitatory synapses (+) with pyramidal neurons and inhibitory synapses (-) with the pyramidal neurons. Inhibitory interneurons establish inhibitory synapses (-) with the pyramidal neurons. Abbreviations: CA1-3, hippocampal fields; DG, dentate gyrus; IN, inhibitory interneuron; MF, mossy fibers; PN, pyramidal neuron; PP, perforant pathway; PYR, pyramidal layer; SCH, Shaffer collaterals; SL, stratum lucidum.

The pipette solution contained (in mmol/l): 150 CsF, 4 CsCl, 2 MgCl₂, 10 N-2-hydroxyethyl piperazine-N-2-ethanesulphonic acid (HEPES), 10 ethylene glycol-bis (b-aminoethylether)

N,N,N',N'-tetraacetic acid (EGTA), 2 adenosine 5'-triphosphate (ATP)-Na₂, 0.2 guanosine 5'-triphosphate (GTP)-Na, 2.5 lidocaine N-ethyl bromide (QX-314) (pH adjusted to 7.2 with CsOH). The patch pipettes had a resistance of 3–5 MΩ when filled with the above solution. Tight seals (<5 GΩ) and the whole cell configuration were obtained by suction according to the standard technique (see (34)).

Voltage-clamp recordings of Na⁺ currents were performed at room temperature (21–22 °C) by means of an Axopatch 200B patch-clamp amplifier (Axon Instruments, Foster City, CA, USA). Series resistance (R_s) was evaluated on line by canceling the whole-cell capacitive transients evoked by -5-mV voltage square pulses with the amplifier built-in compensation section, and reading out the corresponding values. R_s was normally 5–12 MΩ and always <20 MΩ, and was compensated by ~90%. Current signals were acquired in gap-free modality with a personal computer interfaced to a Digidata 1322A interface (Axon Instr.) using the Clampex program of the pClamp 8.2 software package (Axon Instr.). Current signals were low-pass filtered at 5 kHz and digitized at 20 kHz. All drugs applied were preliminarily dissolved in concentrated aliquots and stored at -20°C, then re-dissolved to the final concentrations in ACSF and delivered to the recorded cells via the general perfusion. Tetrodotoxin (TTx) was purchased from Alomone Labs. (Jerusalem, Israel), 1(S),9(R)-(2)-bicuculline methiodide and QX-314 were purchased from Sigma-Aldrich S.r.l.(Milan,Italy), and 2,3-dioxo-6-nitro-1,2,3,4-tetrahydrobenzo[f]-quinoxaline-7-sulfonamide (NBQX), D-(-)-2-amino-5-phosphonopentanoic acid (APV), and (2S,2'R,3'R)-2-(2',3'-dicarboxycyclopropyl) glycine (DCG-IV) from Tocris (Bristol, UK). mEPSCs and mIPSCs, recorded under the conditions specified in the Results, were off-line detected using an automated threshold routine in the LabView environment written and kindly provided by Dr. G. Biella (University of Pavia). All detected events were also visually inspected one-by-one for confirmation or rejection.

3.9 Measurements

Neuron sampling. Series of sections across the whole rostro-caudal extent of the DG were used for reconstruction of DCX-positive and Golgi stained neurons. DCX-positive neurons were sampled in the inner part of the granule cell layer, close to the subgranular zone (Figure 10). The Golgi method casually impregnates a few neurons among a given population and allows one to sample relatively isolated neurons. Golgi-stained neurons were sampled from the outer part of the granule cell layer (Fig. 10). The total number of DCX-positive sampled neurons was 29–52 per animal and the number of sampled Golgi-stained neurons was 10–16 per animal. Only well-impregnated neurons were chosen for the histological analysis. The drawings were made on coded slides so that the drawer was not aware of the animal's treatment.

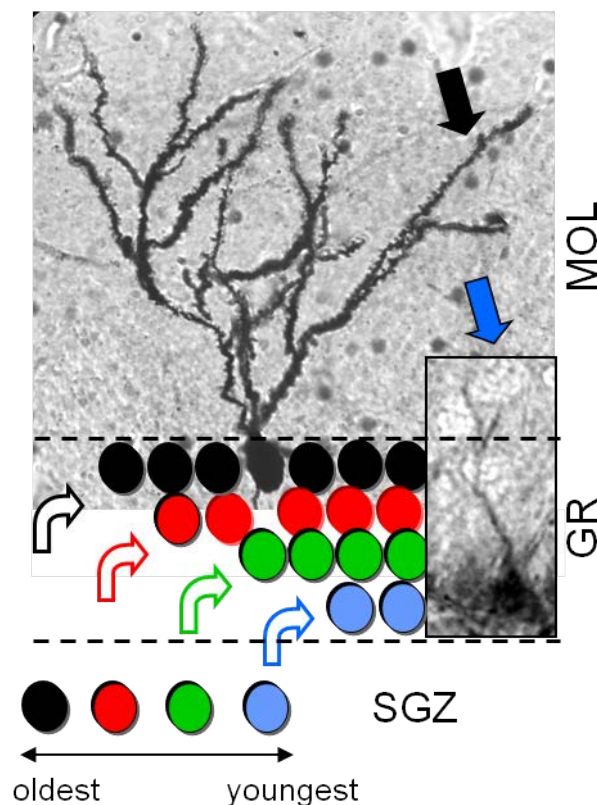


Figure 10 - New granule cells are generated from progenitor cells residing in the subgranular zone (SGZ). The oldest granule cells (black) occupy the outer portion of the granule cell layer (GR) and later born cells are added according to an outside-inside pattern. The photomicrographs show a mature Golgi-stained cell (black arrow) in the outermost portion of the GR and a young doublecortin (DCX)-positive granule cell (blue arrow) in the innermost portion of the GR. The dendrites of the mature granule cells occupy the whole molecular layer (MOL) while those of the young granule cells reach only the innermost portion of this layer.

Measurement of the dendritic tree. The following systems were used: (i) light microscope (Leitz, Hexagon Metrology GmbH, Wetzlar, Germany, Europe) equipped with a motorized stage and focus control system; (ii) color digital video camera attached to the microscope; and (iii) Image Pro Plus (Media Cybernetics, Silver Spring, MD 20910, USA) with the StagePro module for controlling the motorized stage in the x, y and z directions, as primary software. Dendritic trees of DCX-positive and Golgi-stained granule cells of the DG were traced with a dedicated software, custom-designed for dendritic reconstruction (Immagini Computer, Milan, Italy), interfaced with Image Pro Plus. The dendritic tree was traced live, at a final magnification of 500x, by focusing into the depth of the section.

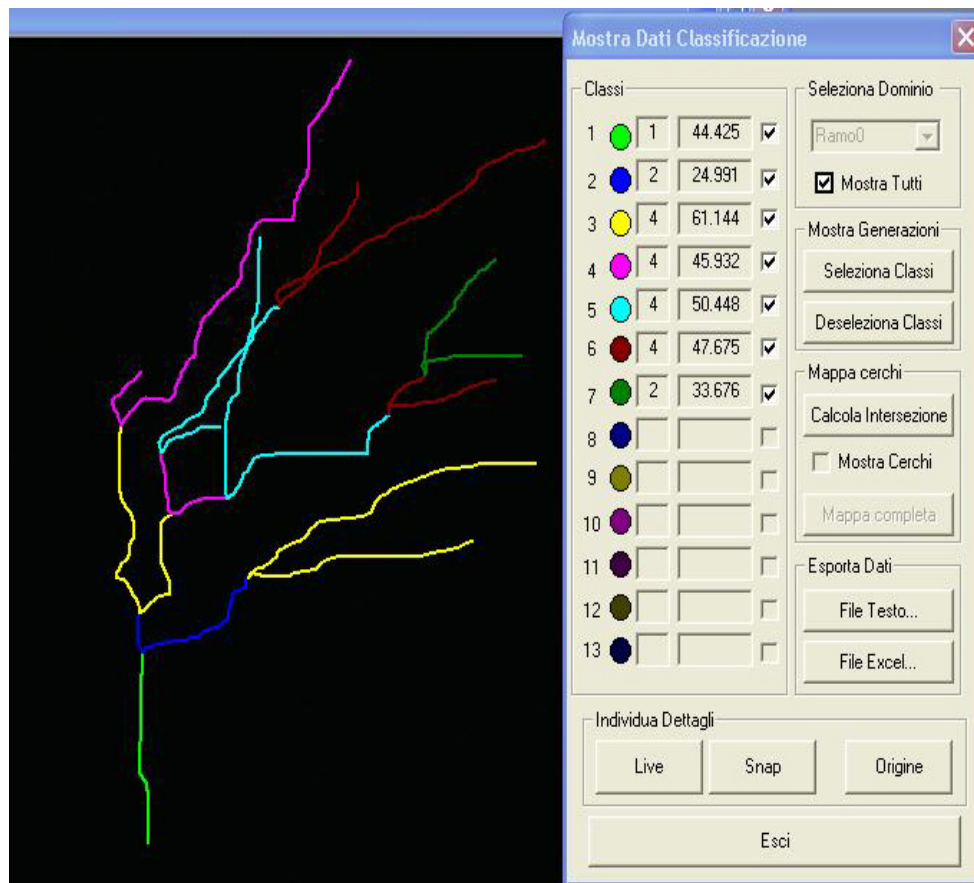


Figure 11 - Computerized reconstruction of granule cell dendrites. Dendrites were traced in a centrifugal direction. Numbers indicate the different dendritic orders (marked by the software with different colors).

The operator starts with branches emerging from the cell soma and after having drawn the first parent branch goes on with all daughter branches of the next order in a centrifugal direction (Fig.

11). At the end of tracing, the program reconstructs the number and length of individual branches, the mean length of branches of each order, and total dendritic length.

Spine density. In Golgi-stained sections, spines of granule cells were counted using a 100x oil immersion objective lens. Spine density values were obtained from dendritic segments in the inner and outer half of the molecular layer. For each neuron, three segments were analyzed in the outer and inner half of the molecular layer, respectively. For each animal, spines were counted in the same neuron population used for dendritic reconstruction. The length of each dendritic segment was determined by tracing the dendritic shaft and the number of spines was counted manually. The linear spine density was calculated by dividing the total number of spines by the length of the dendritic segment. Spine density was expressed as number of spines per 100 μm dendrite.

The axons of the granule cells project to field CA3 and make synaptic contacts with the thorny excrescences located on the proximal part of the dendritic shaft of CA3 pyramidal neurons. The thorny excrescences are protrusions on the dendritic shaft and are formed by 2–5 spine-like structures. Spines of CA3 pyramidal neurons were counted using a 100x oil immersion objective lens. The length of the shaft covered by spinous excrescences was determined and the number of individual spines of the thorny excrescences was counted manually. The linear spine density was calculated by dividing the total number of spines by the length of the dendritic segment. Spine density of CA3 pyramidal neurons was expressed as number of spines per 20 μm dendrite.

DSCAM levels in the molecular layer of the DG. Intensity of DSCAM IR in the molecular layer of the DG was determined by optical densitometry. Fluorescence images were captured using a Nikon Eclipse E600 microscope (see above). The optical density (OD) was evaluated in a box of 1600 μm^2 randomly placed at six different sites in the molecular layer of the upper blade of the DG. The OD of the sampled regions was corrected by the background.

Connectivity in the hippocampal formation. To study innervation of granule cell dendrites and of apical dendrites of CA3 pyramidal neurons, intensity of SYN immunoreactivity (IR) was determined in the molecular layer of the DG and in the stratum lucidum of field CA3, by optical densitometry of immunohistochemically stained sections (n = 3–4 per animal). In the stratum lucidum of field CA3 the IR of VGLUT1 was also evaluated. Fluorescence images were captured using a Nikon Eclipse E600 microscope equipped with a Nikon Digital Camera DXM1200 ATI System (Nikon Instruments Inc., Melville, NY, USA). Densitometric analysis of SYN was carried out using the Nis-Elements Software 3.21.03 (Nikon, Melville, NY, USA). A box of 490 μm^2 was used and placed in the inner, middle and outer third of the molecular layer of the upper blade of the DG and in the stratum lucidum of CA3. Six measurements were taken for each region. For each image, the intensity threshold was estimated by analyzing the distribution of pixel intensities in the image areas that did not contain IR. This value was then subtracted to calculate IR of each sampled area.

Glutamatergic innervation of the hippocampal formation. Dual-channel confocal microscopy was used to study co-localization of SYN with VGLUT1 in the molecular layer of the DG and in the stratum lucidum of field CA3. Sections were scanned with Nikon Ti-E fluorescence microscope coupled with A1R confocal system (Nikon). The lasers were: Multi-Ar (457/488/514) with exciting wavelengths for DyLight 488 and 561 diode-pumped solid state laser (DPSS) with exciting wavelengths for RRX. The conditions for co-localization analysis were: the objective was an oil immersion x60 objective [numerical aperture (NA) 1.4]; laser power was kept low in order to avoid photobleaching; the zoom factor was 6; and software Nis-Elements AR 3.2 was used and image size was 512 x 512 pixels. For each image, the intensity thresholds were estimated by analyzing the distribution of pixel intensities in the image areas that did not contain IR. This value, the

background threshold, was then subtracted, and the green-red co-localization coefficient was calculated.

Density of synaptophysin immunoreactive puncta in the stratum lucidum of field CA3. From the same sections indicated above, we evaluated the density of individual puncta exhibiting SYN immunoreactivity in the stratum lucidum (image size; 512x512 pixels; three images per section).

Thickness of the mossy fiber bundle. The axons of the granule cells, the mossy fibers, can be visualized with PSA-NCAM immunohistochemistry ((171); (165)). In each sampled section, the area of the region occupied by the mossy fibers in field CA3 was first measured by tracing its contour. The length of this area was then obtained by tracing a line at its border with the pyramidal layer of field CA3. The thickness of the mossy fiber system increases, progressing from the hilus of the dentate gyrus toward field CA2. To estimate the mean thickness of the system over field CA3, we divided the area occupied by mossy fibers by its length. Measurements of individual sections were averaged in each animal to obtain the mean thickness of the mossy fiber terminal field.

Statistical analysis. Results are presented as the mean \pm standard deviation (SD) of the mean. Data from single animals were the unity of analysis. Statistical testing was performed with analysis of variance (ANOVA) followed by *post hoc* comparisons with Duncan's test or Bonferroni test. A probability level of $P < 0.05$ was considered to be statistically significant.

4. RESULTS

4.1 *Effect of fluoxetine on the dendritic tree of newborn granule cells in euploid and Ts65Dn mice*

Granule cells are derived from precursors in the subgranular zone of the DG that migrate from the place of birth to the overlying granule cell layer. In rats and mice, only 20% of the granule cells are born before birth and most of the remaining 80% are born in the first two postnatal weeks, with a peak at postnatal day 7 ((7); (10); (168)). At variance with neurons forming the neocortex, granule cells migrate according to an “outside-inside” pattern. Namely, the oldest neurons populate the outer part of the granule cell layer and the youngest populate the inner part (see Fig. 10).

DCX is a microtubule-associated phosphoprotein selectively located in the periphery of the soma with a pattern that overlaps microtubule distribution (49). DCX is expressed widely in migrating neuroblasts and differentiating neurons. Dendritic morphology of newborn granule cells can be analyzed with immunohistochemistry for DCX, taking advantage of the expression of this protein in the cytoplasm of immature neurons during the period of neurite elongation (from 1 to 4 weeks after neuron birth). In view of the time course of DCX expression in the granule cells, DCX-positive cells present in P45 animals are, necessarily, cells born after P15, that is, in the month that followed treatment. To establish the effect of genotype and treatment on dendritic development of granule cells born after cessation of treatment, we examined the dendritic morphology of DCX-positive cells.

In agreement with the morphogenesis of the granule cell layer, DCX-positive cells were located in the innermost portion of the layer, close to the hilus (Fig. 9). In view of their young age, these cells exhibited a dendritic tree with an immature pattern, characterized by a relatively low number of short processes that reached the inner but not the outer part of the molecular layer (Fig. 12A–D). Fig. 12E shows that DCX-positive cells exhibited a range of morphologies, with branches of low orders only (Fig. 12E, neuron “a”), branches of low and intermediate order (Fig. 12E, neuron “b”)

and branches of low, intermediate and high order (Fig. 12E, neuron “c”). Fig. 12F shows that in untreated Ts65Dn mice, DCX-positive cells of each category had fewer processes than in their euploid counterparts. For instance, while in euploid mice most neurons of category “a” had branches of order 2 or 3, in untreated Ts65Dn mice there were numerous cells of category “a” with only a single process. Observation of the neurons reported in Fig. 12A–H shows that treatment with fluoxetine increased the number of branches in neurons of each category both in euploid (Fig. 12C,G) and Ts65Dn (Fig. 12D,H) mice.

We examined the total dendritic length, total number of segments and mean segment length. The latter was obtained by dividing the total dendritic length by the total number of branches. We found that Ts65Dn mice had a shorter dendritic length (-32%; Fig. 12I) and a reduced number of segments (-48%; Fig. 12J) than euploid mice. In contrast, the mean segment length was greater in Ts65Dn than in euploid mice (+33%; Fig. 12K). In euploid mice, treatment with fluoxetine slightly increased the total dendritic length (+20%), with no change in segment size and with a marginally significant increase in the number of segments (Fig. 12I–K). Importantly, in treated Ts65Dn mice the dendritic length (Fig. 12I) and the number of segments (Fig. 12J) underwent a notable increase (+85% and +152% respectively), while the mean segment length underwent a reduction (-28%; Fig. 12K). A comparison between untreated euploid mice and Ts65Dn mice treated with fluoxetine showed that trisomic mice had more segments (although this effect was only marginally significant) (Fig. 12J) and a greater total dendritic length (+30%; Fig. 12I), indicating that not only was dendritic size restored by treatment but it became even greater than that of euploid mice.

To dissect the effects of trisomy and treatment on details of the dendritic architecture, we examined each dendritic order separately. Newborn granule cells of Ts65Dn mice had no high-order dendritic branches and, while in euploid mice DCX-positive cells had up to eight orders of branches, in Ts65Dn mice they had no branches of orders 7 and 8 (Fig. 13A–C arrows).

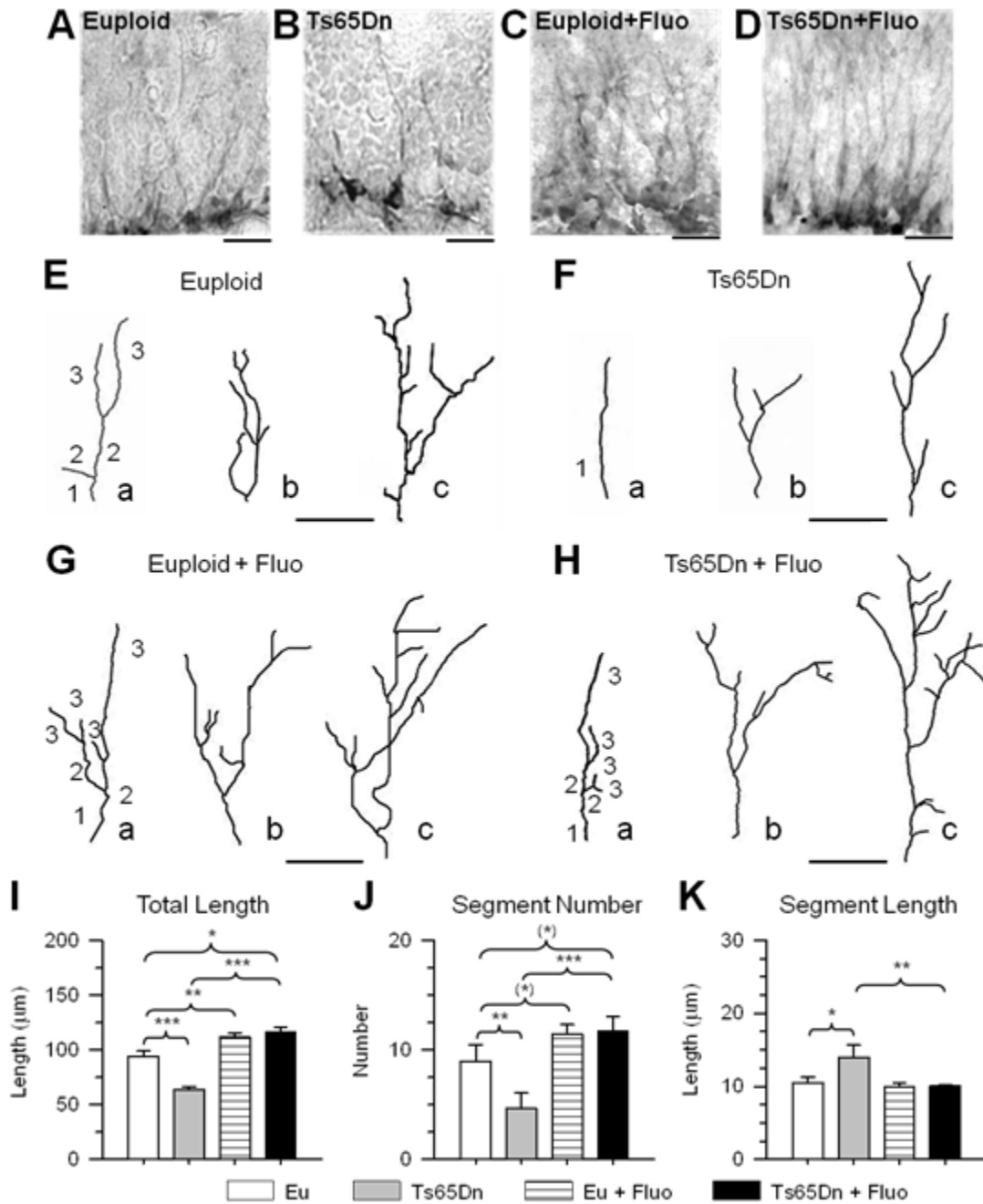


Figure 12 - Effect of fluoxetine on the dendritic size of newborn granule cells. A–D. Photomicrographs of doublecortin (DCX) immunopositive granule cells in an animal from each of the following experimental groups: euploid (A), Ts65Dn (B), treated euploid (C) and treated Ts65Dn (D). E–H. Three examples (a–c) of the reconstructed dendritic tree of granule cells from animals of each of the following experimental groups: euploid (E), Ts65Dn (F), treated euploid (G) and treated Ts65Dn (H). Numbers indicate the different dendritic orders. Calibration in A–H: 20 μm . Mean total dendritic length (I), mean number of dendritic segments (J) and mean segment length (K) in untreated euploid and Ts65Dn mice, and euploid and Ts65Dn mice treated with fluoxetine. Values in I–K represent mean deviation (SD). (*) $P < 0.06$; * $P < 0.05$; ** $P < 0.01$; *** $P < 0.001$ (Duncan’s test after ANOVA).

Analysis of branch length of the individual orders showed that branches of order 1 were notably longer (+86%) in untreated Ts65Dn compared with untreated euploid mice, and that the remaining

orders of Ts65Dn mice had branches with a similar length as those of euploid mice, except for order 6 branches, which were shorter (-80%; Fig. 13A).

Analysis of branch number showed that untreated Ts65Dn mice had a similar number of branches of orders 1 and 2 as untreated euploid mice, but fewer branches of orders 3–6 and no branches of orders 7 and 8 (Fig. 13B). In Ts65Dn mice, there was a progressive worsening in branch number reduction from order 3 to 6 (order 3: -49%, order 4: -66%, order 5: -76%, order 6: -99%). We evaluated the total dendritic surface offered by each order by multiplying the number of branches (Fig. 13B) by the mean branch length (Fig. 13A) of individual orders. In untreated Ts65Dn mice, the dendritic length of order 1 was greater (+86%) than in the euploid counterparts (Fig. 13C). This is in agreement with the greater length of branch 1. Consistently with the reduced number of branches of orders 3–6, in Ts65Dn mice the dendritic length of orders 3, 4, 5 and 6 was smaller (-52%, -62%, -78% and -99% respectively) than that of euploid mice (Fig. 13C).

A comparison between untreated and treated Ts65Dn mice showed that mice treated with fluoxetine underwent a reduction in the length of branches of orders 1, 2 and 4 (-39%, -19% and -17% respectively) which became similar to those of untreated euploid mice and an increase (+260%) in the length of branches of order 6 (Fig. 13A). Importantly, treated Ts65Dn mice acquired branches of orders 7 and 8 (Fig. 13B) and the length of these branches was similar to that of untreated euploid mice (Fig. 13A). In parallel with these effects, in treated Ts65Dn mice there was an increase in the number of branches of orders 2–6 (Fig. 13B). The number of branches became similar to (branches of orders 2, 3, 6–8) or even larger than (branches of orders 4 and 5) the number of branches seen in untreated euploid mice (Fig. 13B). In agreement with these effects, the length of individual orders of treated Ts65Dn mice became similar to or even larger (order 5) than that of untreated euploid mice (Fig. 13C).

A comparison between untreated and treated euploid mice showed that euploid mice treated with fluoxetine underwent a small (-18%) reduction in the length of branches of order 2 (Fig. 13A). They

also showed an increase in the number of branches of orders 3, 4 and 5 (+19%, +59% and +100% respectively; Fig. 13B) and in the total length of orders 4 and 5 (+46% and +100% respectively; Fig. 13C) vs. untreated euploid mice.

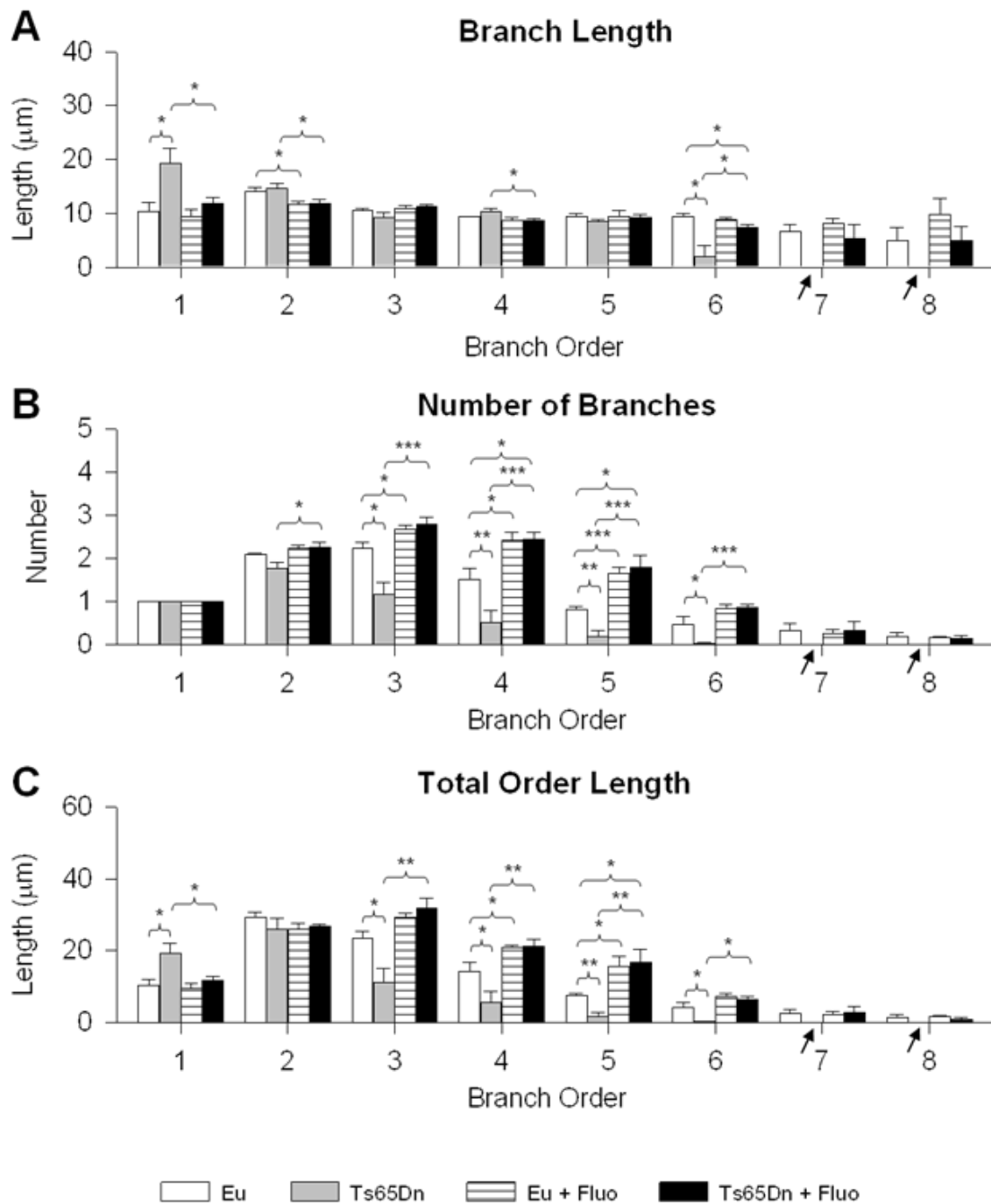


Figure 13 - Effect of fluoxetine on the dendritic architecture of newborn granule cells. A–C. Quantification of the mean length (A) and mean number (B) of branches of the different orders and total length of each order (C) in untreated euploid and Ts65Dn mice, and euploid and Ts65Dn mice treated with fluoxetine. The arrows indicate the absence of branches in untreated Ts65Dn mice. Values in A–C represent mean \pm standard deviation (SD). *P < 0.05; **P < 0.01; ***P < 0.001 (Duncan's test after ANOVA).

Taken together, these data indicate that in Ts65Dn mice the dendritic tree of the granule cells is hypotrophic starting from the early phases of maturation of newborn cells, and that this effect is mainly due to a reduction in the number of branches of intermediate order and a lack of branches of higher order. Treatment with fluoxetine rescued total dendritic length by restoring the number of branches of intermediate order and inducing the appearance *de novo* of higher-order branches. Not only did fluoxetine fully restore this defect but made the total dendritic length larger than that of untreated euploid mice.

The overall effects of genotype and treatment on the dendritic architecture of the newborn granule cells are summarized in the dendrograms of Fig. 14.

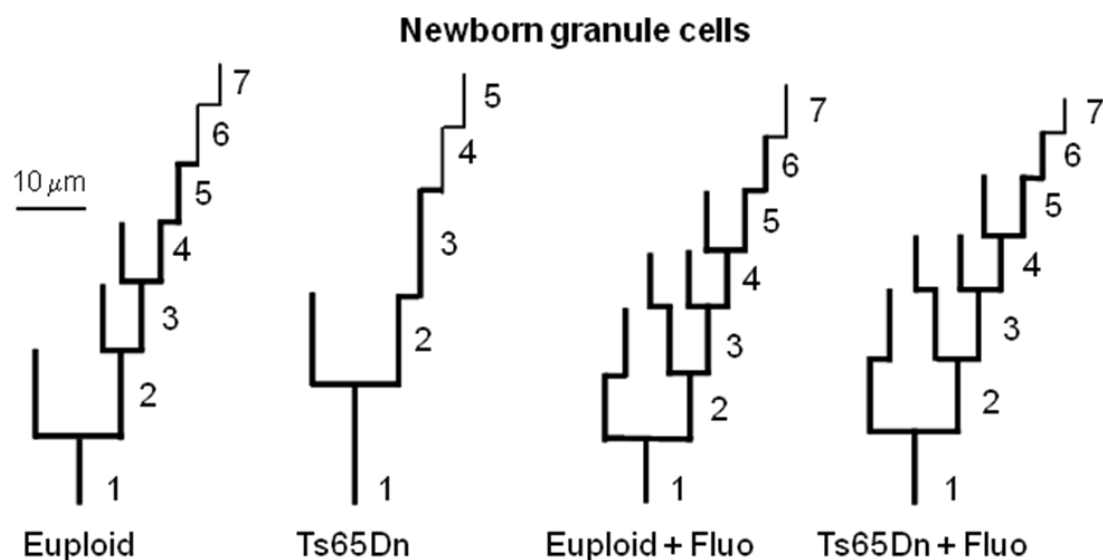


Figure 14 - Dendrograms of the newborn granule cells. The dendrograms were obtained from the mean length and mean number of branches of each order reported in Figure 12. The number of branches was approximated to the nearest integer value (thick lines). Thin lines have been used to indicate a number of branches ranging from 0.1 to 0.5.

4.2 *Effect of fluoxetine on the dendritic tree of the oldest granule cell in euploid and Ts65Dn mice*

Dendritic maturation of the granule cells lasts approximately 50–60 days ((156); (215)). As we were interested in establishing the effect of fluoxetine on granule cells that underwent dendritic maturation during treatment (P3–P15) and accomplished it in the following 30 days (by P45), we

examined Golgi-stained granule neurons located in the outer portion of the granule cell layer (Fig. 10). We chose mature-looking neurons to make sure that those which were oldest were sampled. Fig. 15A–H shows examples of granule cells in the four experimental groups.

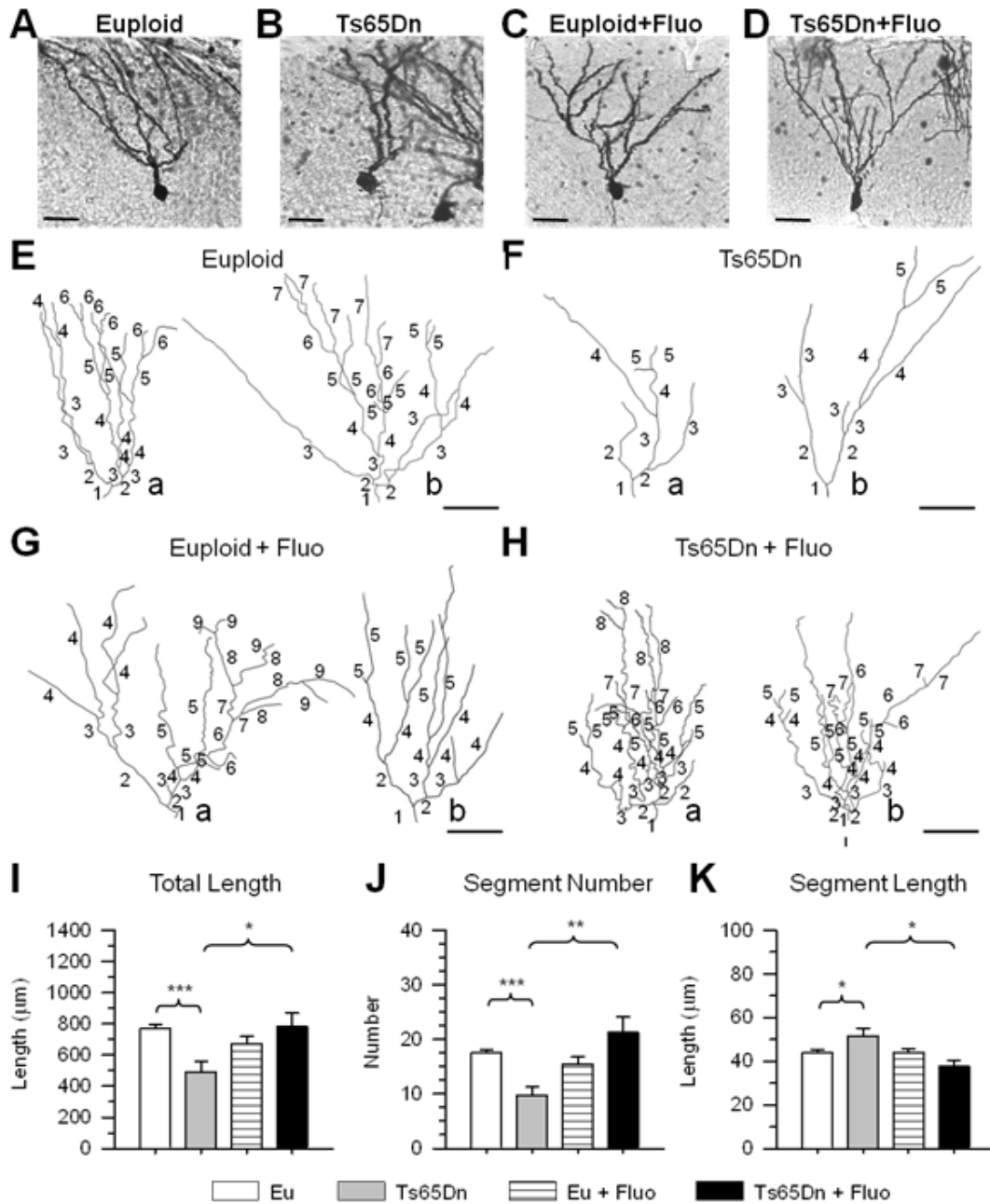


Figure 15 - Effect of fluoxetine on the dendritic size of the oldest granule cells. A–D. Photomicrographs of Golgi-stained granule cells in an animal from each of the following experimental groups: euploid (A), Ts65Dn (B), treated euploid (C) and treated Ts65Dn (D). E–H. Two examples (a and b) of reconstructed dendritic tree of granule cells from animals of each of the following experimental groups: euploid (E), Ts65Dn (F), treated euploid (G) and treated Ts65Dn (H). Numbers indicate the different dendritic orders. Calibration in A–H: 40 μm. I–K. mean total dendritic length (I), mean number of dendritic segments (J) and mean segment length (K) in untreated euploid and Ts65Dn mice, and euploid and Ts65Dn mice treated with fluoxetine. Values in I–K represent mean \pm standard deviation (SD). *P < 0.05; **P < 0.01; ***P < 0.001 (Duncan's test after ANOVA).

It can be noted that in Ts65Dn mice (Fig. 14B,F) the dendritic tree of the granule cells was less developed than in euploid mice (Fig. 15A,E). After treatment with fluoxetine, the dendritic pattern of Ts65Dn mice (Fig. 15D,H) became similar to that of untreated euploid mice.

Quantification of the dendritic size showed that Ts65Dn mice had a shorter dendritic length (-36%; Fig. 15I) and a reduced number of segments (-45%; Fig. 15J) than euploid mice. In contrast, the mean segment length was larger than in euploid mice (+17%; Fig. 15K). While in euploid mice treatment with fluoxetine had no effect on dendritic length, number of segments and segment size (Fig. 15J,K), in treated Ts65Dn mice the dendritic length (Fig. 15I) and the number of segments (Fig. 15J) underwent an increase and the mean segment length underwent a reduction (Fig. 15K). All these parameters became similar to those of untreated euploid mice.

The analysis of each dendritic order showed the absence of branches of higher order in Ts65Dn mice. While euploid mice had up to nine orders of branches, Ts65Dn mice completely lacked branches of orders 7–9 (Fig. 16A–C arrows). Analysis of the branch length of individual orders showed no effects of either genotype or treatment on branches of orders 4–6. In contrast, branches of orders 1–3 were notably longer in untreated Ts65Dn vs. untreated euploid mice (Fig. 16A). Analysis of the number of branches showed that untreated Ts65Dn mice had a similar number of branches of orders 1 and 2 as untreated euploid mice, fewer branches of orders 3–6 and, as noted above, no branches of order higher than 6 (see arrows in Fig. 16B). In Ts65Dn mice, there was a progressive worsening in branch number reduction from order 3 to 6 (order 3: -13%, order 4: -56%, order 5: -70%, order 6: -91%). We evaluated the total dendritic surface offered by each order by multiplying the number of branches (Fig. 16B) by the mean branch length (Fig. 16A) of individual orders. Evaluation of the total dendritic surface offered by each order showed that in untreated Ts65Dn mice, the total length of orders 1, 2 and 3 was larger (+93%, +46% and +26% respectively) compared with the euploid counterparts (Fig. 16C).

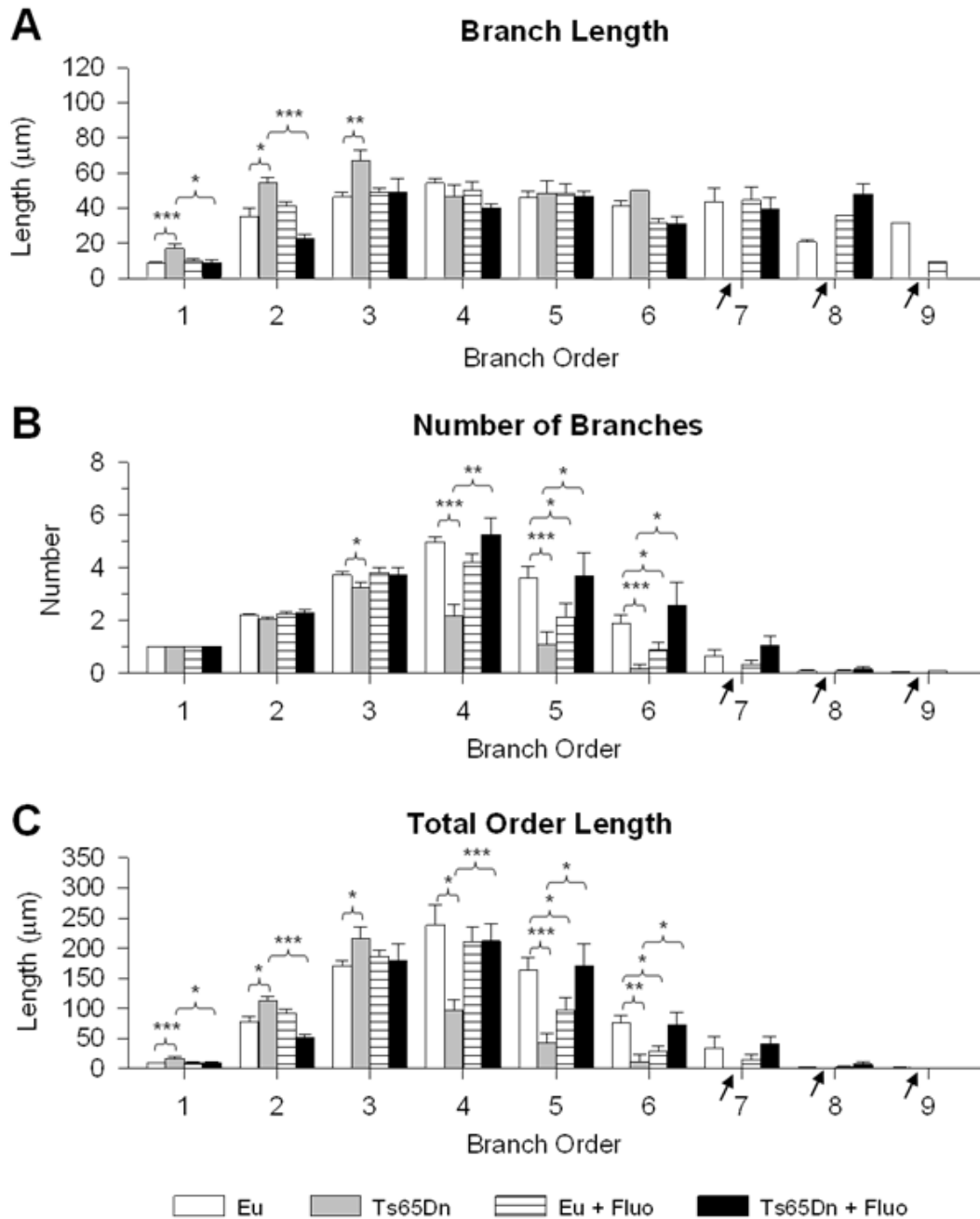


Figure 16 - Effect of fluoxetine on dendritic architecture of the oldest granule cells. A–C. Quantification of the mean length (A) and mean number (B) of branches of the different orders and total length of each order (C) in untreated euploid and Ts65Dn mice, and euploid and Ts65Dn mice treated with fluoxetine. The arrows indicate the absence of branches in untreated Ts65Dn mice. Values in A–C represent mean \pm standard deviation (SD). * $P < 0.05$; ** $P < 0.01$; *** $P < 0.001$ (Duncan's test after ANOVA).

This is in agreement with the greater branch length of these orders in Ts65Dn mice. In agreement with the reduced number of branches of orders 4–6, in Ts65Dn mice the total length of orders 4, 5

and 6 was reduced (-60%, -75% and -8% respectively) compared with that of euploid mice (Fig. 16C).

A comparison between untreated and treated Ts65Dn mice showed that mice treated with fluoxetine underwent a reduction in the length of branches of orders 1–3 (Fig. 16A) and an increase in the number of branches of orders 3–6, thus showing a pattern that became similar to that of untreated euploid mice. Importantly, treated Ts65Dn mice acquired branches of orders 6–8 and the number and length of these branches were similar to that of untreated euploid mice (Fig. 16A,B). In agreement with these effects, the length of individual orders of treated Ts65Dn mice became similar to that of untreated euploid mice (Fig. 16C).

A comparison between untreated and treated euploid mice showed that euploid mice treated with fluoxetine had fewer branches of orders 5 and 6 (-40% and -53% respectively; Fig. 16B), with no change in the mean branch length (Fig. 16A). In agreement with these effects, in treated euploid mice the total length of orders 5 and 6 was reduced (-40% and -62% respectively) compared with that of untreated euploid mice (Fig. 16C).

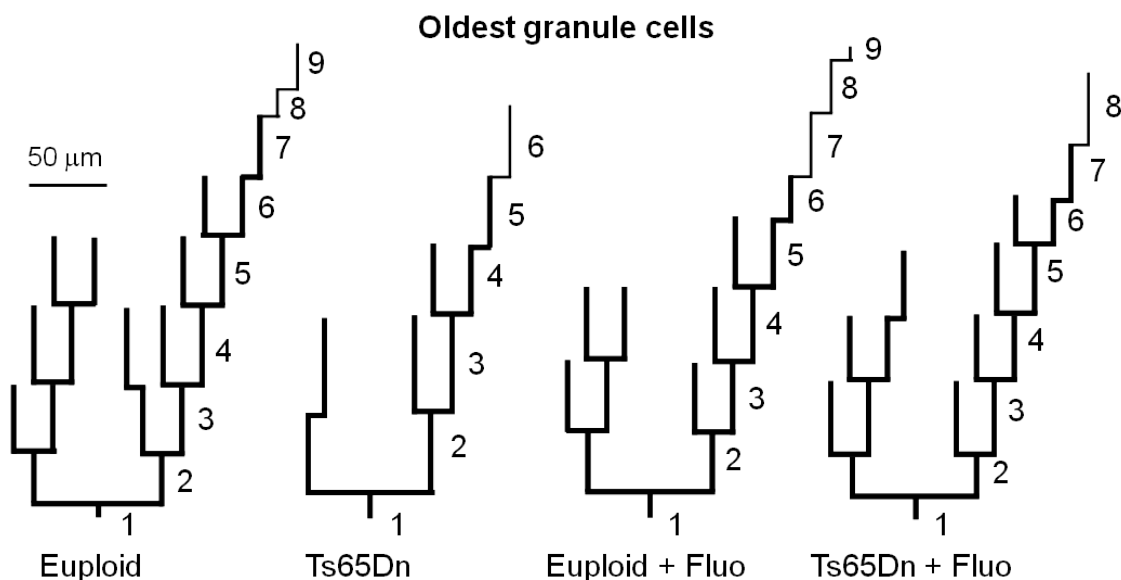


Figure 17 - Dendrograms of the oldest granule cells. The dendrograms were obtained from the mean length and mean number of branches of each order reported in Figure 15. The number of branches was approximated to the nearest integer value (thick lines). Thin lines have been used to indicate a number of branches ranging from 0.1 to 0.5.

Taken together, these results indicate a severe hypotrophy of the dendritic tree of the granule cells of Ts65Dn mice that is mainly due to a notably reduced number of branches of intermediate order and total lack of branches of higher order. Treatment with fluoxetine rescued total dendritic length by restoring the number of intermediate order branches and inducing the appearance *de novo* of higher order branches.

The overall effects of genotype and treatment on the dendritic architecture of the mature granule neurons are summarized in the dendrograms of Fig. 17.

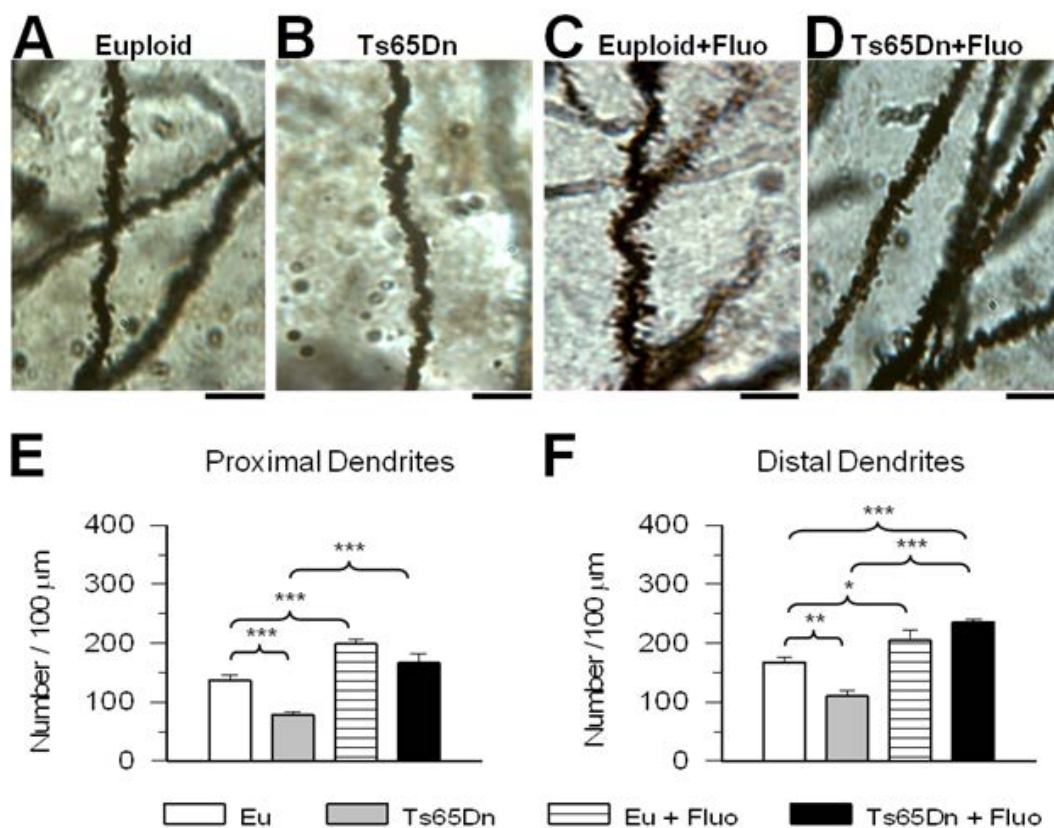


Figure 18 - Effect of fluoxetine on spine density in the oldest granule cells. A–D. Photomicrograph of Golgi-stained granule cells showing distal dendritic branches in an animal from each of the following experimental groups: euploid (A), Ts65Dn (B), treated euploid (C) and treated Ts65Dn (D). Calibration: 10 μ m. E,F. Spine density in the proximal (E) and distal (F) dendritic branches of untreated euploid and Ts65Dn mice, and euploid and Ts65Dn mice treated with fluoxetine. Values represent mean \pm standard deviation (SD). *P < 0.05; **P < 0.01; ***P < 0.001 (Duncan's test after ANOVA).

4.3 Effect of fluoxetine on granule cell spine density in euploid and Ts65Dn mice

Neurons receive their excitatory inputs through dendritic spines. Evidence in two mouse models of DS shows a spine density reduction along the dendritic tree of the granule cells ((23); (22)). To establish whether fluoxetine rescues this defect, we examined spine density in untreated and treated mice. Figure A–D shows that in untreated Ts65Dn mice the dendrites of the granule cells had fewer spines (Fig. 18B) compared with euploid mice (Fig. 18A) and that treatment increased spine number (Fig. 18 7D).

Quantification of spine density showed that in untreated Ts65Dn mice, spine density was notably lower than that of untreated euploid mice, both at the level of the inner (-43%; Fig. 18E) and outer (-35%; Fig. 18F) portions of the molecular layer. After treatment with fluoxetine, Ts65Dn mice underwent a notable increase in spine density that became similar to that of untreated euploid mice in the inner half of the molecular layer (Fig. 18E), and became even larger in comparison with euploid mice in the outer half (Fig. 18F). In treated euploid mice, spine density increased compared with that of untreated mice, both in the inner half (+44%; Fig. 18E) and outer half (+22%; Fig. 18F) of the molecular layer.

4.4 Effect of fluoxetine on hippocampal SYN levels in euploid and Ts65Dn mice

It is likely that a reduction in connectivity is the counterpart of the severe dendritic hypotrophy that characterizes the granule cells of Ts65D mice. SYN (also known as p38) is a synaptic vesicle glycoprotein that is a specific marker of presynaptic terminals.

Evaluation of SYN levels in the hippocampal formation (DG plus hippocampus proper) by Western blot analysis showed that Ts65Dn mice had reduced SYN levels and that treatment restored SYN levels (Fig. 19A,B). SYN levels also increased in treated euploid mice and became higher than in untreated euploid mice (Fig. 19A,B). Next, we examined SYN IR in order to obtain specific information on SYN levels in the molecular layer of the DG. Fig. 19C shows representative images

from animals of each group. It can be readily appreciated that IR for SYN was reduced in Ts65Dn mice compared with untreated euploid mice and that it was increased by treatment with fluoxetine. Quantitative analysis showed that in untreated Ts65Dn mice, the optical density (OD) of SYN was significantly lower than in untreated euploid mice in the middle (-35%) and outer (-48%) molecular layers. A marginally significant reduction was present also in the inner molecular layer (Fig. 19D). In Ts65Dn mice treated with fluoxetine, the OD of SYN underwent a large increase in all zones of the molecular layer and became even greater than that found in untreated euploid mice (Fig. 19D). An increase in the OD of SYN also took place in treated euploid mice in all zones of the molecular layer (Fig. 19D).

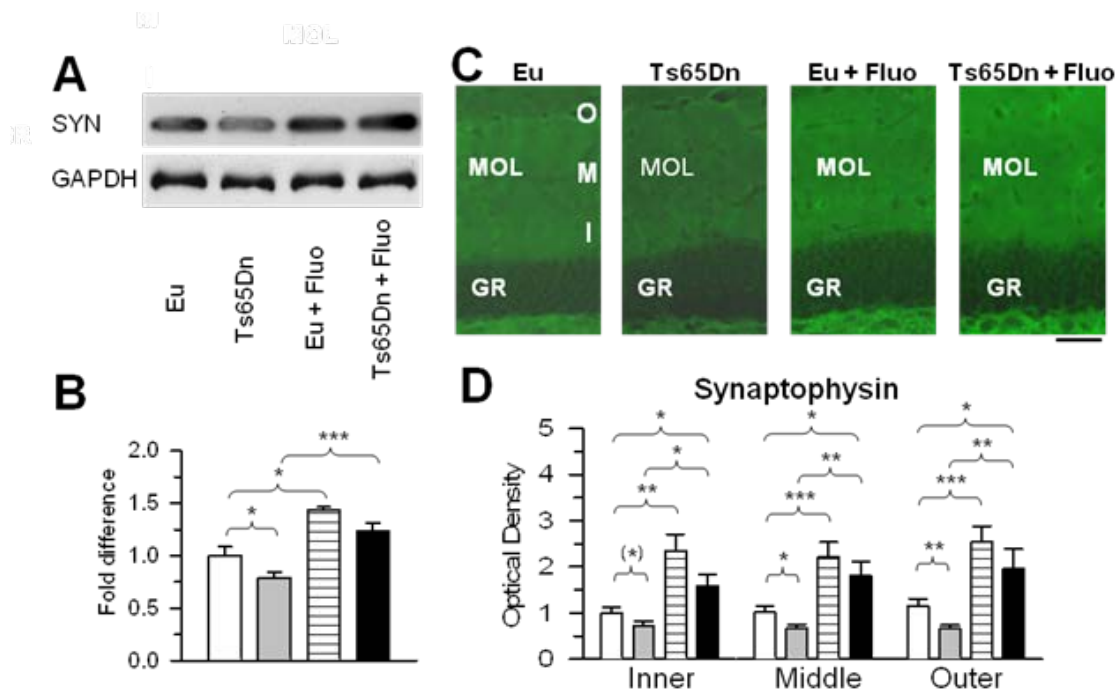


Figure 19 - Effect of fluoxetine on connectivity in the molecular layer. A,B. Western blot analysis of synaptophysin levels in the hippocampal formation of untreated and treated mice. Western immunoblots in (A) are examples from animals of each experimental group. Histograms in (B) show synaptophysin levels normalized to glyceraldehyde-3-phosphate dehydrogenase (GAPDH) and expressed as fold difference in comparison to untreated euploid mice. C. Images of sections processed for synaptophysin immunofluorescence from the dentate gyrus (DG) of an animal from each experimental group. Calibration: 50 μ m. D. Optical density of synaptophysin immunoreactivity in the inner, middle and outer third of the molecular layer of untreated and treated euploid and Ts65Dn mice. Data are given as fold difference vs. inner molecular layer of untreated euploid mice. Values in B, D represent mean \pm standard deviation (SD). (*) $P < 0.06$; * $P < 0.05$; ** $P < 0.01$; *** $P < 0.001$ (Duncan's test after ANOVA).

4.5 Effect of fluoxetine on the glutamatergic innervation of the granule cells in euploid and Ts65Dn mice

Perforant path fibers, which take their origin from the entorhinal cortex and use glutamate as a neurotransmitter, innervate the middle and outer third of the molecular layer (10). In view of the key role of this input in hippocampus-dependent memory functions, we examined the effects of trisomy and treatment on glutamatergic terminals in the DG. To this purpose, we evaluated the co-localization of SYN and the VGLUT1 in the outer and middle third of the molecular layer.

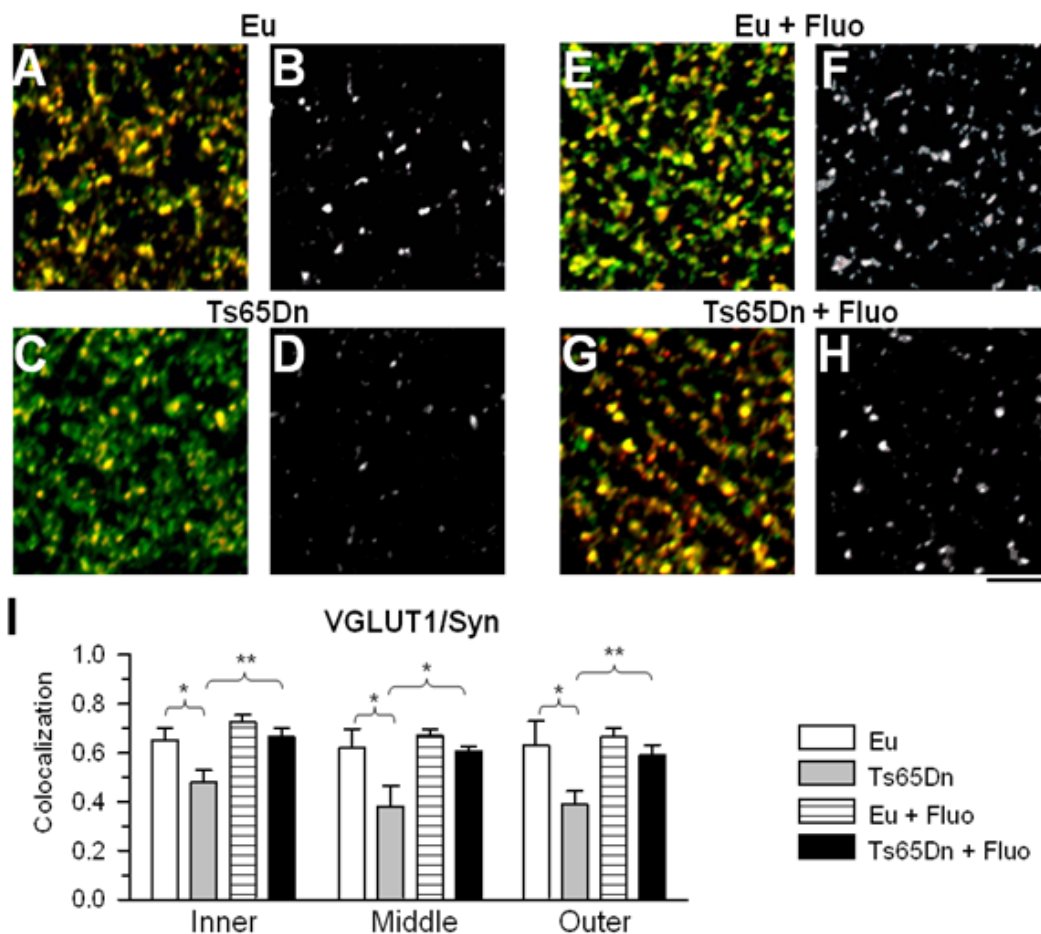


Figure 20 - Effect of fluoxetine on the glutamatergic input in the molecular layer. A–H. Images of sections processed for double-labeling immunofluorescence with an anti-synaptophysin antibody (green) and an anti-vesicular glutamate transporter 1 (VGLUT1) antibody (red) from the outer molecular layer of the DG of an animal from each of the following experimental groups: euploid (A,B), Ts65Dn (C,D), treated euploid (E,F) and treated Ts65Dn (G,H). Images in B, D, F, H represent co-localization (white) between synaptophysin (SYN) and VGLUT1. Calibration: 5 μ m (applies to A–H). M. Coefficient of co-localization of SYN and VGLUT1 in the inner, middle and outer third of the molecular layer of untreated and treated euploid and Ts65Dn mice. Values in I represent mean \pm standard deviation (SD). (*) $P < 0.06$; * $P < 0.05$; ** $P < 0.01$; *** $P < 0.001$ (Duncan's test after ANOVA).

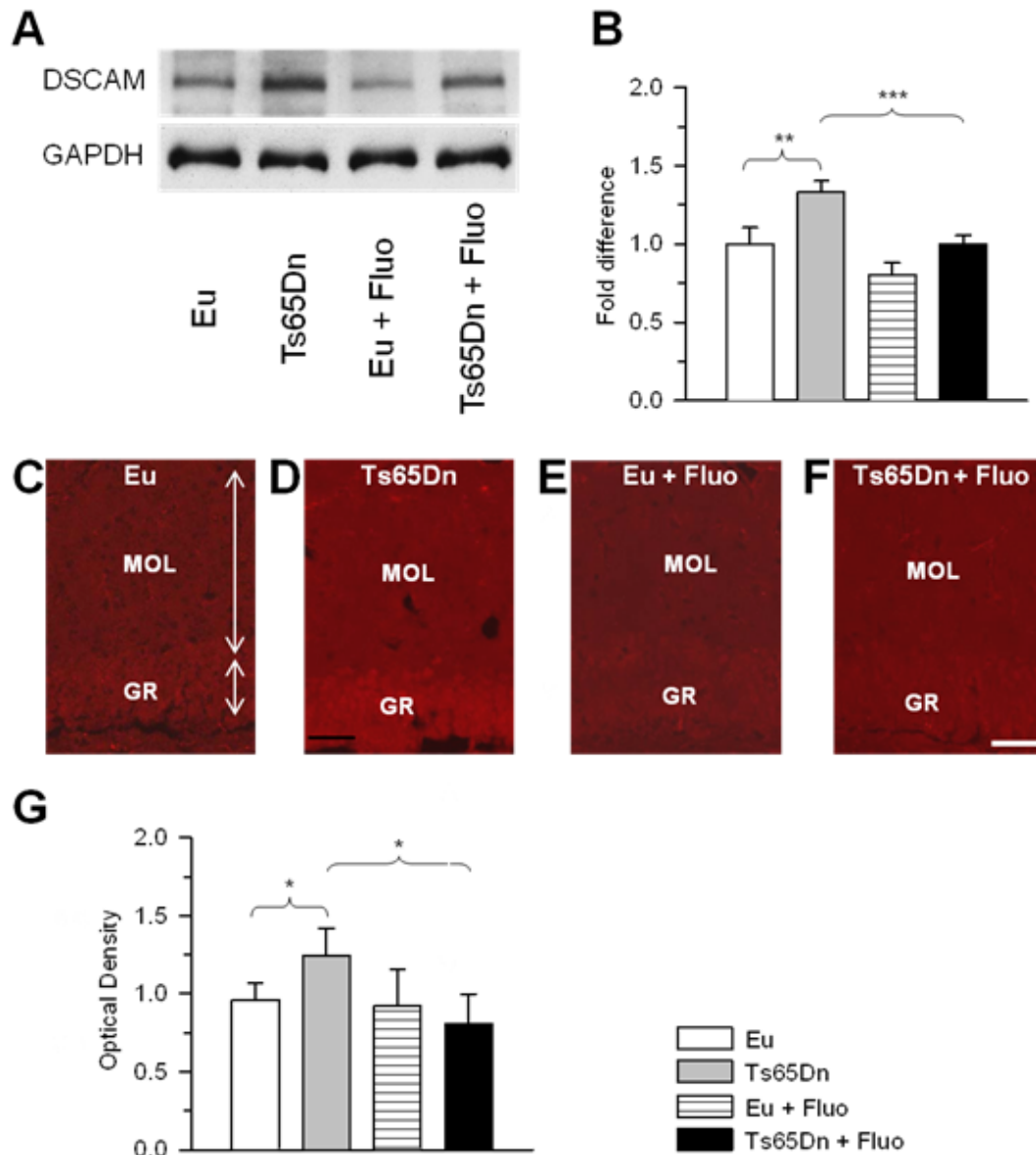


Figure 21 - Effect of fluoxetine on Down syndrome cell adhesion molecule (DSCAM) immunoreactivity in the dentate gyrus. A,B. Western blot analysis of DSCAM levels in the hippocampal formation of untreated and treated mice. Western immunoblots in (A) are examples from animals of each experimental group. Histograms in (B) show DSCAM levels normalized to glyceraldehyde-3-phosphate dehydrogenase (GAPDH) and expressed as fold difference in comparison to untreated euploid mice. C–F. Images of sections processed for DSCAM immunoreactivity from the dentate gyrus (DG) of an animal from each of the following experimental groups: euploid (C), Ts65Dn (D), treated euploid (E) and treated Ts65Dn (F). Calibration: 50 μ m (applies to C–F). G. Optical density of DSCAM immunoreactivity in the molecular layer of untreated and treated euploid and Ts65Dn mice. Data are given as fold difference vs. untreated euploid mice. Values in B, G represent mean \pm standard deviation (SD). * $P < 0.05$; ** $P < 0.01$; *** $P < 0.001$ (Duncan's test after ANOVA).

We additionally examined the inner third, which mainly contains glutamatergic terminals of the mossy cells (10). We found that co-localization of SYN and VGLUT1 was reduced in untreated Ts65Dn as compared with euploid mice in the inner, middle and outer third of the molecular layer

(Fig. 19A–I), indicating a generalized reduction of excitatory afferents. Importantly, in treated Ts65Dn mice, co-localization of SYN and VGLUT1 increased in all zones of the molecular layer and became similar to that of untreated euploid mice (Fig. 20A–I), suggesting restoration of the glutamatergic inputs. In euploid mice, treatment had no effect on co-localization of SYN and VGLUT1.

4.6 Effect of fluoxetine on DSCAM levels in the DG of euploid and Ts65Dn mice

The mechanisms underlying dendritic pathology in DS have not been elucidated and there is no clear evidence as to the role played by triplicated genes in the DS aberrant dendritic phenotype. DSCAM is a triplicated gene of HSA21.

Over-expression in hippocampal neurons of DSCAM dramatically inhibits dendritic branching, strongly suggesting that DSCAM over-expression may be a determinant of the dendritic pathology in DS (9). DSCAM mRNA has been shown to be localized to dendrites where it is translated (9). Dendritic levels of DSCAM protein are regulated by synaptic activity at the NMDA receptor (NMDAR). In particular, activation of this receptor increases DSCAM levels. Evaluation of DSCAM levels in the hippocampal formation (hippocampus plus DG) by Western blot analysis showed that Ts65Dn mice had higher DSCAM levels than untreated euploid mice (Fig. 21A,B). After treatment with fluoxetine, Ts65Dn mice underwent a reduction in DSCAM levels that became similar to those of untreated euploid mice (Fig. 21A,B). In sections immunostained for DSCAM, we quantified DSCAM IR in the DG. We found that the OD of DSCAM in untreated Ts65Dn mice, similarly to Ts1Cej mice (9), was higher than euploid mice (Fig. 21C–G). In the DG of Ts65Dn mice treated with fluoxetine, the OD of DSCAM became similar to that of untreated euploid mice (Fig. 21C–G), suggesting that this reduction may underlie the recovery of granule cell dendritic architecture.

4.7 Effect of fluoxetine on the hippocampal serotonergic system in euploid and Ts65Dn mice

A profuse network of serotonin (5-HT) containing axons originating from the dorsal and medial raphe nuclei innervates the hippocampus and DG (16). In a previous study, we found that Ts65Dn mice aged 15 days had no differences in serotonin levels but reduced levels of the 5-HT_{1A} receptor ((28)).

Quantification of 5-HT by HPLC in the hippocampal region (hippocampus plus DG) of treated and untreated P45 mice showed that Ts65Dn mice had a lower 5-HT concentration (Fig. 22A), and a lower concentration of the 5-HT metabolite 5-HIAA (Fig. 21B) than euploid mice. However, there was a similar expression of the serotonin transporter (SERT) (Fig. 22C). After treatment with fluoxetine, the levels of 5-HT and 5-HIAA underwent an increase and became similar to those of euploid mice (Fig. 22A,B), with no changes in the expression of SERT (Fig. 22C). Taken together these data suggest impairment of the serotonergic input to the hippocampal formation in Ts65Dn mice that can be restored by treatment. This is in agreement with the overall connectivity increase found in the DG of treated trisomic mice (Fig. 19A–D).

At P45, unlike P15 (28), the hippocampal expression of the 5-HT_{1A} receptor was similar in Ts65Dn and euploid mice (Fig. 22D). After treatment with fluoxetine, both Ts65Dn and euploid mice exhibited a reduction in the expression of the 5-HT_{1A} receptor compared with their untreated counterparts (Fig. 22D). This may represent a compensatory mechanism caused by the increased bioavailability of serotonin induced by treatment. In view of the role of the 5-HT_{1A} receptor in neurogenesis and dendritic development ((33); (64); (210)), we compared its expression in euploid and Ts65Dn mice at three different ages. We found that both in euploid and Ts65Dn mice the expression of the 5-HT_{1A} receptor increased with age (Fig. 22E). Importantly, its expression was lower in Ts65Dn mice compared with the euploid counterparts at P2 and P15, but not at P45. This indicates failure of the 5-HT_{1A} receptor in a period (P2–P15) that is critical for two fundamental processes: neurogenesis and dendritogenesis.

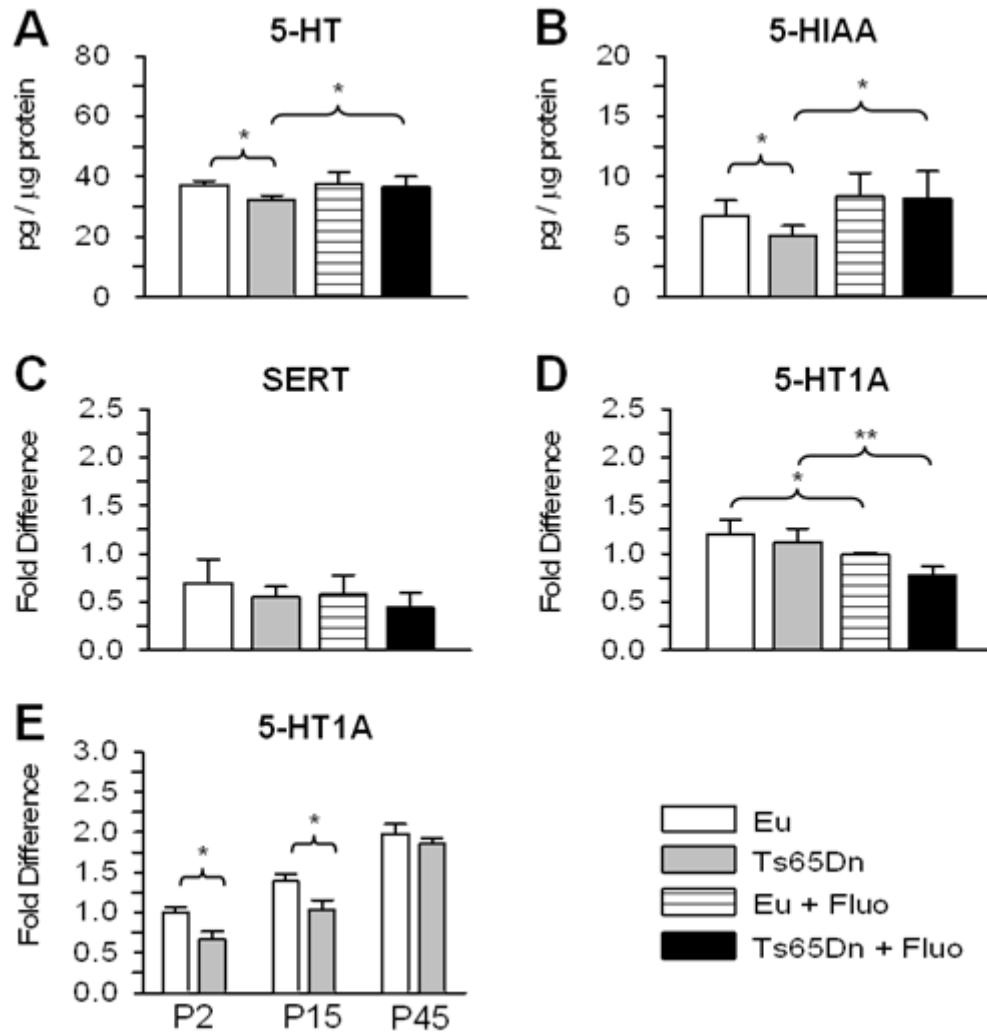


Figure 22 – Effect of fluoxetine on serotonin levels and serotonin receptor expression in the hippocampal formation. A,B. Levels of serotonin (5-HT) (A) and of the serotonin metabolite hydroxy indolic acid (5-HIAA) (B) measured with high-performance liquid chromatography (HPLC) in the hippocampal formation of P45 untreated euploid and Ts65Dn mice and P45 euploid and Ts65Dn mice treated with fluoxetine. Values represent mean \pm standard deviation (SD). C–E. RNA expression levels quantified by real-time quantitative PCR (RT-qPCR) of the serotonin transporter (SERT) (C), 5-HT1A receptor (D) in the hippocampal formation of P45 untreated and treated euploid and Ts65Dn mice, and in the hippocampal formation of untreated euploid and Ts65Dn mice at P2, P15 and P45 (E). Data are expressed as fold difference in comparison with untreated P45 euploid mice (C, D) or compared with P2 euploid mice (E). Data of P45 mice in E are the same as those in D. Values represent the mean \pm standard deviation (SD). *P < 0.05; **P < 0.01. (Duncan's test after ANOVA).

4.8 Effect of fluoxetine on spine density on the proximal shaft of CA3 pyramidal neurons in euploid and Ts65Dn mice

The mossy fiber axons establish multiple asymmetrical synapses with the thorny excrescences on the proximal portion of the apical dendritic tree of CA3 pyramidal neurons. Recent evidence shows

a decreased number of thorns on the thorny excrescences of Ts65Dn mice aged six months (142). We were interested in establishing whether a reduction in the density of spines forming the thorny excrescences is already present in mice aged 45 days and whether fluoxetine rescues this defect. Images in Fig. 23A show that in untreated Ts65Dn mice there were patently fewer spines compared to euploid mice and that treatment increased their number. An increase in spine density also took place in treated euploid mice (Fig. 23A).

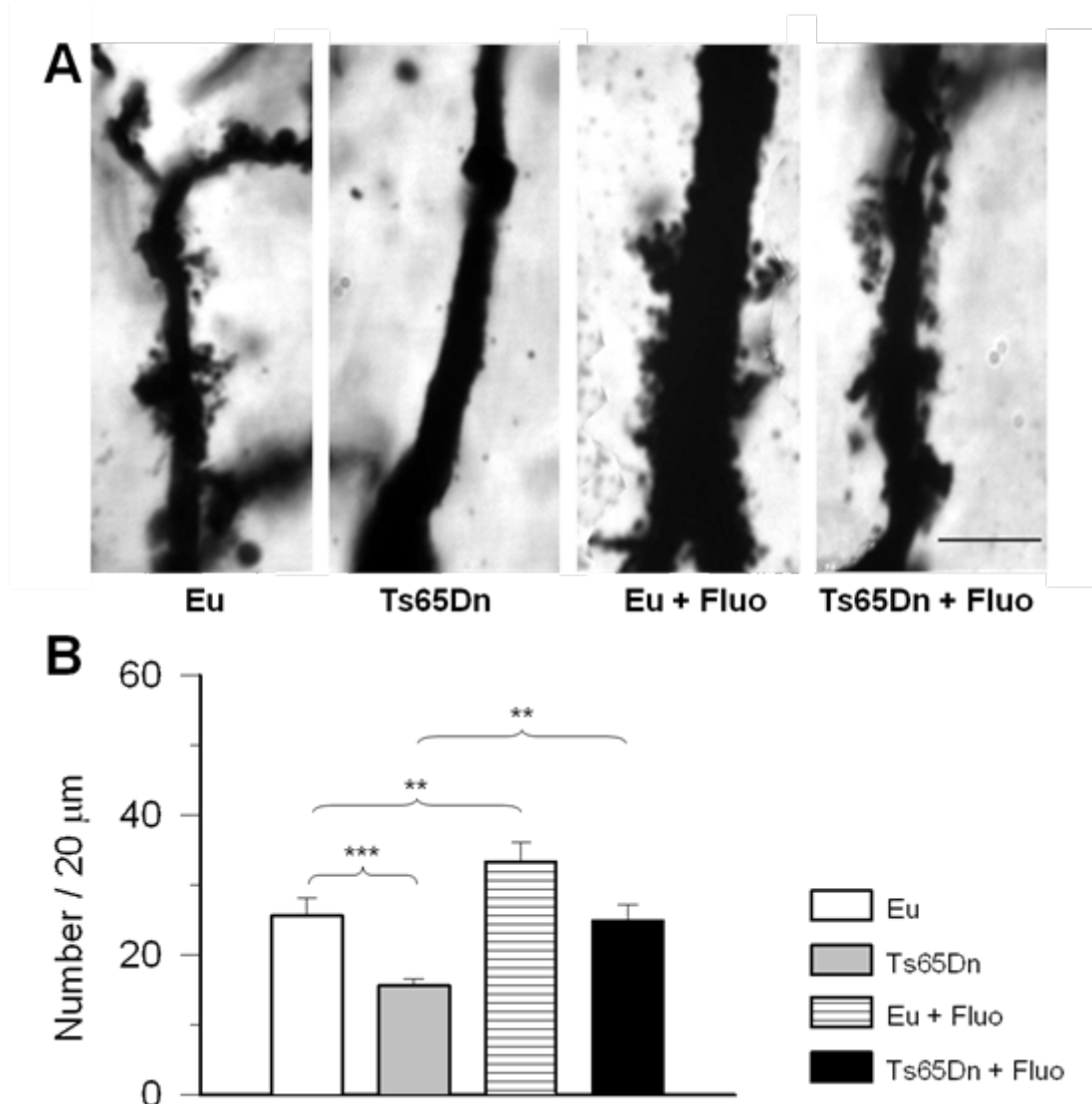


Figure 23 - Effect of fluoxetine on CA3 pyramidal neuron spine density. A: Photomicrograph of Golgi-stained field CA3 pyramidal cells showing the spinous excrescences on the proximal apical dendritic shaft in an animal from each experimental group. Scale bar = 10 μm. B: Density of spines on the proximal apical dendritic shaft in the stratum lucidum of field CA3 of untreated euploid, untreated Ts65Dn, treated euploid and treated Ts65Dn mice. Spine density is expressed as number of spines per 20 μm of dendrite. Values represent mean ± standard deviation (SD). * P < 0.05; ** P < 0.01; *** P < 0.001 (Duncan's test after ANOVA).

Quantification of spine density showed that in untreated Ts65Dn mice spine density was notably lower (-40%) than that of untreated euploid mice (Fig. 23B). After treatment with fluoxetine, Ts65Dn mice underwent an increase in spine density that became similar to that of untreated euploid mice (Fig. 23B).

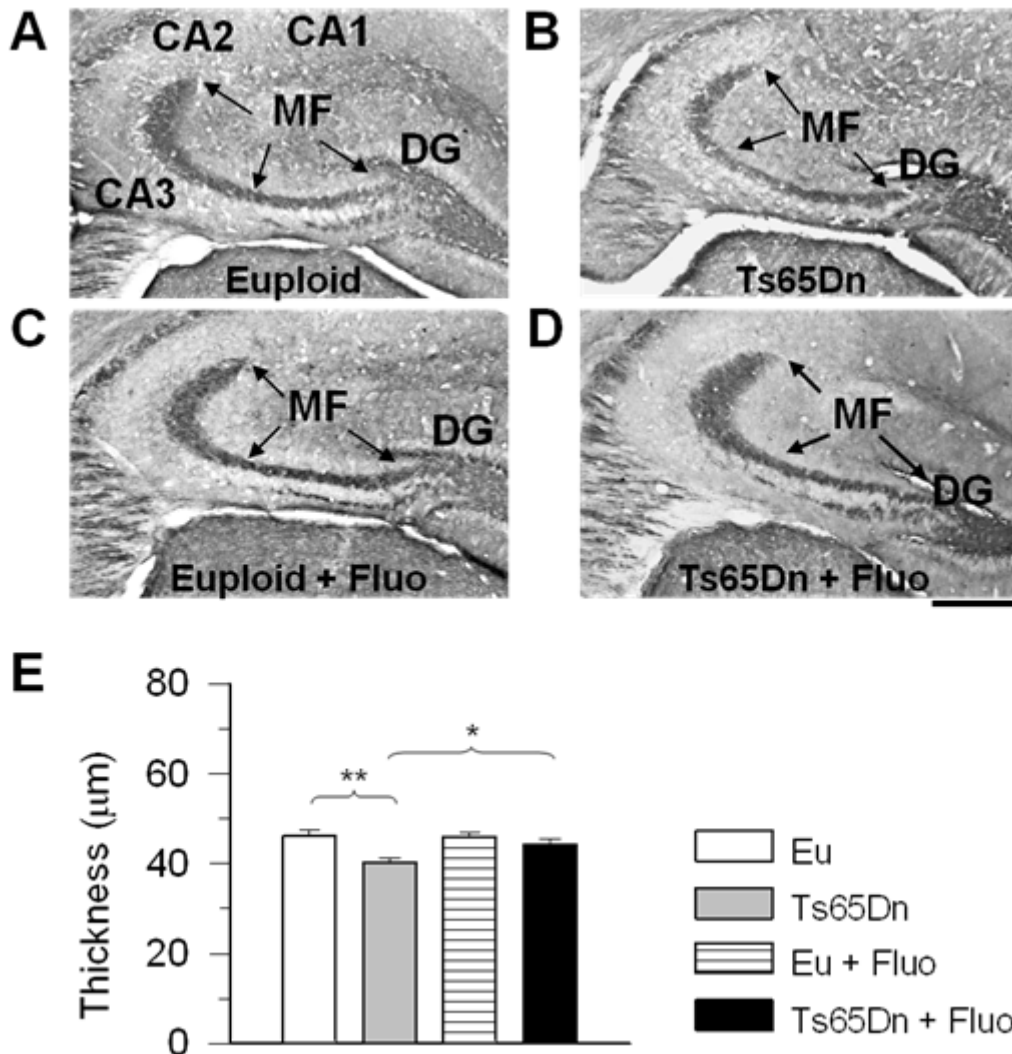


Figure 24 - Effect of fluoxetine on the thickness of the mossy fiber terminal field. A–D: Examples of coronal sections, processed for PSA-NCAM immunohistochemistry, across the hippocampal formation of an animal from each of the following experimental groups: euploid (A), Ts65Dn (B), treated euploid (C), and treated Ts65Dn (D). Sections were taken at approximately the same distance from the rostral border of the hippocampal formation. The mossy fiber system (indicated by arrows) can be clearly recognized for its dark color and its abrupt termination at the border between CA3 and CA2. The scale bar = 300 μm applies to A–D. Abbreviations: DG, dentate gyrus; MF, mossy fibers. E: Mean thickness of the mossy fiber terminal field in CA3 in untreated euploid, untreated Ts65Dn, treated euploid and treated Ts65Dn mice. The mean thickness was obtained by dividing the area occupied by the mossy fibers by the length of CA3. Values represent mean ± standard deviation (SD). * P < 0.05; ** P < 0.01 (Duncan’s test after ANOVA).

Treatment also induced a significant increase in spine density in euploid mice (+30% compared to untreated mice).

4.9 Effect of fluoxetine on the size of the mossy fiber bundle in euploid and Ts65Dn mice

The granule cells send their axons, the mossy fibers, to field CA3. The region of synaptic contact forms a layer called the stratum lucidum (Fig. 9A). The mossy fiber axons express PSA-NCAM ((171); (165)), which makes it possible to examine this bundle in sections immunoprocessed for PSA-NCAM. Ts65Dn mice have a reduced number of granule cells in comparison with euploid mice ((28)), which implies a reduction in the number of mossy fibers reaching the stratum lucidum. A reduced number of fibers may result in a reduced thickness of the terminal field of the mossy fibers in field CA3. To obtain information regarding this issue we examined the size of the mossy fiber system in the stratum lucidum of field CA3. Fig. 24A,B shows that the mossy fiber system was patently less prominent in Ts65Dn than in euploid mice.

Quantification of the mean thickness of the mossy fiber bundle within CA3 showed that in Ts65Dn mice it was smaller (-13%) than in euploid mice (Fig. 24E). In euploid mice, treatment with fluoxetine did not change the mean thickness of the mossy fiber bundle (Fig. 24A–E). Importantly, in trisomic mice treated with fluoxetine the thickness of the mossy fiber bundle increased and became similar to that of untreated euploid mice (Fig. 24A–E).

4.10 Effect of fluoxetine on overall innervation in the stratum lucidum of euploid and Ts65Dn mice

In order to obtain information on overall connectivity to the stratum lucidum, we examined the immunoreactivity for SYN in this layer. Fig. 25A shows representative images from animals of each group. It can be readily appreciated that the immunoreactivity for SYN was reduced in Ts65Dn mice compared to untreated euploid mice and that treatment with fluoxetine increased SYN

immunoreactivity both in Ts65Dn and euploid mice. Quantitative analysis showed that in untreated Ts65Dn mice the optical density (OD) of SYN was significantly lower (-20%) than in untreated euploid mice. In Ts65Dn mice treated with fluoxetine, the OD of SYN underwent a large increase and became similar to that found in untreated euploid mice (Fig. 25B). An increase in the OD of SYN also took place in treated euploid mice with an increase of 60% in comparison with untreated euploid mice (Fig. 25B).

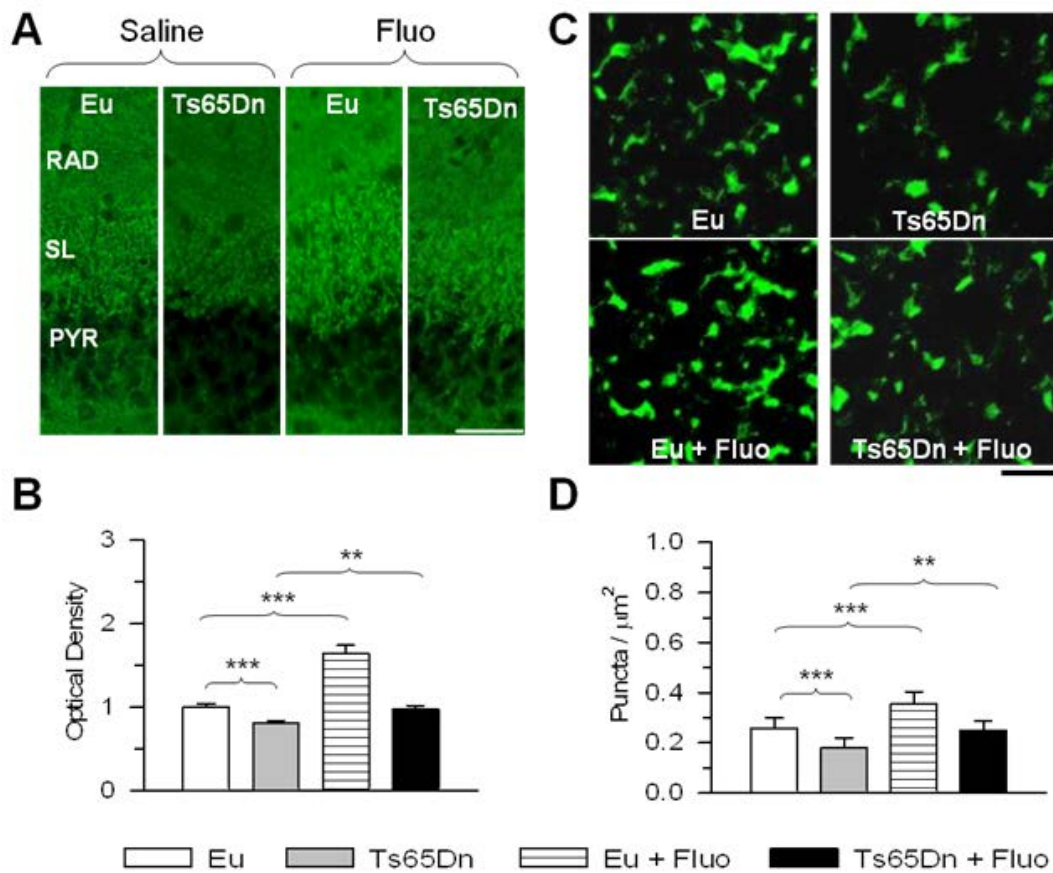


Figure 25 - Effect of fluoxetine on overall innervation in stratum lucidum of field CA3. A: Images of sections processed for synaptophysin immunofluorescence from field CA3 from an animal of each experimental group. Scale bar = 50 μm. B: Optical density of synaptophysin immunoreactivity in the stratum lucidum of untreated euploid, untreated Ts65Dn, treated euploid and treated Ts65Dn mice. Data are given as fold difference vs. the stratum lucidum of untreated euploid mice. C: Images, taken with the confocal microscope, of sections processed for synaptophysin immunofluorescence from the stratum lucidum of field CA3 from an animal of each experimental group. Scale bar = 5 μm. D: Number of puncta per μm² exhibiting synaptophysin immunoreactivity in untreated euploid, untreated Ts65Dn, treated euploid and treated Ts65Dn mice. Values in B and D represent mean ± standard deviation (SD). ** P < 0.01; *** P < 0.001 (Duncan's test after ANOVA).

Differences in SYN immunoreactivity among groups may be attributable to differences in the number of synaptic terminals and/or to differences in the number of synaptic vesicles contained in each terminal. To establish possible differences among groups in the overall number of synaptic contacts, we evaluated the density of individual puncta exhibiting SYN immunoreactivity in the stratum lucidum. Fig. 25C shows representative images from animals of each experimental group. We found that untreated Ts65Dn mice had fewer puncta (-31%) exhibiting SYN immunoreactivity than the euploid counterparts (Fig. 25D), suggesting that fewer synapses overall are established on CA3 pyramidal neurons. Treatment with fluoxetine increased the density of SYN puncta both in Ts65Dn and euploid mice (Fig. 25D).

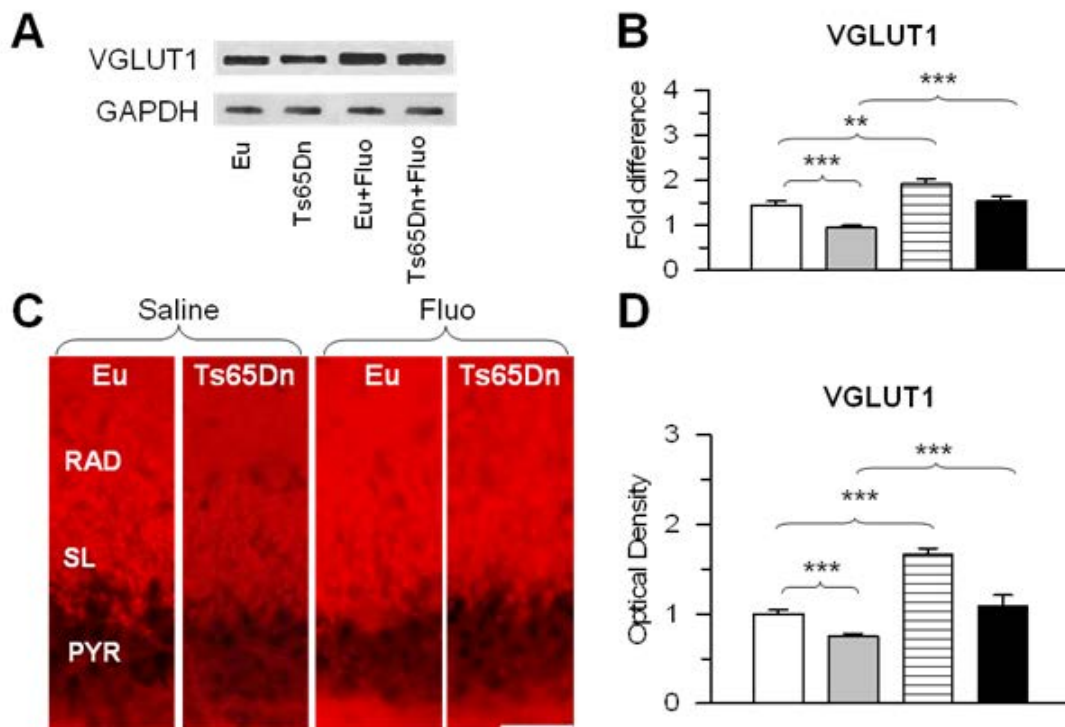


Figure 26 – Effect of fluoxetine on hippocampal VGLUT1 levels. A–B: Western blot analysis of VGLUT1 levels in the hippocampal formation of untreated euploid, untreated Ts65Dn, treated euploid and treated Ts65Dn mice. Western immunoblots in (A) are examples from an animal of each experimental group. Histograms in (B) show VGLUT1 levels normalized to GAPDH and expressed as fold difference in comparison with untreated euploid mice. C: Images of sections processed for VGLUT1 immunofluorescence from field CA3 of an animal of each experimental group. Scale bar = 50 μ m. D: Optical density of VGLUT1 immunoreactivity in the stratum lucidum of untreated euploid, untreated Ts65Dn, treated euploid and treated Ts65Dn mice. Number of analyzed sections: 3–4 per animal. Data are given as fold difference vs. stratum lucidum of untreated euploid mice. Values in B and D represent mean \pm standard deviation (SD). ** $P < 0.01$; *** $P < 0.001$ (Duncan's test after ANOVA).

A comparison between treated and untreated euploid mice showed that the former had significantly more SYN puncta (+38%) than the latter (Fig. 25D), suggesting an increase in the number of synaptic terminals also in euploid mice.

4.11 Effect of fluoxetine on glutamatergic innervation in the stratum lucidum of euploid and Ts65Dn mice

The granule cells use glutamate as a neurotransmitter. Their axons form large complex “mossy” synapses on the thorny excrescences covering the proximal apical dendritic shaft of CA3 pyramidal neurons. In addition, the granule cell axons give origin to thin filopodial extensions and small en passant boutons onto local circuit inhibitory interneurons primarily located within the stratum lucidum ((2); (109)) (Fig. 9B).

To establish the effect of trisomy and treatment on the glutamatergic input we evaluated the glutamate vesicular transporter 1 (VGLUT1) levels in the hippocampal formation (dentate gyrus plus hippocampus proper) using Western blot analysis. Results showed that Ts65Dn mice had reduced VGLUT1 levels that were restored with treatment (Fig. 26A,B). VGLUT1 levels also increased in treated euploid mice and became higher than in untreated euploid mice (Fig. 26A,B).

To specifically establish the effect of trisomy and treatment on the glutamatergic terminals from the DG, we evaluated immunoreactivity for the glutamate vesicular transporter 1 (VGLUT1) in the stratum lucidum of treated and untreated mice. Fig. 26C shows representative images from animals of each group. It can be noted that the immunoreactivity for VGLUT1 was reduced in Ts65Dn mice compared to untreated euploid mice and that treatment with fluoxetine increased VGLUT1 immunoreactivity both in Ts65Dn and euploid mice. In untreated Ts65Dn mice the OD of VGLUT1 was significantly lower (-25%) than in untreated euploid mice (Fig. 26D). In Ts65Dn mice treated with fluoxetine, the OD of VGLUT1 underwent an increase and became similar to that found in untreated euploid mice (Fig. 26D).

The OD of VGLUT1 also increased by 66% in treated euploid mice compared with untreated euploid mice (Fig. 26D).

The stratum lucidum harbors, in addition to excitatory projections from the granule cells of the DG, inhibitory interneurons that impinge upon the proximal shaft of field CA3 pyramidal neurons ((2), (109)). In order to establish the effect of trisomy and treatment on the relative abundance of glutamatergic terminals we examined the co-localization of SYN and VGLUT1 in the stratum lucidum of treated and untreated mice.

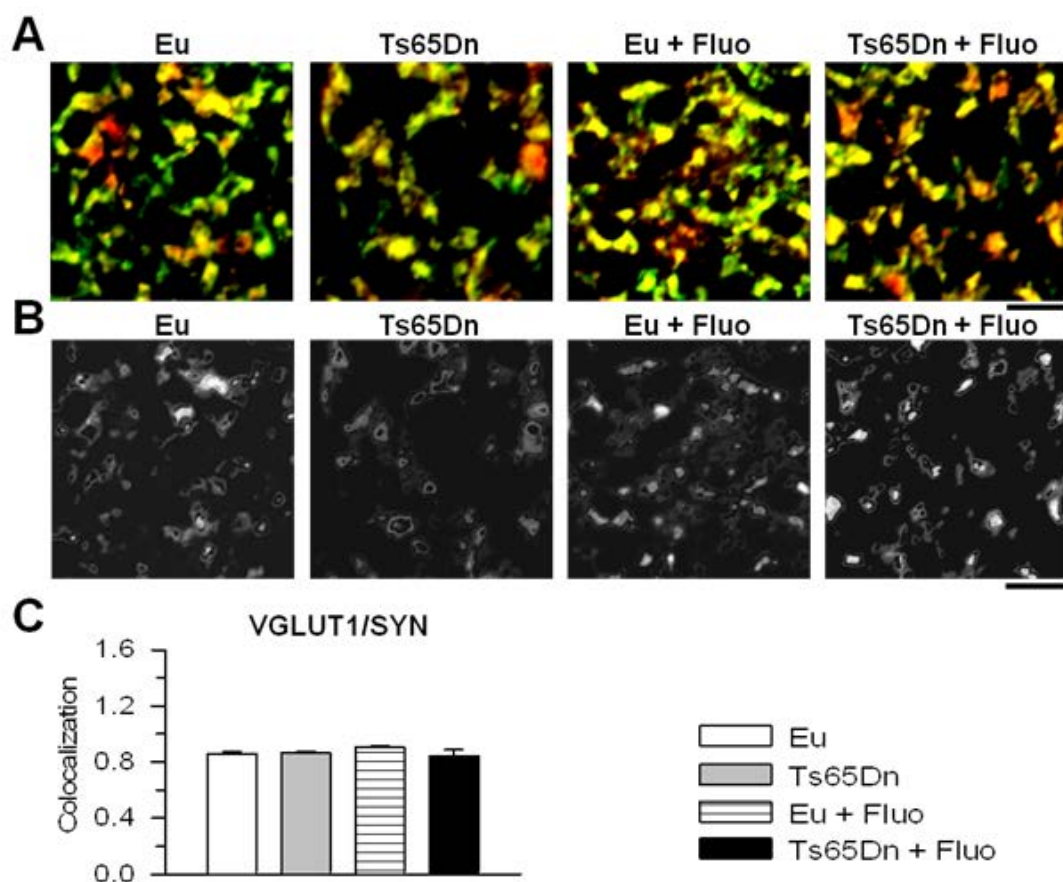


Figure 27 - Effect of fluoxetine on the glutamatergic innervation in stratum lucidum of field CA3. A, B: Images, taken with the confocal microscope, of sections processed for double-labeling immunofluorescence with an anti-synaptophysin antibody (green) and an anti-VGLUT1 antibody (red) from the stratum lucidum of an animal from each experimental group. Images in (B) represent colocalization (white) between these two markers. Images correspond to the same images shown in Figure 24C. Scale bar = 5 μ m. C: Coefficient of colocalization of synaptophysin (SYN) and VGLUT1 in stratum lucidum of untreated euploid, untreated Ts65Dn, treated euploid and treated Ts65Dn mice. Values in B and D represent mean \pm standard deviation (SD). (Duncan's test after ANOVA).

Fig. 25A shows representative images processed for double-labeling immunofluorescence with an anti-synaptophysin antibody (green) and an anti-VGLUT1 antibody (red) and Fig. 27B shows the colocalization (white) of these markers. We found no differences among groups in the colocalization of SYN and VGLUT1 (Fig. 26C). The colocalization coefficient had a high value (approximately 0.8), which is consistent with the prevalence of glutamatergic projections to the stratum lucidum. The similarity in the co-localization coefficient between euploid and Ts65Dn mice indicates that, though in trisomic mice there were fewer synaptic terminals, the ratio of glutamatergic (excitatory) and non-glutamatergic (inhibitory) synapses was similar to that of euploid mice. Likewise, in trisomic and euploid mice treated with fluoxetine, the finding that the co-localization coefficient was unchanged in comparison with the untreated counterparts indicates that the overall increase in the number of synaptic contacts involved, in a proportional manner, excitatory and inhibitory synapses.

4.12 Effect of fluoxetine on basal synaptic input in CA3 neurons

“Miniature” synaptic events reflect the spontaneous release of neurotransmitters from all presynaptic terminals converging on the recorded neuron. The frequency of these events is related to the total number of presynaptic terminals and the probability of release at each terminal. To functionally evaluate the basal excitatory and inhibitory synaptic input to CA3 pyramidal neurons, we recorded spontaneous miniature excitatory postsynaptic currents (mEPSCs) and miniature inhibitory postsynaptic currents (mIPSCs) from individual pyramidal neurons by performing whole-cell, patch-clamp experiments in the voltage-clamp mode. Miniature events were recorded in the presence of tetrodotoxin (TTx, 1 μ M) in the perfusing solution, so as to prevent spontaneous synaptic events due to presynaptic action-potential firing. In each cell, mEPSC and mIPSC activity was continuously recorded for a period of at least 5 min and up to 10 min.

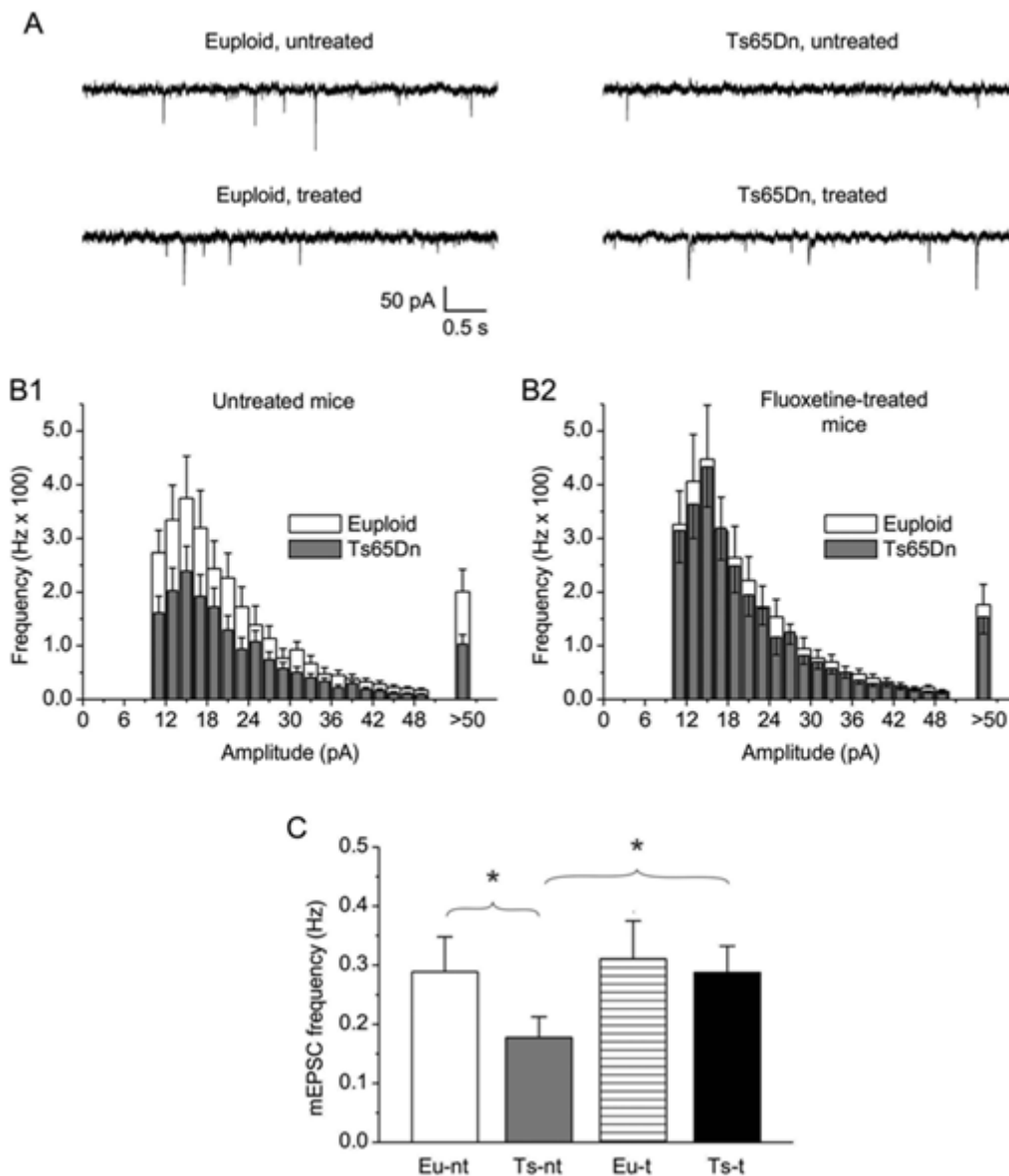


Figure 28 - Effect of fluoxetine on mEPSC frequency in CA3 pyramidal neurons. A: Exemplary current tracings recorded in the gap-free mode in four representative cells from untreated euploid and Ts65Dn mice and euploid and Ts65Dn mice treated with fluoxetine, showing mEPSC activity. B: Average frequency- distribution diagrams of mEPSC amplitude for untreated euploid and Ts65Dn mice (B1) and euploid and Ts65Dn mice treated with fluoxetine (B2). Numbers of observations are: 8 (euploid, untreated mice), 4 (Ts65Dn, untreated mice), 7 (euploid, fluoxetine-treated mice), and 5 (Ts65Dn, fluoxetine- treated mice) (these values indicate the number of animals of each group from which recordings were obtained; 2 to 4 cells were recorded from each animal). C: Average, overall mEPSC frequency in the four animal groups (n: as above). One-way ANOVA revealed the existence of a statistically significant difference among groups ($P = 0.007$). *, $P < 0.05$ (Bonferroni post-test; the same test also revealed a significant difference, at the 0.01 level, between Ts65Dn, untreated mice and euploid, fluoxetine-treated mice).

For mEPSC recording, the holding potential was set at -70 mV, a level that, under our experimental conditions, was close to the theoretical equilibrium potential of chloride ions (-71.5 mV), and therefore to the reversal potential of GABAergic currents: this allowed for mEPSC recording in

virtual isolation from mEPSCs. Fig. 28A shows examples of mEPSCs recorded, under the above conditions, in representative cells from untreated and fluoxetine-treated euploid and trisomic mice.

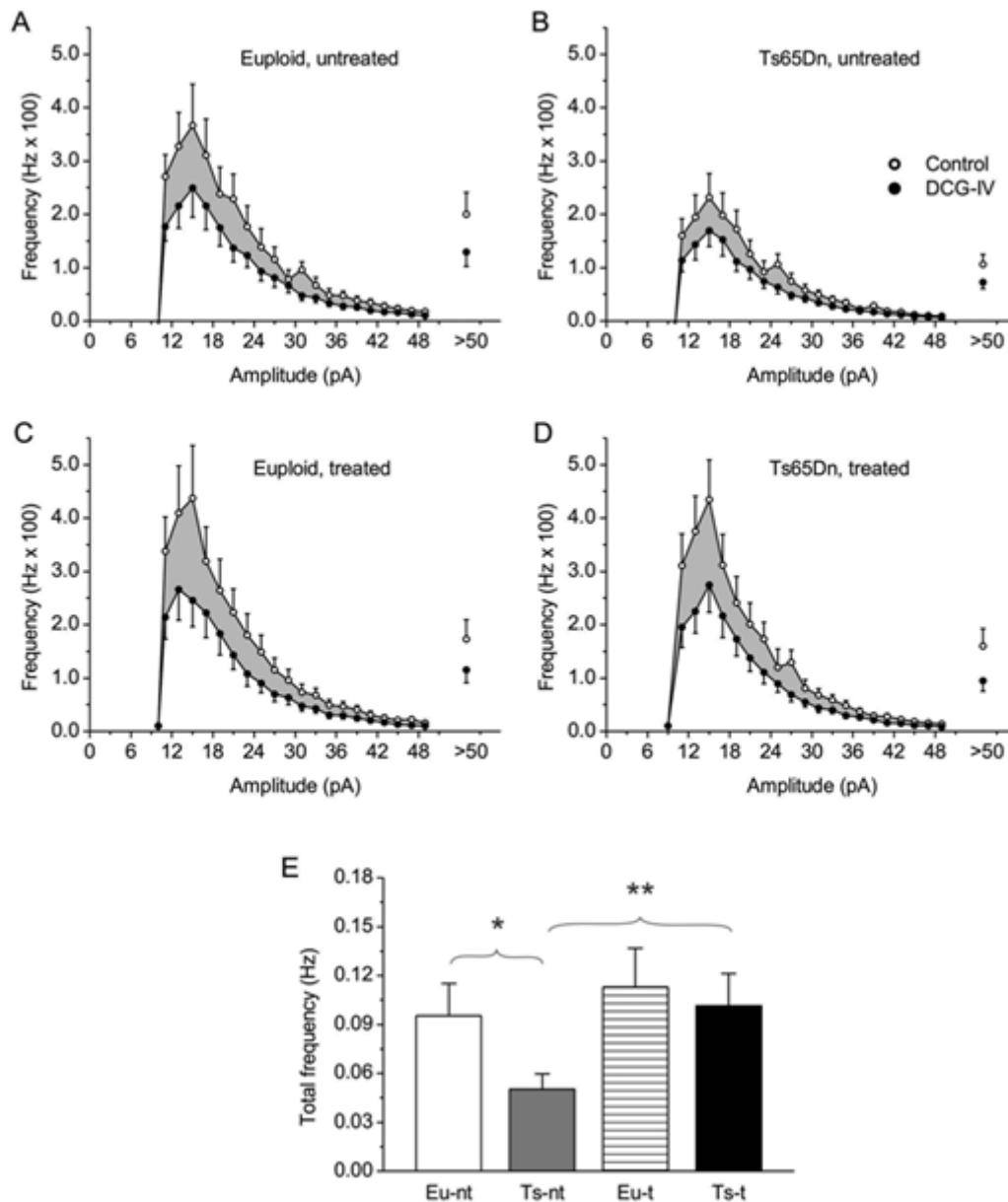


Figure 29 - Effects of fluoxetine on mEPSCs due to mossy-fiber input to CA3 pyramidal neurons. A–D: Average frequency-distribution diagrams of mEPSC amplitude for untreated euploid (A) and Ts65Dn (B) mice, and fluoxetine-treated euploid (C) and Ts65Dn (D) mice, before (open symbols) and during (filled symbols) application of the group-II metabotropic glutamate receptor (mGluR) agonist, DCG-IV plus APV. The shadowed areas correspond to the frequency of the mEPSC activity removed by this drug treatment. Numbers of observations are: 8 (euploid, untreated mice), 4 (Ts65Dn, untreated mice), 6 (euploid, fluoxetine-treated mice), and 5 (Ts65Dn, fluoxetine-treated mice). E: Average, overall frequency of the mEPSC activity removed by DCG-IV+APV treatment, obtained by subtraction, in the four animal groups (n: as above). One-way ANOVA revealed the existence of a statistically significant difference among groups ($P < 0.001$). * and **, $p < 0.05$ and 0.01 , respectively (Bonferroni post-test; the same test also revealed a significant difference, at the 0.001 level, between Ts65Dn, untreated mice and euploid, fluoxetine-treated mice).

No spontaneous synaptic events were observable any longer after application of the glutamatergic inhibitors, NBQX (10 μ M)+APV (50 μ M) (n=4 cells; not shown). Due to baseline noise levels normally observed at -70 mV, events of less than 10 pA in peak amplitude were ignored. Accepted events were then used to construct frequency-distribution diagrams of mEPSC amplitude. Data were averaged among the cells from each animal (n = 2 to 4), and then among the animals pertaining to the same experimental group (untreated euploid or trisomic mice, fluoxetine-treated euploid or trisomic mice). The plots thus obtained are shown in Fig. 28B. In untreated mice, the trisomic condition was associated with a clear reduction in mEPSC frequency for all amplitude classes, with no evident changes in frequency-distribution shape (Fig. 28B1), in accordance with previous observations (85). The overall mEPSC frequency was significantly reduced in trisomic animals by ~39% (Fig. 28C).

The frequency distribution of mEPSC amplitude was also qualitatively similar in fluoxetine-treated mice (Fig. 28B2).

The overall mEPSC frequency was found to be slightly, albeit non significantly, higher in fluoxetine-treated euploid mice than in untreated euploid mice. However, in fluoxetine-treated trisomic mice it was significantly higher than in untreated trisomic mice and not significantly different from the mEPSC frequency found in euploid untreated or treated mice (Fig. 28C).

The above data show that in trisomic animals fluoxetine treatment increased the basal, excitatory synaptic input to pyramidal CA3 neurons to nearly normal levels. The sources of this synaptic input include both granule-cell mossy fibers and association afferents from other pyramidal neurons.

To ascertain whether the synaptic input specifically due to mossy fibers was restored in fluoxetine-treated trisomic animals, we adopted the same experimental strategy described by Hanson et al. (85).

In a subset of cells of each animal group, after mEPSC recording under basal conditions, the group-II metabotropic glutamate receptor (mGluR) agonist, DCG-IV (3 μ M) was applied in association

with the NMDA-receptor antagonist, APV (50 μ M). Under these conditions, group-II mGluR activation is known to selectively inhibit synaptic transmission in mossy-fiber inputs (85) but not in associational connections (97).

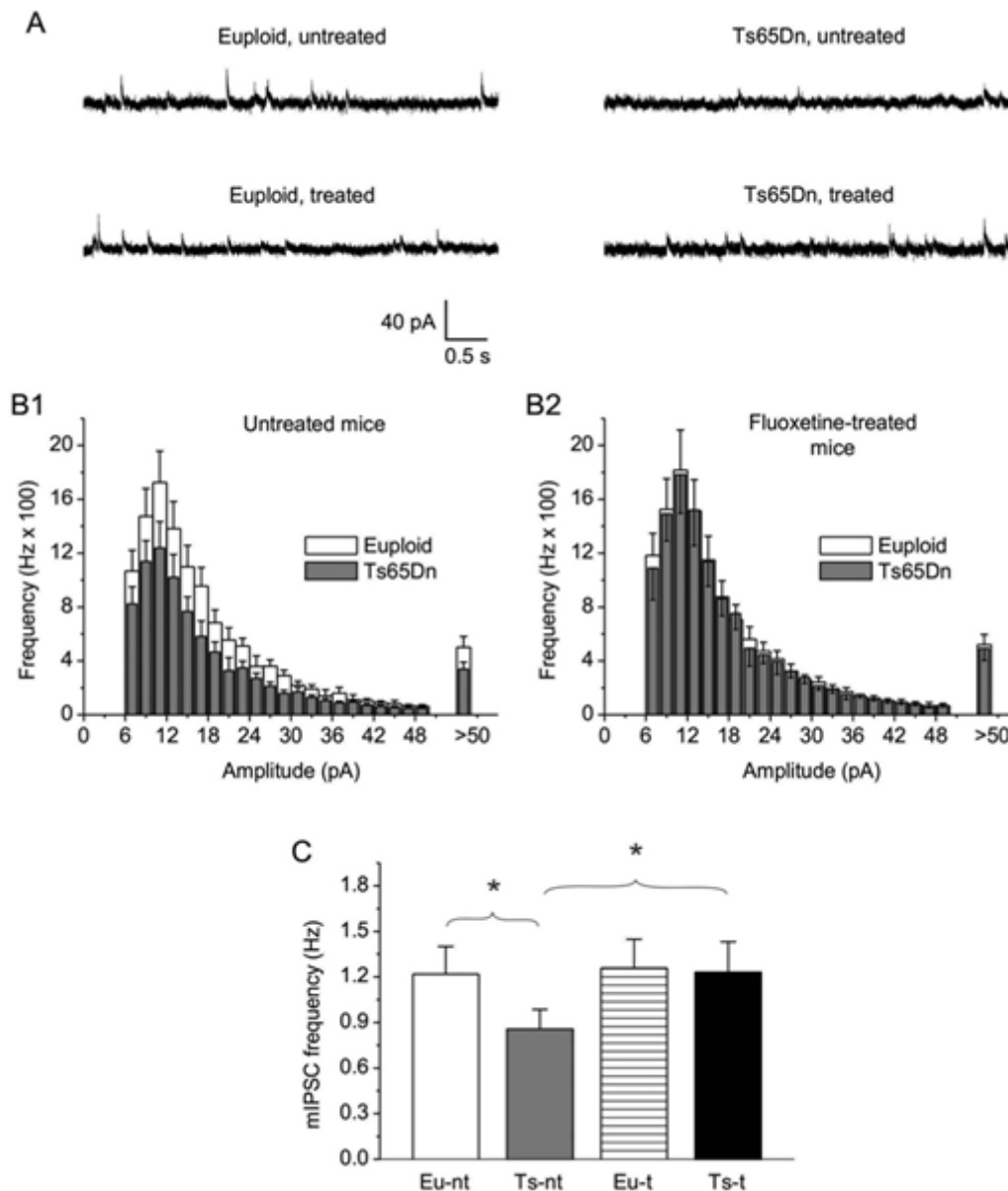


Figure 30 - Effects of fluoxetine on mIPSC frequency in CA3 pyramidal neurons. A: Exemplary current tracings recorded in the gap-free mode in four representative cells from untreated euploid and Ts65Dn mice and euploid and Ts65Dn mice treated with fluoxetine, showing mIPSC activity.

B: Average frequency-distribution diagrams of mIPSC amplitude for untreated euploid and Ts65Dn mice (B1) and euploid and Ts65Dn mice treated with fluoxetine (B2). Numbers of observations are: 8 (euploid, untreated mice), 4 (Ts65Dn, untreated mice), 7 (euploid, fluoxetine-treated mice), and 5 (Ts65Dn, fluoxetine-treated mice). C: Average, overall mIPSC frequency in the four animal groups (n: as above). One-way ANOVA revealed the existence of a statistically significant difference among groups ($P < 0.01$). *, $P < 0.05$ (Bonferroni post-test; the same test also revealed a significant difference, at the 0.05 level, between Ts65Dn, untreated mice and euploid, fluoxetine-treated mice).

DGC-IV+APV application markedly reduced mEPSC frequency at all amplitude classes in each animal group (Fig. 29A-D). The mEPSC activity abolished by DGCIV, quantified by subtracting the overall mEPSC frequency in the presence of DCG-IV+APV from the overall mEPSC frequency in control conditions, was significantly reduced in untreated trisomic animals as compared to euploid animals, but was restored to nearly normal levels in fluoxetine-treated trisomic animals (Fig. 29E). These results suggest that fluoxetine treatment was able to recover functionally normal synaptic inputs from mossy fibers in CA3 pyramidal neurons.

mIPSCs were recorded by setting the holding potential at 0 mV, a level close to the reversal potential of glutamatergic currents, which allowed for virtual elimination of visible mEPSC activity. Examples of mIPSCs recorded in representative cells from the four animal groups considered are shown in Fig. 30A. mIPSC activity was abolished by application of the GABA_A-ergic inhibitor, bicuculline (20 μM) (n =3 cells; not shown). Detected events of >6 pA in peak amplitude were used to construct frequency-distribution diagrams of mIPSC amplitude, and data were averaged among cells from each animal (n = 2 to 4) and then among animals, as above (Fig. 30B).

In untreated mice, the trisomic condition was associated with a significant reduction (~30%) in mIPSC frequency (Fig. 30B1, C), again in accordance with previous observations (85).

Fluoxetine treatment of trisomic mice restored mIPSC frequency to levels not significantly different from those observed in euploid animals (Fig. 30B2, C).

4.13 Effect of fluoxetine on BDNF expression

Neurotrophins and, in particular, the brain-derived neurotrophic factor (BDNF) are important regulators of neuronal plasticity. Synaptic reorganization mediated by BDNF is thought to be a critical process which shapes neuronal networks. Reduced BDNF expression has been documented in the frontal cortex of Ts65Dn mice (29). We previously found that in the hippocampus of Ts65Dn

mice aged 15 days BDNF expression was lower than in euploid mice and that BDNF levels were restored by treatment with fluoxetine (28).

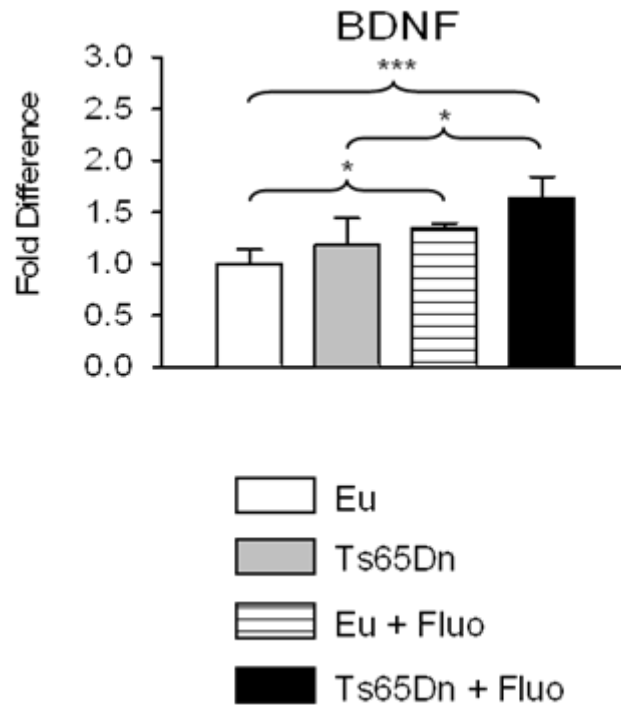


Figure 31 - Effect of fluoxetine on hippocampal BDNF levels. RNA expression levels of BDNF, quantified by RT-qPCR, in homogenates of the hippocampal formation from untreated euploid, untreated Ts65Dn, treated euploid and treated Ts65Dn mice. Data are given as fold difference in comparison with untreated euploid mice. Values represent mean \pm standard deviation (SD). * $P < 0.05$; *** $P < 0.001$ (Duncan's test after ANOVA).

This suggests that reduced BDNF levels may take part in developmental alterations in the trisomic brain and that restoration of BDNF levels may be a determinant of the beneficial effects of treatment with fluoxetine. We evaluated here BDNF levels in the hippocampus of mice aged 45 days. At this age, we found no differences in BDNF levels between untreated euploid and Ts65Dn mice (Fig. 31). Normal BDNF levels have been detected in the hippocampus of adult mice, (141) suggesting that failure of BDNF production is not a permanent defect in the trisomic hippocampus. However, after treatment with fluoxetine in the period P3-P15, Ts65Dn mice and euploid mice aged 45 days exhibited higher BDNF levels than the untreated counterparts (Fig. 31). This increase was approximately +35% in treated vs. untreated euploid mice, and +38% in treated vs. untreated

Ts65Dn mice. The increase in BDNF levels in treated mice is consistent with the effects of antidepressants on brain BDNF expression (115).

5. DISCUSSION

The current study provides novel evidence that a brief pharmacological therapy with fluoxetine in the early postnatal period fully rescues dendritic pathology and connectivity in the hippocampal DG of the Ts65Dn mouse model of DS. This study also shows that in Ts65Dn mice the connectivity from the granule cells to field CA3 is impaired and that neonatal treatment with fluoxetine restores the anatomy and function of the mossy fiber system, in parallel with total granule cell number.

In view of the key role of DG and CA3 in declarative memory, these effects are essential for the recovery of the trisynaptic network properties and, hence, of hippocampus-dependent memory performance.

In untreated Ts65Dn mice, newborn (DCX-positive) granule cells had abnormally long branches of low order and very few branches of higher order (Fig. 14). The dendritic architecture of the **newborn granule cells** of Ts65Dn mice treated with fluoxetine underwent notable changes. In particular, total dendritic length notably increased and became even larger than that of untreated euploid mice (Figure 12I). This effect was due to a full restoration of the mean branch length and of the number of branches of all orders. Importantly, after treatment with fluoxetine both these dendritic parameters became similar to those of untreated euploid mice and the absence of high order branches was compensated by the *de novo* appearance of high order branches. Consequently, the total length of all individual orders became similar or even larger than that of untreated euploid mice (Figure 13).

The dendritic architecture of the **older granule cells** of untreated Ts65Dn mice, examined in Golgi-stained material, closely recapitulated the proximodistal defects of newborn granule cells. (Fig.17). This indicates that dendritic hypotrophy starts at the initial stages of granule cell development and is retained at later stages. Also in the older granule cells of Ts65Dn mice there was a restoration of the

excessive length of low order branches, an increase in the number of branches of intermediate order and the *de novo* appearance of highest order branches after treatment with fluoxetine. Because of these readjustments, the total length of the dendritic tree (Fig. 15I) and its architecture (Fig. 17) were fully restored. Moreover, in trisomic mice treated with fluoxetine there was a full restoration in **spine density** both in the inner half (Fig. 18E) and outer half (Fig. 18F) of the molecular layer of DG, which may also notably concur to a more efficient processing of signals.

In view of the restoration of both dendritic architecture and spine density it is expected that after treatment with fluoxetine the superficial granule cells of trisomic mice process entorhinal signal in a manner similar to that of the untreated euploid counterpart.

5.1 *Fluoxetine rescues connectivity of trisomic granule cells*

SYN immunohistochemistry revealed an overall reduction of the inputs to the molecular layer in trisomic mice (Fig. 19D). Since synaptogenesis and neuron maturation take place in the first few postnatal weeks, treatment with fluoxetine during this critical time window is expected to have a significant impact on altered connectivity in the trisomic brain. Consistently with this idea, we found that, after treatment with fluoxetine, Ts65Dn mice showed an increase in SYN IR throughout the molecular layer. Although it cannot be ruled out that an increase in SYN expression may be due to increased levels of the protein contained in individual synapses, the increase in the number of dendritic spines in treated trisomic mice is consistent with a treatment-induced increase in the overall connectivity of the molecular layer. VGLUT1 immunohistochemistry showed that in trisomic mice the glutamatergic input to the molecular layer was reduced, which is consistent with the paucity of dendrites and spines of trisomic granule cells. Consistently with restoration of the dendritic arbor, treated trisomic mice underwent an increase in the glutamatergic input (Fig. 20I). Perforant path fibers convey signals from the entorhinal cortex to the granule cells (10) and the hippocampal processing of these signals is essential for long-term declarative memory. Current

results suggest that reduction of the glutamatergic input from the entorhinal cortex may be a key determinant of memory impairment in trisomic mice. It is likely that recovery of this input contributes to the rescue of hippocampus-dependent memory performance previously observed in trisomic mice treated with fluoxetine (28).

5.2 *Fluoxetine normalizes DSCAM levels in the DG of Ts65Dn mice*

The abnormally long low-order dendritic branches and the scanty number of higher-order branches in trisomic granule cells suggest that dendritic hypotrophy is due to the failure of the mechanism/s that trigger dendritic branching. We found over-expression of DSCAM IR in the DG of trisomic mice and that fluoxetine restored DSCAM levels (Fig. 21B,G). This suggests that the dendritic hypotrophy of the trisomic brain is underpinned by DSCAM over-expression and that fluoxetine rescues this defect by reducing DSCAM levels.

DSCAM mRNA is translated at dendritic level through an NMDA dependent mechanism. NMDAR activation increases dendritic levels of DSCAM protein, while NMDAR inhibition has an opposite effect (9). Interestingly, serotonin appears to suppress NMDAR function by activating the 5-HT1A receptor (213). This provides a potential mechanism whereby fluoxetine restores dendritic development in trisomic mice. The impairment of the serotonergic system in trisomic mice (see above) implies a reduced suppression of NMDAR function, which, in turn, may lead to high levels of DSCAM protein. Increased serotonin availability, following treatment with fluoxetine, may reduce NMDAR function, which, in turn, may reduce DSCAM protein levels, thereby restoring dendritic branching.

5.3 Restoration of granule cell dendritic development parallels restoration of the serotonergic system

The dendritic branching pattern of trisomic DCX-positive cells was rescued by fluoxetine (Fig. 11 and 12). This indicates a positive impact of treatment on neurons born after the end of treatment.

The time course of granule cell development (215) implies that the cells we sampled in the outer granule cell layer of mice aged 45 days were exposed to treatment during the early period of their dendritic maturation. The full dendritic recovery of these cells in treated trisomic mice shows that a relatively short period of treatment (13 days) was sufficient to rescue dendritic development, and that this effect was retained for up to 1 month after treatment cessation.

Serotonin is fundamental for granule cell dendritic development through the 5-HT_{1A} receptor, and the first 2 postnatal weeks represent a critical time window for serotonin action (210). We previously found that in P15 trisomic mice, the serotonergic system was impaired because of reduced expression of the 5-HT_{1A} receptor, but with normal levels of serotonin (28). We found here that the expression of the 5-HT_{1A} receptor, which was reduced at P2 and P15, recovered by P45 (Fig. 22D). In P45 trisomic mice, however, the serotonergic system was impaired because of a reduced serotonin level (Fig. 22A). In a study of euploid and Ts65Dn mice by Megias et al (122), no differences in the cellularity of the dorsal and medial raphe nuclei (the source of the serotonergic input to the forebrain) were detected. In view of the reduced dendritic surface of trisomic granule cells, it is likely that the reduced serotonin levels in trisomic mice are the result of a reduction in the number of serotonergic terminals. The finding that in treated trisomic mice serotonin levels became similar to those in euploid mice suggests recovery of the serotonergic input (Fig. 22A).

The reduced expression of the 5HT_{1A} receptor at P2 and P15 (Fig. 22E), a time when most of the granule cells are beginning maturation, is likely to adversely affect dendritic growth, in spite of normal serotonin levels. The outcome of a reduced dendritic growth is a reduction in the number of synaptic contacts established by afferent systems to the granule cells, including the serotonergic system. A reduction in the serotonergic input causes, in turn, a reduction in serotonin levels and,

hence, further impairs dendritic development. Thus, for different reasons, the serotonergic system appears to be altered across critical phases of granule cell formation and maturation. The system begins to be deranged because of a low expression of the 5-HT1A receptor. This defect leads to a negative process that reinforces itself with time: the fewer the dendrites, the fewer the serotonergic synaptic contacts, and so on.

Treatment with fluoxetine in the P3–P15 period restored the expression of the 5-HT1A receptor in P15 trisomic mice (28) and, as found here, restored serotonin levels in P45 mice. By the same line of reasoning used above, normalization of the 5-HT1A receptor at P15 may be fundamental in order to trigger proper dendritic development during the early phases of granule cell maturation and to prevent the entry in the vicious cycle mentioned above. Namely, early normalization of the dendritic material may favor the establishment of a proper number of synaptic contacts with serotonergic terminals. Correct serotonin levels will further favor dendritic growth and, consequently, create a milieu, which is favorable for the dendritic formation of granule cells born after treatment cessation.

5.4 Impaired connectivity in the stratum lucidum of field CA3 of Ts65Dn mice

In Ts65Dn mice, consistently with the reduced number of granule cells in the DG (28) and, hence, a reduction in mossy fiber axons, the thickness of the mossy fiber bundle in the stratum lucidum of CA3 was reduced in comparison with that of euploid mice (Fig. 24E). In agreement with previous evidence (106), we found that Ts65Dn mice had overall fewer synaptic terminals and fewer glutamatergic terminals in the stratum lucidum (Fig. 25B,D and Fig. 26D) The density reduction of the glutamatergic terminals is consistent with the reduced number of granule cells that are the source of the glutamatergic input to the stratum lucidum. Since excitatory inputs terminate on dendritic spines, the reduced spine density on the thorny excrescences of trisomic mice (Fig. 24B) is the counterpart of the reduced density of the glutamatergic terminals. Consistently with the

hypotrophy of the glutamatergic system in the stratum lucidum, in Ts65Dn mice mEPSC frequency was notably reduced (Fig. 29E).

Taken together these data indicate a reduced excitatory drive from the granule cells to the pyramidal neurons of CA3 and, consequently, impaired signal processing. The mossy fibers additionally innervate inhibitory interneurons in the stratum lucidum that exert a feedforward inhibitory control on pyramidal neuron discharge ((2), (109)). If the reduction in the density of the glutamatergic terminals in the stratum lucidum of Ts65Dn mice includes synapses on inhibitory interneurons, this will result in a reduction in feedforward inhibition, matching the reduction in direct excitation. In field CA3 of Ts65Dn mice there was a reduction in the frequency of mIPSCs, which is in line with the reduction in the density of non-glutamatergic synapses in the stratum lucidum and suggests a reduced inhibitory control on CA3 pyramidal neurons (Fig. 30C). It is important to note that, though in absolute terms Ts65Dn mice had fewer excitatory and inhibitory synaptic contacts, the ratio of these inputs was similar to that of euploid mice (Fig. 27C) This confirms that in field CA3, unlike in the dentate gyrus (103), a shift towards over-inhibition is not present (85).

5.5 Fluoxetine restores the mossy fiber projections and functional connectivity in the stratum lucidum of Ts65Dn mice

In agreement with the treatment-induced restoration of total granule cell number (28), the thickness of the mossy fiber bundle of treated Ts65Dn mice underwent an increase and became similar to that of euploid mice (Fig. 24E). Moreover, after treatment with fluoxetine, Ts65Dn mice showed an increase in the overall number of synaptic terminals in the stratum lucidum (Fig. 25B,D). This increase was due to a proportionally similar increase in the number of glutamatergic and non glutamatergic terminals (Fig. 27C). In parallel, in Ts65Dn mice there was an increase in spine density on the proximal shaft of CA3 pyramidal neurons in the stratum lucidum (Fig. 23B). These

two effects were accompanied by an increase in the frequency of mEPSC, indicating that the new connections were functionally effective (Fig. 28E).

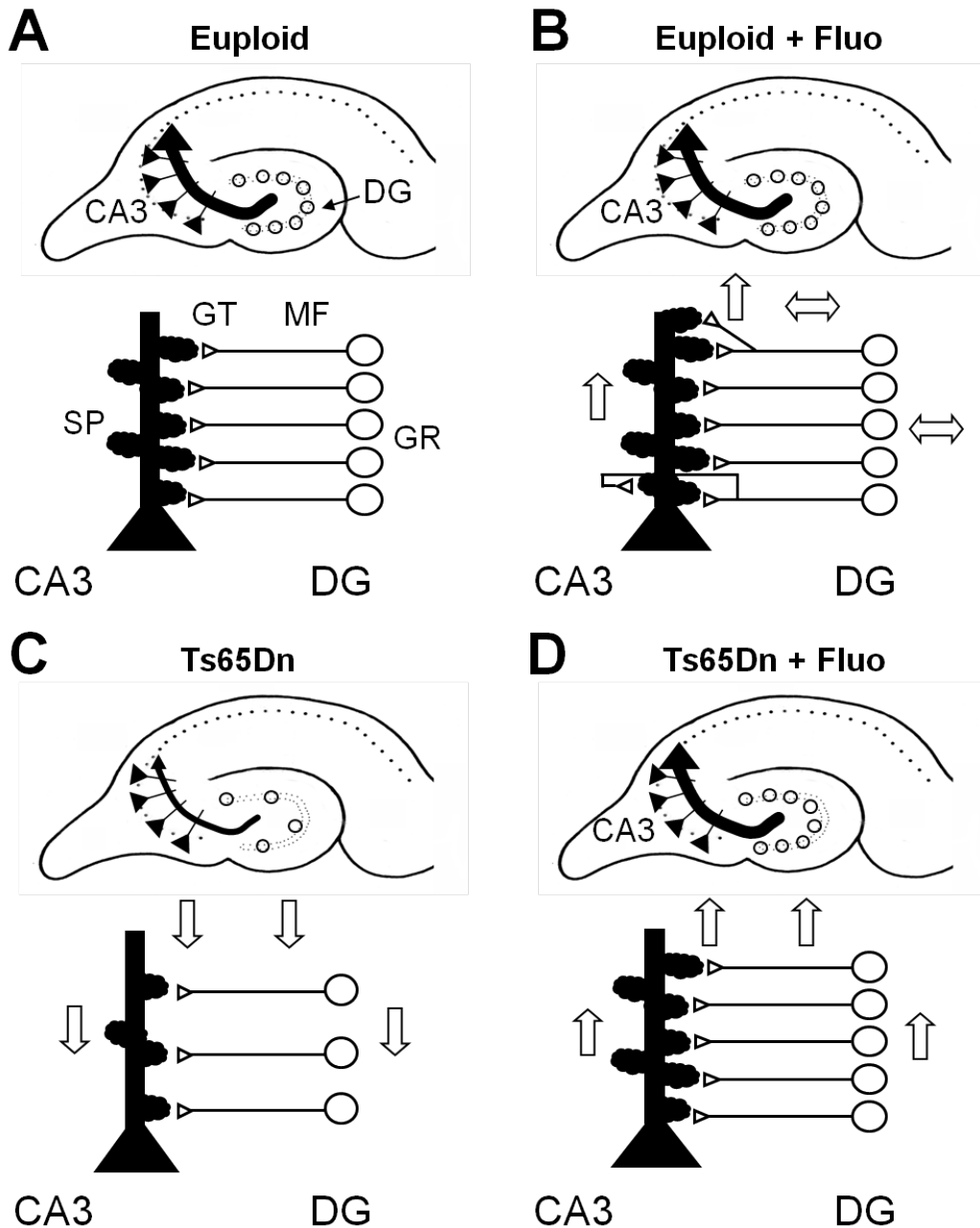


Figure 32 - Summary of the effect of fluoxetine on connectivity in the stratum lucidum. A–D: Connectivity between the dentate gyrus (DG) and field CA3 in euploid mice (A), euploid mice treated with fluoxetine (B), Ts65Dn mice (C) and Ts65Dn mice treated with fluoxetine (D). Ts65Dn mice have a reduced number of granule cells (GC), mossy fibers (MF), glutamatergic terminals (GT) in the stratum lucidum and spines (SP) on the thorny excrescences (C). Treatment with fluoxetine rescues all these defects and restores the input from the DG to CA3 (D). The direction of the arrows indicates the direction of the defect and the effect of the therapy in comparison with untreated euploid mice. The double-headed arrows indicate no effect.

Importantly, in treated Ts65Dn mice there was also an increase in the frequency of mIPSCs, indicating an increase in the inhibitory input to the pyramidal cells (Fig. 30C). In the stratum lucidum of field CA3, feedforward inhibition is fundamental for shaping the pattern and duration of pyramidal neuron discharge in response to the mossy fiber input (109).

A reduction in feedforward inhibition would lead to excessive recruitment of pyramidal cells and predisposition to epileptiform activity. It appears, thus, of relevance that in treated trisomic mice the increase in the number of excitatory synapses was matched by a parallel increase in the inhibitory input. The fully recovery of the input from the DG to field CA3 is summarized in Fig. 31.

5.6 BDNF may contribute to synaptic remodeling in field CA3 of Ts65Dn mice treated with fluoxetine

BDNF is one of the most potent modulators of synaptic plasticity and spine formation (39);. The mossy fiber pathway contains the highest levels of BDNF in the CNS, and BDNF appears to regulate both direct excitatory and indirect inhibitory inputs to CA3 pyramidal cells (53). The increase in BDNF levels in trisomic mice treated with fluoxetine (Fig. 31) suggests that BDNF may concur, in conjunction with the increase in the number of mossy fibers, to favor the formation of glutamatergic synapses. BDNF is also present in mossy fiber terminals contacting inhibitory neurons (53), suggesting that the increase in the inhibitory innervation in the stratum lucidum of treated Ts65Dn mice may also be mediated by mossy fiber BDNF.

5.7 Fluoxetine has moderate or no effects in euploid mice

In euploid mice, fluoxetine caused an increase in SYN levels in the DG similar to trisomic mice (Fig. 19D). Treatment, however, had smaller effects on dendritic length and spine density of the granule cells than in trisomic mice (Fig. 12I, 15I and Fig. 18E,F). The oldest granule cells of

euploid mice even underwent a reduction in the number of some branches. Likewise, no effects of fluoxetine were observed on serotonin and DSCAM levels (Fig. 22A and Fig. 21B).

The thickness of the mossy fiber bundle was not affected by treatment in euploid mice (Fig. 24E), which fits with the absence of a significant increase in total granule cell number (28). The large increase in synaptophysin immunoreactivity in the stratum lucidum of treated euploid mice (Fig. 25B) was accompanied by a more moderate increase in the number of synaptophysin immunoreactive puncta (Fig. 25D) and the large increase in VGLUT1 immunoreactivity (Fig. 26D) was accompanied by a less prominent increase in spine density (Fig. 23B). The similarity in the colocalization coefficient of synaptophysin and VGLUT1 between treated and untreated euploid mice suggests that, similarly to trisomic mice, treatment increased glutamatergic and nonglutamatergic terminals in a proportional manner (Fig. 27C). In treated euploid mice, the frequency of mEPSCs and mIPSCs underwent a moderate but not statistically significant increase, suggesting that among the surplus of synaptic terminals there were silent terminals (Fig. 29E and Fig. 30C).

It is possible that a relatively short period of treatment, such as the one used here, has large effects on brain plasticity under adverse brain conditions but weaker effects in the normal brain. The idea that the impact of fluoxetine on normal animals may have relatively scarce advantages, or even disadvantages, is strengthened by the observation that in euploid but not in trisomic mice treatment with fluoxetine caused a reduction in brain weight and no improvement in hippocampus-dependent memory performance (28).

5.8 Conclusions

Neuron generation and dendritic maturation with consequent alteration in connectivity are heavily compromised in DS. Thus, therapies to improve brain development should be aimed at restoring all these processes. Treatment with fluoxetine in adult Ts65Dn mice has been shown to restore

neurogenesis in the DG (43). No studies have examined the effects of fluoxetine during adulthood on dendritic architecture and connectivity. It should be noted that treatments in adulthood are likely to moderately impact on brain cellularity and wiring that mainly occur in the very early phases of brain development. We previously found that neonatal treatment with fluoxetine fully restores hippocampal neurogenesis and memory performance in trisomic mice (28).

Current results show that treatment with fluoxetine restores dendritic architecture and spine density of trisomic granule cells, indicating that the same treatment is able to restore not only the number of granule neurons but also their “quality” in terms of correct maturation. Moreover, the rescue of dendritic development was accompanied by the rescue of connectivity to the DG .

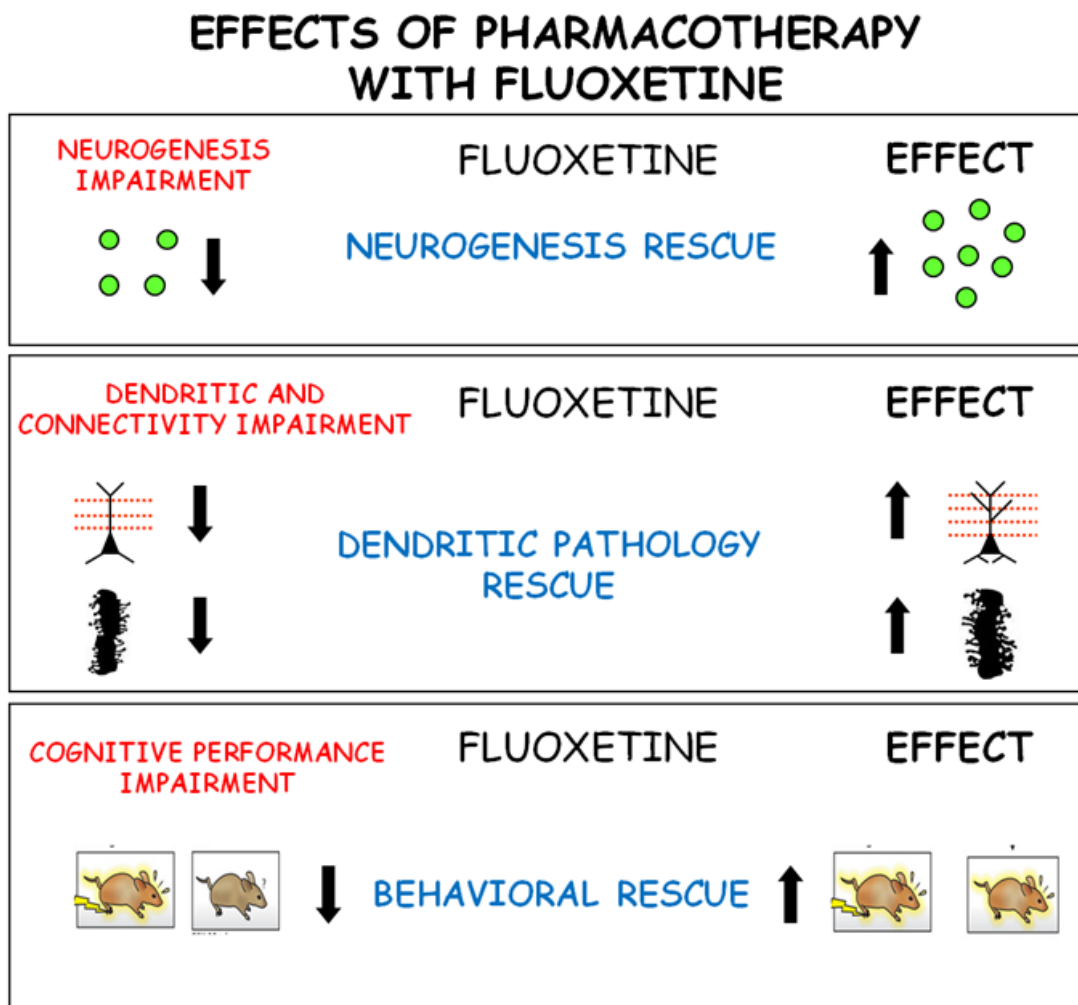


Figure 33 - Summary of the effects of neonatal treatment with fluoxetine on the hippocampal formation in Ts65Dn mice.

The fluoxetine-induced rescue of the total number of granule neurons in Ts65Dn mice (28) is an essential but not sufficient condition for the functional recovery of the trisynaptic circuit. It is equally important that the surplus of granule cells establishes appropriate synaptic contacts with CA3, the second element of the trisynaptic circuit. We found here that in trisomic mice treated with fluoxetine there was the fully recovery of the input from the DG to field CA3.

This recovery includes restoration of i) the number of granule cells and, hence, of mossy fibers; ii) the density of glutamatergic terminals in the stratum lucidum; and, iii) the density of spines forming the thorny excrescences. In addition, electrophysiological evidence showed that the increased excitatory connectivity was functionally effective and that the inhibitory input to CA3 was also restored.

Taken together, these data suggest that the restoration of cognitive performance is due not only to the rescue of neurogenesis but also to restoration of the organization of the hippocampal circuits. The widespread beneficial effects of fluoxetine on the hippocampal formation (Fig. 33) suggest that early treatment with fluoxetine can be a suitable therapy, possibly usable in humans, to restore the physiology of the hippocampal networks and, hence, memory functions. These findings may open the way for future clinical trials in children and adolescents with DS.

6. REFERENCES

1. Abraham H, Tornoczky T, Kosztolanyi G, Seress L (2001) Cell formation in the cortical layers of the developing human cerebellum. *Int J Dev Neurosci* 19:53-62.
2. Acsady L, Kamondi A, Sik A, Freund T, Buzsaki G (1998) GABAergic cells are the major postsynaptic targets of mossy fibers in the rat hippocampus. *J Neurosci* 18:3386-3403.
3. Ahn JK, Seo JM, Yu J, Oh FS, Chung H, Yu HG (2005) Down-regulation of IFN-gamma-producing CD56+ T cells after combined low-dose cyclosporine/prednisone treatment in patients with Behcet's uveitis. *Invest Ophthalmol Vis Sci* 46:2458-2464.
4. Ahn KJ, Jeong HK, Choi HS, Ryoo SR, Kim YJ, Goo JS, Choi SY, Han JS, Ha I, Song WJ (2006) DYRK1A BAC transgenic mice show altered synaptic plasticity with learning and memory defects. *Neurobiol Dis* 22:463-472.
5. Aldridge K, Reeves RH, Olson LE, Richtsmeier JT (2007) Differential effects of trisomy on brain shape and volume in related aneuploid mouse models. *Am J Med Genet A* 143A:1060-1070.
6. Altafaj X, Dierssen M, Baamonde C, Marti E, Visa J, Guimera J, Oset M, Gonzalez JR, Florez J, Fillat C and others (2001) Neurodevelopmental delay, motor abnormalities and cognitive deficits in transgenic mice overexpressing Dyrk1A (minibrain), a murine model of Down's syndrome. *Hum Mol Genet* 10:1915-1923.
7. Altman J, Bayer S (1975) Postnatal development of the hippocampal dentate gyrus under normal and experimental conditions. In: Isaacson RL and Pribram KH, editors. *The hippocampus*, Vol 1. Plenum Press, New York and London. p 95-122.:95-122.
8. Altman J, Bayer SA (1990) Prolonged sojourn of developing pyramidal cells in the intermediate zone of the hippocampus and their settling in the stratum pyramidale. *J Comp Neurol* 301:343-364.
9. Alves-Sampaio A, Troca-Marin JA, Montesinos ML (2010) NMDA-mediated regulation of DSCAM dendritic local translation is lost in a mouse model of Down's syndrome. *J Neurosci* 30:13537-13548.
10. Amaral DG, Witter MP (1995) Hippocampal formation. In: "The Rat Nervous System", G. Paxinos, Academic Press,:443-492.
11. Antonarakis SE, Lyle R, Dermitzakis ET, Reymond A, Deutsch S (2004) Chromosome 21 and down syndrome: from genomics to pathophysiology. *Nat Rev Genet* 5:725-738.
12. Arai Y, Ijuin T, Takenawa T, Becker LE, Takashima S (2002) Excessive expression of synaptotagmin in brains with Down syndrome. *Brain Dev* 24:67-72.
13. Azmitia EC, Rubinstein VJ, Strafaci JA, Rios JC, Whitaker-Azmitia PM (1995) 5-HT1A agonist and dexamethasone reversal of para-chloroamphetamine induced loss of MAP-2 and synaptophysin immunoreactivity in adult rat brain. *Brain Res* 677:181-192.
14. Bahn S, Mimmack M, Ryan M, Caldwell MA, Jauniaux E, Starkey M, Svendsen CN, Emson P (2002) Neuronal target genes of the neuron-restrictive silencer factor in neurospheres derived from fetuses with Down's syndrome: a gene expression study. *Lancet* 359:310-315.
15. Bairy KL, Madhyastha S, Ashok KP, Bairy I, Malini S (2007) Developmental and behavioral consequences of prenatal fluoxetine. *Pharmacology* 79:1-11.
16. Banasr M, Hery M, Printemps R, Daszuta A (2004) Serotonin-induced increases in adult cell proliferation and neurogenesis are mediated through different and common 5-HT receptor subtypes in the dentate gyrus and the subventricular zone. *Neuropsychopharmacology* 29:450-460.

17. Bar-Peled O, Gross-Isseroff R, Ben-Hur H, Hoskins I, Groner Y, Biegon A (1991) Fetal human brain exhibits a prenatal peak in the density of serotonin 5-HT_{1A} receptors. *Neurosci Lett* 127:173-176.
18. Bartesaghi R, Guidi S, Ciani E (2011) Is it possible to improve neurodevelopmental abnormalities in Down syndrome? *Rev Neurosci* 22:419-455.
19. Baxter LL, Moran TH, Richtsmeier JT, Troncoso J, Reeves RH (2000) Discovery and genetic localization of Down syndrome cerebellar phenotypes using the Ts65Dn mouse. *Hum Mol Genet* 9:195-202.
20. Becker L, Mito T, Takashima S, Onodera K (1991) Growth and development of the brain in Down syndrome. *Prog Clin Biol Res* 373:133-152.
21. Belichenko NP, Belichenko PV, Kleschevnikov AM, Salehi A, Reeves RH, Mobley WC (2009) The "Down syndrome critical region" is sufficient in the mouse model to confer behavioral, neurophysiological, and synaptic phenotypes characteristic of Down syndrome. *J Neurosci* 29:5938-5948.
22. Belichenko PV, Kleschevnikov AM, Salehi A, Epstein CJ, Mobley WC (2007) Synaptic and cognitive abnormalities in mouse models of Down syndrome: exploring genotype-phenotype relationships. *J Comp Neurol* 504:329-345.
23. Belichenko PV, Masliah E, Kleschevnikov AM, Villar AJ, Epstein CJ, Salehi A, Mobley WC (2004) Synaptic structural abnormalities in the Ts65Dn mouse model of Down Syndrome. *J Comp Neurol* 480:281-298.
24. Benavides-Piccione R, Ballesteros-Yanez I, de Lagran MM, Elston G, Estivill X, Fillat C, Defelipe J, Dierssen M (2004) On dendrites in Down syndrome and DS murine models: a spiny way to learn. *Prog Neurobiol* 74:111-126.
25. Best TK, Siarey RJ, Galdzicki Z (2007) Ts65Dn, a mouse model of Down syndrome, exhibits increased GABA_B-induced potassium current. *J Neurophysiol* 97:892-900.
26. Bialowas-McGoey LA, Lesicka A, Whitaker-Azmitia PM (2008) Vitamin E increases S100B-mediated microglial activation in an S100B-overexpressing mouse model of pathological aging. *Glia* 56:1780-1790.
27. Bianchi M, Shah AJ, Fone KC, Atkins AR, Dawson LA, Heidbreder CA, Hows ME, Hagan JJ, Marsden CA (2009) Fluoxetine administration modulates the cytoskeletal microtubular system in the rat hippocampus. *Synapse* 63:359-364.
28. Bianchi P, Ciani E, Guidi S, Trazzi S, Felice D, Grossi G, Fernandez M, Giuliani A, Calza L, Bartesaghi R (2010) Early pharmacotherapy restores neurogenesis and cognitive performance in the Ts65Dn mouse model for Down syndrome. *J Neurosci* 30:8769-8779.
29. Bimonte-Nelson HA, Hunter CL, Nelson ME, Granholm AC (2003) Frontal cortex BDNF levels correlate with working memory in an animal model of Down syndrome. *Behav Brain Res* 139:47-57.
30. Boylan K, Romero S, Birmaher B (2007) Psychopharmacologic treatment of pediatric major depressive disorder. *Psychopharmacology (Berl)* 191:27-38.
31. Brazel CY, Romanko MJ, Rothstein RP, Levison SW (2003) Roles of the mammalian subventricular zone in brain development. *Prog Neurobiol* 69:49-69.
32. Brezun JM, Daszuta A (1999) Depletion in serotonin decreases neurogenesis in the dentate gyrus and the subventricular zone of adult rats. *Neuroscience* 89:999-1002.
33. Caccia S, Cappi M, Fracasso C, Garattini S (1990) Influence of dose and route of administration on the kinetics of fluoxetine and its metabolite norfluoxetine in the rat. *Psychopharmacology (Berl)* 100:509-514.
34. Castelli L, Nigro MJ, Magistretti J (2007) Analysis of resurgent sodium-current expression in rat parahippocampal cortices and hippocampal formation. *Brain Res* 1163:44-55.
35. Cataldo AM, Petanceska S, Peterhoff CM, Terio NB, Epstein CJ, Villar A, Carlson EJ, Staufienbiel M, Nixon RA (2003) App gene dosage modulates endosomal abnormalities of

- Alzheimer's disease in a segmental trisomy 16 mouse model of down syndrome. *J Neurosci* 23:6788-6792.
36. Chakrabarti L, Best TK, Cramer NP, Carney RS, Isaac JT, Galdzicki Z, Haydar TF (2010) Olig1 and Olig2 triplication causes developmental brain defects in Down syndrome. *Nat Neurosci* 13:927-934.
 37. Chakrabarti L, Galdzicki Z, Haydar TF (2007) Defects in embryonic neurogenesis and initial synapse formation in the forebrain of the Ts65Dn mouse model of Down syndrome. *J Neurosci* 27:11483-11495.
 38. Chang KT, Shi YJ, Min KT (2003) The Drosophila homolog of Down's syndrome critical region 1 gene regulates learning: implications for mental retardation. *Proc Natl Acad Sci U S A* 100:15794-15799.
 39. Chapleau CA, Pozzo-Miller L (2012) Divergent Roles of p75(NTR) and Trk Receptors in BDNF's Effects on Dendritic Spine Density and Morphology. *Neural Plast* 2012:578057.
 40. Chapman RS, Hesketh LJ (2000) Behavioral phenotype of individuals with Down syndrome. *Ment Retard Dev Disabil Res Rev* 6:84-95.
 41. Chatterjee A, Dutta S, Mukherjee S, Mukherjee N, Dutta A, Mukherjee A, Sinha S, Panda CK, Chaudhuri K, Roy AL and others (2013) Potential contribution of SIM2 and ETS2 functional polymorphisms in Down syndrome associated malignancies. *BMC Med Genet* 14:12.
 42. Chen-Hwang MC, Chen HR, Elzinga M, Hwang YW (2002) Dynamin is a minibrain kinase/dual specificity Yak1-related kinase 1A substrate. *J Biol Chem* 277:17597-17604.
 43. Clark S, Schwalbe J, Stasko MR, Yarowsky PJ, Costa AC (2006) Fluoxetine rescues deficient neurogenesis in hippocampus of the Ts65Dn mouse model for Down syndrome. *Exp Neurol* 200:256-261.
 44. Contestabile A, Benfenati F, Gasparini L (2010) Communication breaks-Down: from neurodevelopment defects to cognitive disabilities in Down syndrome. *Prog Neurobiol* 91:1-22.
 45. Contestabile A, Fila T, Bartesaghi R, Ciani E (2008) Cell cycle elongation impairs proliferation of cerebellar granule cell precursors in the Ts65Dn mouse, an animal model for Down syndrome. *Brain Pathol* in press.
 46. Contestabile A, Fila T, Ceccarelli C, Bonasoni P, Bonapace L, Santini D, Bartesaghi R, Ciani E (2007) Cell cycle alteration and decreased cell proliferation in the hippocampal dentate gyrus and in the neocortical germinal matrix of fetuses with Down syndrome and in Ts65Dn mice. *Hippocampus* 17:665-678.
 47. Cortez MA, Shen L, Wu Y, Aleem IS, Trepanier CH, Sadeghnia HR, Ashraf A, Kanawaty A, Liu CC, Stewart L and others (2009) Infantile spasms and Down syndrome: a new animal model. *Pediatr Res* 65:499-503.
 48. Costa AC, Scott-McKean JJ (2013) Prospects for improving brain function in individuals with down syndrome. *CNS Drugs* 27:679-702.
 49. Couillard-Despres S, Winner B, Schaubeck S, Aigner R, Vroemen M, Weidner N, Bogdahn U, Winkler J, Kuhn HG, Aigner L (2005) Doublecortin expression levels in adult brain reflect neurogenesis. *Eur J Neurosci* 21:1-14.
 50. Cvetkovska V, Hibbert AD, Emran F, Chen BE (2013) Overexpression of Down syndrome cell adhesion molecule impairs precise synaptic targeting. *Nat Neurosci* 16:677-682.
 51. da Nobrega AM, Nunesmaia HG, Viana Nde O, Filgueiras MA (1999) [Electroencephalographic modification in Down syndrome]. *Arq Neuropsiquiatr* 57:580-586.
 52. Dahmane N, Charron G, Lopes C, Yaspo ML, Maunoury C, Decorte L, Sinet PM, Bloch B, Delabar JM (1995) Down syndrome-critical region contains a gene homologous to

- Drosophila sim* expressed during rat and human central nervous system development. *Proc Natl Acad Sci U S A* 92:9191-9195.
53. Danzer SC, McNamara JO (2004) Localization of brain-derived neurotrophic factor to distinct terminals of mossy fiber axons implies regulation of both excitation and feedforward inhibition of CA3 pyramidal cells. *J Neurosci* 24:11346-11355.
 54. Davisson MT, Schmidt C, Akeson EC (1990) Segmental trisomy of murine chromosome 16: a new model system for studying Down syndrome. *Prog Clin Biol Res* 360:263-280.
 55. DeVane CL (1994) Pharmacokinetics of the newer antidepressants: clinical relevance. *Am J Med* 97:13S-23S.
 56. Devinsky O, Sato S, Conwit RA, Schapiro MB (1990) Relation of EEG alpha background to cognitive function, brain atrophy, and cerebral metabolism in Down's syndrome. Age-specific changes. *Arch Neurol* 47:58-62.
 57. Dierssen M, Benavides-Piccione R, Martinez-Cue C, Estivill X, Florez J, Elston GN, DeFelipe J (2003) Alterations of neocortical pyramidal cell phenotype in the Ts65Dn mouse model of Down syndrome: effects of environmental enrichment. *Cereb Cortex* 13:758-764.
 58. Dorsey RR, Songer TJ, Zgibor JC, Orchard TJ (2006) Influences on screening for chronic diabetes complications in type 1 diabetes. *Dis Manag* 9:93-101.
 59. Dowjat WK, Adayev T, Kuchna I, Nowicki K, Palminiello S, Hwang YW, Wegiel J (2007) Trisomy-driven overexpression of DYRK1A kinase in the brain of subjects with Down syndrome. *Neurosci Lett* 413:77-81.
 60. Downes EC, Robson J, Grailly E, Abdel-All Z, Xuereb J, Brayne C, Holland A, Honer WG, Mukaetova-Ladinska EB (2008) Loss of synaptophysin and synaptosomal-associated protein 25-kDa (SNAP-25) in elderly Down syndrome individuals. *Neuropathol Appl Neurobiol* 34:12-22.
 61. Einarson A, Choi J, Einarson TR, Koren G (2009) Incidence of major malformations in infants following antidepressant exposure in pregnancy: results of a large prospective cohort study. *Can J Psychiatry* 54:242-246.
 62. Engidawork E, Gulesserian T, Fountoulakis M, Lubec G (2003) Aberrant protein expression in cerebral cortex of fetus with Down syndrome. *Neuroscience* 122:145-154.
 63. Epstein CJ (1986) Developmental genetics. *Experientia* 42:1117-1128.
 64. Faber KM, Haring JH (1999) Synaptogenesis in the postnatal rat fascia dentata is influenced by 5-HT1a receptor activation. *Brain Res Dev Brain Res* 114:245-252.
 65. Fernandez F, Trinidad JC, Blank M, Feng DD, Burlingame AL, Garner CC (2009) Normal protein composition of synapses in Ts65Dn mice: a mouse model of Down syndrome. *J Neurochem* 110:157-169.
 66. Ferrari L, Seregini E, Aliberti G, Martinetti A, Pallotti F, Villano C, Lucignani G, Bombardieri E (2004) Comparative evaluation of two methods to assay thyroglobulin serum concentrations in patients with differentiated thyroid carcinomas. *Q J Nucl Med Mol Imaging* 48:237-242.
 67. Ferrer I, Gullotta F (1990) Down's syndrome and Alzheimer's disease: dendritic spine counts in the hippocampus. *Acta Neuropathol* 79:680-685.
 68. Fitzpatrick GV, Soloway PD, Higgins MJ (2002) Regional loss of imprinting and growth deficiency in mice with a targeted deletion of KvDMR1. *Nat Genet* 32:426-431.
 69. Fuentes JJ, Genesca L, Kingsbury TJ, Cunningham KW, Perez-Riba M, Estivill X, de la Luna S (2000) DSCR1, overexpressed in Down syndrome, is an inhibitor of calcineurin-mediated signaling pathways. *Hum Mol Genet* 9:1681-1690.
 70. Galante M, Jani H, Vanes L, Daniel H, Fisher EM, Tybulewicz VL, Bliss TV, Morice E (2009) Impairments in motor coordination without major changes in cerebellar plasticity in the Tc1 mouse model of Down syndrome. *Hum Mol Genet* 18:1449-1463.

71. Galdzicki Z, Siarey R, Pearce R, Stoll J, Rapoport SI (2001) On the cause of mental retardation in Down syndrome: extrapolation from full and segmental trisomy 16 mouse models. *Brain Res Brain Res Rev* 35:115-145.
72. Galdzicki Z, Siarey RJ (2003) Understanding mental retardation in Down's syndrome using trisomy 16 mouse models. *Genes Brain Behav* 2:167-178.
73. Gandolfi A, Horoupian DS, De Teresa RM (1981) Pathology of the auditory system in autosomal trisomies with morphometric and quantitative study of the ventral cochlear nucleus. *J Neurol Sci* 51:43-50.
74. Gardiner K, Davisson M (2000) The sequence of human chromosome 21 and implications for research into Down syndrome. *Genome Biol* 1:REVIEWS0002.
75. Golden JA, Hyman BT (1994) Development of the superior temporal neocortex is anomalous in trisomy 21. *J Neuropathol Exp Neurol* 53:513-520.
76. Granholm AC, Sanders L, Seo H, Lin L, Ford K, Isacson O (2003) Estrogen alters amyloid precursor protein as well as dendritic and cholinergic markers in a mouse model of Down syndrome. *Hippocampus* 13:905-914.
77. Griffin WS, Sheng JG, McKenzie JE, Royston MC, Gentleman SM, Brumback RA, Cork LC, Del Bigio MR, Roberts GW, Mrak RE (1998) Life-long overexpression of S100beta in Down's syndrome: implications for Alzheimer pathogenesis. *Neurobiol Aging* 19:401-405.
78. Gropp A, Kolbus U, Giers D (1975) Systematic approach to the study of trisomy in the mouse. II. *Cytogenet Cell Genet* 14:42-62.
79. Grossi G, Bargossi AM, Lucarelli C, Paradisi R, Sprovieri C, Sprovieri G (1991) Improvements in automated analysis of catecholamine and related metabolites in biological samples by column-switching high-performance liquid chromatography. *J Chromatogr* 541:273-284.
80. Guidi S, Bonasoni P, Ceccarelli C, Santini D, Gualtieri F, Ciani E, Bartesaghi R (2008) Neurogenesis impairment and increased cell death reduce total neuron number in the hippocampal region of fetuses with Down syndrome. *Brain Pathol* 18:180-197.
81. Guidi S, Ciani E, Bonasoni P, Santini D, Bartesaghi R (2011) Widespread Proliferation Impairment and Hypocellularity in the Cerebellum of Fetuses with Down Syndrome. *Brain Pathol* 21:361-373.
82. Gulesserian T, Kim SH, Fountoulakis M, Lubec G (2002) Aberrant expression of centractin and capping proteins, integral constituents of the dynactin complex, in fetal down syndrome brain. *Biochem Biophys Res Commun* 291:62-67.
83. Hajszan T, MacLusky NJ, Leranth C (2005) Short-term treatment with the antidepressant fluoxetine triggers pyramidal dendritic spine synapse formation in rat hippocampus. *Eur J Neurosci* 21:1299-1303.
84. Hammerle B, Elizalde C, Galceran J, Becker W, Tejedor FJ (2003) The MNB/DYRK1A protein kinase: neurobiological functions and Down syndrome implications. *J Neural Transm Suppl*:129-137.
85. Hanson JE, Blank M, Valenzuela RA, Garner CC, Madison DV (2007) The functional nature of synaptic circuitry is altered in area CA3 of the hippocampus in a mouse model of Down's syndrome. *J Physiol* 579:53-67.
86. Harashima C, Jacobowitz DM, Stoffel M, Chakrabarti L, Haydar TF, Siarey RJ, Galdzicki Z (2006) Elevated expression of the G-protein-activated inwardly rectifying potassium channel 2 (GIRK2) in cerebellar unipolar brush cells of a Down syndrome mouse model. *Cell Mol Neurobiol* 26:719-734.
87. Hattori M, Fujiyama A, Taylor TD, Watanabe H, Yada T, Park HS, Toyoda A, Ishii K, Totoki Y, Choi DK and others (2000) The DNA sequence of human chromosome 21. *Nature* 405:311-319.

88. Haydar TF, Blue ME, Molliver ME, Krueger BK, Yarowsky PJ (1996) Consequences of trisomy 16 for mouse brain development: corticogenesis in a model of Down syndrome. *J Neurosci* 16:6175-6182.
89. Haydar TF, Nowakowski RS, Yarowsky PJ, Krueger BK (2000) Role of founder cell deficit and delayed neurogenesis in microencephaly of the trisomy 16 mouse. *J Neurosci* 20:4156-4164.
90. Hayes A, Batshaw ML (1993) Down syndrome. *Pediatr Clin North Am* 40:523-535.
91. Hewitt CA, Ling KH, Merson TD, Simpson KM, Ritchie ME, King SL, Pritchard MA, Smyth GK, Thomas T, Scott HS and others (2010) Gene network disruptions and neurogenesis defects in the adult Ts1Cje mouse model of Down syndrome. *PLoS One* 5:e11561.
92. Holtzman DM, Santucci D, Kilbridge J, Chua-Couzens J, Fontana DJ, Daniels SE, Johnson RM, Chen K, Sun Y, Carlson E and others (1996) Developmental abnormalities and age-related neurodegeneration in a mouse model of Down syndrome. *Proc Natl Acad Sci U S A* 93:13333-13338.
93. Insausti AM, Megias M, Crespo D, Cruz-Orive LM, Dierssen M, Vallina IF, Insausti R, Florez J (1998) Hippocampal volume and neuronal number in Ts65Dn mice: a murine model of Down syndrome. *Neurosci Lett* 253:175-178.
94. Irving C, Basu A, Richmond S, Burn J, Wren C (2008) Twenty-year trends in prevalence and survival of Down syndrome. *Eur J Hum Genet* 16:1336-1340.
95. Ishihara K, Amano K, Takaki E, Shimohata A, Sago H, Epstein CJ, Yamakawa K (2010) Enlarged brain ventricles and impaired neurogenesis in the Ts1Cje and Ts2Cje mouse models of Down syndrome. *Cereb Cortex* 20:1131-1143.
96. Ivanov A, Esclapez M, Ferhat L (2009) Role of drebrin A in dendritic spine plasticity and synaptic function: Implications in neurological disorders. *Commun Integr Biol* 2:268-270.
97. Kamiya H, Shinozaki H, Yamamoto C (1996) Activation of metabotropic glutamate receptor type 2/3 suppresses transmission at rat hippocampal mossy fibre synapses. *J Physiol* 493 (Pt 2):447-455.
98. Karlsson B, Gustafsson J, Hedov G, Ivarsson SA, Anneren G (1998) Thyroid dysfunction in Down's syndrome: relation to age and thyroid autoimmunity. *Arch Dis Child* 79:242-245.
99. Kaufmann WE, Moser HW (2000) Dendritic anomalies in disorders associated with mental retardation. *Cereb Cortex* 10:981-991.
100. Kemper TL (1988) Neuropathology of Down syndrome. *The psychobiology of Down syndrome*.
101. Khoshnood B, De Vigan C, Blondel B, Lhomme A, Vodovar V, Garel M, Goffinet F (2006) Women's interpretation of an abnormal result on measurement of fetal nuchal translucency and maternal serum screening for prenatal testing of Down syndrome. *Ultrasound Obstet Gynecol* 28:242-248.
102. Kim SH, Yoo BC, Broers JL, Cairns N, Lubec G (2000) Neuroendocrine-specific protein C, a marker of neuronal differentiation, is reduced in brain of patients with Down syndrome and Alzheimer's disease. *Biochem Biophys Res Commun* 276:329-334.
103. Kleschevnikov AM, Belichenko PV, Villar AJ, Epstein CJ, Malenka RC, Mobley WC (2004) Hippocampal long-term potentiation suppressed by increased inhibition in the Ts65Dn mouse, a genetic model of Down syndrome. *J Neurosci* 24:8153-8160.
104. Koo BK, Blaser S, Harwood-Nash D, Becker LE, Murphy EG (1992) Magnetic resonance imaging evaluation of delayed myelination in Down syndrome: a case report and review of the literature. *J Child Neurol* 7:417-421.
105. Kurt MA, Davies DC, Kidd M, Dierssen M, Florez J (2000) Synaptic deficit in the temporal cortex of partial trisomy 16 (Ts65Dn) mice. *Brain Res* 858:191-197.

106. Kurt MA, Kafa MI, Dierssen M, Davies DC (2004) Deficits of neuronal density in CA1 and synaptic density in the dentate gyrus, CA3 and CA1, in a mouse model of Down syndrome. *Brain Res* 1022:101-109.
107. Lacey-Casem ML, Oster-Granite ML (1994) The neuropathology of the trisomy 16 mouse. *Crit Rev Neurobiol* 8:293-322.
108. Lana-Elola E, Watson-Scales SD, Fisher EM, Tybulewicz VL (2011) Down syndrome: searching for the genetic culprits. *Dis Model Mech* 4:586-595.
109. Lawrence JJ, McBain CJ (2003) Interneuron diversity series: containing the detonation--feedforward inhibition in the CA3 hippocampus. *Trends Neurosci* 26:631-640.
110. Lieberman DN, Mody I (1994) Regulation of NMDA channel function by endogenous Ca(2+)-dependent phosphatase. *Nature* 369:235-239.
111. Liu DP, Schmidt C, Billings T, Davisson MT (2003) Quantitative PCR genotyping assay for the Ts65Dn mouse model of Down syndrome. *Biotechniques* 35:1170-1174, 1176, 1178 passim.
112. Lorenzi HA, Reeves RH (2006) Hippocampal hypocellularity in the Ts65Dn mouse originates early in development. *Brain Res* 1104:153-159.
113. Lubec B, Weitzdoerfer R, Fountoulakis M (2001) Manifold reduction of moesin in fetal Down syndrome brain. *Biochem Biophys Res Commun* 286:1191-1194.
114. Luscher C, Jan LY, Stoffel M, Malenka RC, Nicoll RA (1997) G protein-coupled inwardly rectifying K⁺ channels (GIRKs) mediate postsynaptic but not presynaptic transmitter actions in hippocampal neurons. *Neuron* 19:687-695.
115. Malberg JE, Blendy JA (2005) Antidepressant action: to the nucleus and beyond. *Trends Pharmacol Sci* 26:631-638.
116. Malberg JE, Eisch AJ, Nestler EJ, Duman RS (2000) Chronic antidepressant treatment increases neurogenesis in adult rat hippocampus. *J Neurosci* 20:9104-9110.
117. Mann DM, Yates PO, Marcyniuk B, Ravindra CR (1985) Pathological evidence for neurotransmitter deficits in Down's syndrome of middle age. *J Ment Defic Res* 29 (Pt 2):125-135.
118. Mansuy IM (2003) Calcineurin in memory and bidirectional plasticity. *Biochem Biophys Res Commun* 311:1195-1208.
119. Mao R, Zielke CL, Zielke HR, Pevsner J (2003) Global up-regulation of chromosome 21 gene expression in the developing Down syndrome brain. *Genomics* 81:457-467.
120. Marin-Padilla M (1976) Pyramidal cell abnormalities in the motor cortex of a child with Down's syndrome. A Golgi study. *J Comp Neurol* 167:63-81.
121. Matsumoto N, Ohashi H, Tsukahara M, Kim KC, Soeda E, Niikawa N (1997) Possible narrowed assignment of the loci of monosomy 21-associated microcephaly and intrauterine growth retardation to a 1.2-Mb segment at 21q22.2. *Am J Hum Genet* 60:997-999.
122. Megias M, Verduga R, Dierssen M, Florez J, Insausti R, Crespo D (1997) Cholinergic, serotonergic and catecholaminergic neurons are not affected in Ts65Dn mice. *Neuroreport* 8:3475-3478.
123. Mito T, Becker LE (1993) Developmental changes of S-100 protein and glial fibrillary acidic protein in the brain in Down syndrome. *Exp Neurol* 120:170-176.
124. Moller RS, Kubart S, Hoeltzenbein M, Heye B, Vogel I, Hansen CP, Menzel C, Ullmann R, Tommerup N, Ropers HH and others (2008) Truncation of the Down syndrome candidate gene DYRK1A in two unrelated patients with microcephaly. *Am J Hum Genet* 82:1165-1170.
125. Morice E, Andreae LC, Cooke SF, Vanes L, Fisher EM, Tybulewicz VL, Bliss TV (2008) Preservation of long-term memory and synaptic plasticity despite short-term impairments in the Tc1 mouse model of Down syndrome. *Learn Mem* 15:492-500.

126. Nadel L (2003) Down's syndrome: a genetic disorder in biobehavioral perspective. *Genes Brain Behav* 2:156-166.
127. Noble J (1998) Natural history of Down's syndrome: a brief review for those involved in antenatal screening. *J Med Screen* 5:172-177.
128. O'Doherty A, Ruf S, Mulligan C, Hildreth V, Errington ML, Cooke S, Sesay A, Modino S, Vanes L, Hernandez D and others (2005) An aneuploid mouse strain carrying human chromosome 21 with Down syndrome phenotypes. *Science* 309:2033-2037.
129. Ohara S, Tsukada M, Ikeda S (1999) On the occurrence of neuronal sprouting in the frontal cortex of a patient with Down's syndrome. *Acta Neuropathol* 97:85-90.
130. Olson LE, Richtsmeier JT, Leszl J, Reeves RH (2004) A chromosome 21 critical region does not cause specific Down syndrome phenotypes. *Science* 306:687-690.
131. Olson LE, Roper RJ, Baxter LL, Carlson EJ, Epstein CJ, Reeves RH (2004) Down syndrome mouse models Ts65Dn, Ts1Cje, and Ms1Cje/Ts65Dn exhibit variable severity of cerebellar phenotypes. *Dev Dyn* 230:581-589.
132. Olson LE, Roper RJ, Sengstaken CL, Peterson EA, Aquino V, Galdzicki Z, Siarey R, Pletnikov M, Moran TH, Reeves RH (2007) Trisomy for the Down syndrome 'critical region' is necessary but not sufficient for brain phenotypes of trisomic mice. *Hum Mol Genet* 16:774-782.
133. Park J, Oh Y, Yoo L, Jung MS, Song WJ, Lee SH, Seo H, Chung KC (2010) Dyrk1A phosphorylates p53 and inhibits proliferation of embryonic neuronal cells. *J Biol Chem* 285:31895-31906.
134. Patterson D (2009) Molecular genetic analysis of Down syndrome. *Hum Genet* 126:195-214.
135. Pennington BF, Moon J, Edgin J, Stedron J, Nadel L (2003) The neuropsychology of Down syndrome: evidence for hippocampal dysfunction. *Child Dev* 74:75-93.
136. Pereira PL, Magnol L, Sahun I, Brault V, Duchon A, Prandini P, Gruart A, Bizot JC, Chadeaux-Vekemans B, Deutsch S and others (2009) A new mouse model for the trisomy of the Abcg1-U2af1 region reveals the complexity of the combinatorial genetic code of down syndrome. *Hum Mol Genet* 18:4756-4769.
137. Perez-Cremades D, Hernandez S, Blasco-Ibanez JM, Crespo C, Nacher J, Varea E (2010) Alteration of inhibitory circuits in the somatosensory cortex of Ts65Dn mice, a model for Down's syndrome. *J Neural Transm* 117:445-455.
138. Phillips RG, LeDoux JE (1992) Differential contribution of amygdala and hippocampus to cued and contextual fear conditioning. *Behav Neurosci* 106:274-285.
139. Pinter JD, Eliez S, Schmitt JE, Capone GT, Reiss AL (2001) Neuroanatomy of Down's syndrome: a high-resolution MRI study. *Am J Psychiatry* 158:1659-1665.
140. Pollak D, Cairns N, Lubec G (2003) Cytoskeleton derangement in brain of patients with Down syndrome, Alzheimer's disease and Pick's disease. *J Neural Transm Suppl*:149-158.
141. Pollonini G, Gao V, Rabe A, Palmieriello S, Albertini G, Alberini CM (2008) Abnormal expression of synaptic proteins and neurotrophin-3 in the Down syndrome mouse model Ts65Dn. *Neuroscience* 156:99-106.
142. Popov VI, Kleschevnikov AM, Klimenko OA, Stewart MG, Belichenko PV (2011) Three-dimensional synaptic ultrastructure in the dentate gyrus and hippocampal area CA3 in the Ts65Dn mouse model of down syndrome. *J Comp Neurol* 519:1338-1354.
143. Priller C, Bauer T, Mitteregger G, Krebs B, Kretschmar HA, Herms J (2006) Synapse formation and function is modulated by the amyloid precursor protein. *J Neurosci* 26:7212-7221.
144. Pueschel SM (1990) Clinical aspects of Down syndrome from infancy to adulthood. *Am J Med Genet Suppl* 7:52-56.

145. Purohit AA, Li W, Qu C, Dwyer T, Shao Q, Guan KL, Liu G (2012) Down syndrome cell adhesion molecule (DSCAM) associates with uncoordinated-5C (UNC5C) in netrin-1-mediated growth cone collapse. *J Biol Chem* 287:27126-27138.
146. Purpura DP (1979) Pathobiology of cortical neurons in metabolic and unclassified amentias. *Res Publ Assoc Res Nerv Ment Dis* 57:43-68.
147. Rachidi M, Lopes C (2007) Mental retardation in Down syndrome: from gene dosage imbalance to molecular and cellular mechanisms. *Neurosci Res* 59:349-369.
148. Rachidi M, Lopes C (2008) Mental retardation and associated neurological dysfunctions in Down syndrome: a consequence of dysregulation in critical chromosome 21 genes and associated molecular pathways. *Eur J Paediatr Neurol* 12:168-182.
149. Rachidi M, Lopes C, Charron G, Delezoide AL, Paly E, Bloch B, Delabar JM (2005) Spatial and temporal localization during embryonic and fetal human development of the transcription factor SIM2 in brain regions altered in Down syndrome. *Int J Dev Neurosci* 23:475-484.
150. Rachidi M, Lopes C, Delezoide AL, Delabar JM (2006) C21orf5, a human candidate gene for brain abnormalities and mental retardation in Down syndrome. *Cytogenet Genome Res* 112:16-22.
151. Radley JJ, Jacobs BL (2002) 5-HT1A receptor antagonist administration decreases cell proliferation in the dentate gyrus. *Brain Res* 955:264-267.
152. Raz N, Torres IJ, Briggs SD, Spencer WD, Thornton AE, Loken WJ, Gunning FM, McQuain JD, Driesen NR, Acker JD (1995) Selective neuroanatomic abnormalities in Down's syndrome and their cognitive correlates: evidence from MRI morphometry. *Neurology* 45:356-366.
153. Reeves RH, Gearhart JD, Littlefield JW (1986) Genetic basis for a mouse model of Down syndrome. *Brain Res Bull* 16:803-814.
154. Reeves RH, Irving NG, Moran TH, Wohn A, Kitt C, Sisodia SS, Schmidt C, Bronson RT, Davisson MT (1995) A mouse model for Down syndrome exhibits learning and behaviour deficits. *Nat Genet* 11:177-184.
155. Reymond A, Marigo V, Yaylaoglu MB, Leoni A, Ucla C, Scamuffa N, Caccioppoli C, Dermitzakis ET, Lyle R, Banfi S and others (2002) Human chromosome 21 gene expression atlas in the mouse. *Nature* 420:582-586.
156. Rhin LL, Claiborne BJ (1990) Dendritic growth and regression in rat dentate granule cells during late postnatal development. *Dev. Brain Res.* 54:115-124.
157. Risser D, Lubec G, Cairns N, Herrera-Marschitz M (1997) Excitatory amino acids and monoamines in parahippocampal gyrus and frontal cortical pole of adults with Down syndrome. *Life Sci* 60:1231-1237.
158. Roizen NJ, Patterson D (2003) Down's syndrome. *Lancet* 361:1281-1289.
159. Roper RJ, Reeves RH (2006) Understanding the basis for Down syndrome phenotypes. *PLoS Genet* 2:e50.
160. Ross MH, Galaburda AM, Kemper TL (1984) Down's syndrome: is there a decreased population of neurons? *Neurology* 34:909-916.
161. Roubertoux PL, Bichler Z, Pinoteau W, Seregaza Z, Fortes S, Jamon M, Smith DJ, Rubin E, Migliore-Samour D, Carlier M (2005) Functional analysis of genes implicated in Down syndrome: 2. Laterality and corpus callosum size in mice transpolygenic for Down syndrome chromosomal region -1 (DCR-1). *Behav Genet* 35:333-341.
162. Sago H, Carlson EJ, Smith DJ, Rubin EM, Crnic LS, Huang TT, Epstein CJ (2000) Genetic dissection of region associated with behavioral abnormalities in mouse models for Down syndrome. *Pediatr Res* 48:606-613.

163. Sairanen M, Lucas G, Ernfors P, Castren M, Castren E (2005) Brain-derived neurotrophic factor and antidepressant drugs have different but coordinated effects on neuronal turnover, proliferation, and survival in the adult dentate gyrus. *J Neurosci* 25:1089-1094.
164. Salehi A, Faizi M, Colas D, Valletta J, Laguna J, Takimoto-Kimura R, Kleschevnikov A, Wagner SL, Aisen P, Shamloo M and others (2009) Restoration of norepinephrine-modulated contextual memory in a mouse model of Down syndrome. *Sci Transl Med* 1:7ra17.
165. Sandi C, Cordero MI, Merino JJ, Kruyt ND, Regan CM, Murphy KJ (2004) Neurobiological and endocrine correlates of individual differences in spatial learning ability. *Learn Mem* 11:244-252.
166. Santarelli L, Saxe M, Gross C, Surget A, Battaglia F, Dulawa S, Weisstaub N, Lee J, Duman R, Arancio O and others (2003) Requirement of hippocampal neurogenesis for the behavioral effects of antidepressants. *Science* 301:805-809.
167. Schapiro MB, Creasey H, Schwartz M, Haxby JV, White B, Moore A, Rapoport SI (1987) Quantitative CT analysis of brain morphometry in adult Down's syndrome at different ages. *Neurology* 37:1424-1427.
168. Schlessinger AR, Cowan WM, Gottlieb DI (1975) An autoradiographic study of the time of origin and the pattern of granule cell migration in the dentate gyrus of the rat. *J Comp Neurol* 159:149-175.
169. Schmid RG, Tirsch WS, Rappelsberger P, Weinmann HM, Poppl SJ (1992) Comparative coherence studies in healthy volunteers and Down's syndrome patients from childhood to adult age. *Electroencephalogr Clin Neurophysiol* 83:112-123.
170. Schwartz N, Schohl A, Ruthazer ES (2009) Neural activity regulates synaptic properties and dendritic structure in vivo through calcineurin/NFAT signaling. *Neuron* 62:655-669.
171. Seki T, Arai Y (1993) Highly polysialylated neural cell adhesion molecule (NCAM-H) is expressed by newly generated granule cells in the dentate gyrus of the adult rat. *J Neurosci* 13:2351-2358.
172. Shankaran M, King C, Lee J, Busch R, Wolff M, Hellerstein MK (2006) Discovery of novel hippocampal neurogenic agents by using an in vivo stable isotope labeling technique. *J Pharmacol Exp Ther* 319:1172-1181.
173. Shapiro BL (1997) Whither Down syndrome critical regions? *Hum Genet* 99:421-423.
174. Shim KS, Lubec G (2002) Drebrin, a dendritic spine protein, is manifold decreased in brains of patients with Alzheimer's disease and Down syndrome. *Neurosci Lett* 324:209-212.
175. Shin JH, Gulesserian T, Weitzdoerfer R, Fountoulakis M, Lubec G (2004) Derangement of hypothetical proteins in fetal Down's syndrome brain. *Neurochem Res* 29:1307-1316.
176. Shulz D, Fregnac Y (1992) Cellular analogs of visual cortical epigenesis. II. Plasticity of binocular integration. *J Neurosci* 12:1301-1318.
177. Siarey RJ, Villar AJ, Epstein CJ, Galdzicki Z (2005) Abnormal synaptic plasticity in the Ts1Cje segmental trisomy 16 mouse model of Down syndrome. *Neuropharmacology* 49:122-128.
178. Smith DJ, Stevens ME, Sudanagunta SP, Bronson RT, Makhinson M, Watabe AM, O'Dell TJ, Fung J, Weier HU, Cheng JF and others (1997) Functional screening of 2 Mb of human chromosome 21q22.2 in transgenic mice implicates minibrain in learning defects associated with Down syndrome. *Nat Genet* 16:28-36.
179. Smith DJ, Zhu Y, Zhang J, Cheng JF, Rubin EM (1995) Construction of a panel of transgenic mice containing a contiguous 2-Mb set of YAC/P1 clones from human chromosome 21q22.2. *Genomics* 27:425-434.
180. Sommer CA, Henrique-Silva F (2008) Trisomy 21 and Down syndrome: a short review. *Braz J Biol* 68:447-452.

181. Strovel J, Stamberg J, Yarowsky PJ (1999) Interphase FISH for rapid identification of a down syndrome animal model. *Cytogenet Cell Genet* 86:285-287.
182. Sudarov A, Joyner AL (2007) Cerebellum morphogenesis: the foliation pattern is orchestrated by multi-cellular anchoring centers. *Neural Dev* 2:26.
183. Suetsugu M, Mehraein P (1980) Spine distribution along the apical dendrites of the pyramidal neurons in Down's syndrome. A quantitative Golgi study. *Acta Neuropathol* 50:207-210.
184. Sylvester PE (1986) The anterior commissure in Down's syndrome. *J Ment Defic Res* 30 (Pt 1):19-26.
185. Takashima S, Becker LE, Armstrong DL, Chan F (1981) Abnormal neuronal development in the visual cortex of the human fetus and infant with down's syndrome. A quantitative and qualitative Golgi study. *Brain Res* 225:1-21.
186. Takashima S, Ieshima A, Nakamura H, Becker LE (1989) Dendrites, dementia and the Down syndrome. *Brain Dev* 11:131-133.
187. Takashima S, Iida K, Mito T, Arima M (1994) Dendritic and histochemical development and ageing in patients with Down's syndrome. *J Intellect Disabil Res* 38 (Pt 3):265-273.
188. Teipel SJ, Bayer W, Alexander GE, Bokde AL, Zebuhr Y, Teichberg D, Muller-Spahn F, Schapiro MB, Moller HJ, Rapoport SI and others (2003) Regional pattern of hippocampus and corpus callosum atrophy in Alzheimer's disease in relation to dementia severity: evidence for early neocortical degeneration. *Neurobiol Aging* 24:85-94.
189. Trazzi S, Mitrugno VM, Valli E, Fuchs C, Rizzi S, Guidi S, Perini G, Bartesaghi R, Ciani E (2011) APP-dependent up-regulation of Ptch1 underlies proliferation impairment of neural precursors in Down syndrome. *Hum Mol Genet* 20:1560-1573.
190. Turner PR, O'Connor K, Tate WP, Abraham WC (2003) Roles of amyloid precursor protein and its fragments in regulating neural activity, plasticity and memory. *Prog Neurobiol* 70:1-32.
191. Vacik T, Ort M, Gregorova S, Strnad P, Blatny R, Conte N, Bradley A, Bures J, Forejt J (2005) Segmental trisomy of chromosome 17: a mouse model of human aneuploidy syndromes. *Proc Natl Acad Sci U S A* 102:4500-4505.
192. Vicari S (2006) Motor development and neuropsychological patterns in persons with Down syndrome. *Behav Genet* 36:355-364.
193. Villar AJ, Belichenko PV, Gillespie AM, Kozy HM, Mobley WC, Epstein CJ (2005) Identification and characterization of a new Down syndrome model, Ts[Rb(12.1716)]2Cje, resulting from a spontaneous Robertsonian fusion between T(171)65Dn and mouse chromosome 12. *Mamm Genome* 16:79-90.
194. Voronov SV, Frere SG, Giovedi S, Pollina EA, Borel C, Zhang H, Schmidt C, Akeson EC, Wenk MR, Cimasoni L and others (2008) Synaptojanin 1-linked phosphoinositide dyshomeostasis and cognitive deficits in mouse models of Down's syndrome. *Proc Natl Acad Sci U S A* 105:9415-9420.
195. Vuksic M, Petanjek Z, Rasin MR, Kostovic I (2002) Perinatal growth of prefrontal layer III pyramids in Down syndrome. *Pediatr Neurol* 27:36-38.
196. Wang JW, David DJ, Monckton JE, Battaglia F, Hen R (2008) Chronic fluoxetine stimulates maturation and synaptic plasticity of adult-born hippocampal granule cells. *J Neurosci* 28:1374-1384.
197. Wang PP, Doherty S, Hesselink JR, Bellugi U (1992) Callosal morphology concurs with neurobehavioral and neuropathological findings in two neurodevelopmental disorders. *Arch Neurol* 49:407-411.
198. Weis S, Weber G, Neuhold A, Rett A (1991) Down syndrome: MR quantification of brain structures and comparison with normal control subjects. *AJNR Am J Neuroradiol* 12:1207-1211.

199. Weitzdoerfer R, Dierssen M, Fountoulakis M, Lubec G (2001) Fetal life in Down syndrome starts with normal neuronal density but impaired dendritic spines and synaptosomal structure. *J Neural Transm Suppl* 61:59-70.
200. Weitzdoerfer R, Fountoulakis M, Lubec G (2002) Reduction of actin-related protein complex 2/3 in fetal Down syndrome brain. *Biochem Biophys Res Commun* 293:836-841.
201. Whitaker-Azmitia PM (2001) Serotonin and brain development: role in human developmental diseases. *Brain Res Bull* 56:479-485.
202. White NS, Alkire MT, Haier RJ (2003) A voxel-based morphometric study of nondemented adults with Down Syndrome. *Neuroimage* 20:393-403.
203. Whittle N, Sartori SB, Dierssen M, Lubec G, Singewald N (2007) Fetal Down syndrome brains exhibit aberrant levels of neurotransmitters critical for normal brain development. *Pediatrics* 120:e1465-1471.
204. Winter TC, Ostrovsky AA, Komarniski CA, Uhrich SB (2000) Cerebellar and frontal lobe hypoplasia in fetuses with trisomy 21: usefulness as combined US markers. *Radiology* 214:533-538.
205. Wiseman FK (2009) Cognitive enhancement therapy for a model of Down syndrome. *Sci Transl Med* 1:7ps9.
206. Wisniewski KE (1990) Down syndrome children often have brain with maturation delay, retardation of growth, and cortical dysgenesis. *Am J Med Genet Suppl* 7:274-281.
207. Wisniewski KE, Dalton AJ, McLachlan C, Wen GY, Wisniewski HM (1985) Alzheimer's disease in Down's syndrome: clinicopathologic studies. *Neurology* 35:957-961.
208. Wisniewski KE, Schmidt-Sidor B (1989) Postnatal delay of myelin formation in brains from Down syndrome infants and children. *Clin Neuropathol* 8:55-62.
209. Yamaki A, Noda S, Kudoh J, Shindoh N, Maeda H, Minoshima S, Kawasaki K, Shimizu Y, Shimizu N (1996) The mammalian single-minded (SIM) gene: mouse cDNA structure and diencephalic expression indicate a candidate gene for Down syndrome. *Genomics* 35:136-143.
210. Yan W, Wilson CC, Haring JH (1997) 5-HT_{1a} receptors mediate the neurotrophic effect of serotonin on developing dentate granule cells. *Brain Res Dev Brain Res* 98:185-190.
211. Yang EJ, Ahn YS, Chung KC (2001) Protein kinase Dyrk1 activates cAMP response element-binding protein during neuronal differentiation in hippocampal progenitor cells. *J Biol Chem* 276:39819-39824.
212. Yu T, Liu C, Belichenko P, Clapcote SJ, Li S, Pao A, Kleschevnikov A, Bechard AR, Asrar S, Chen R and others (2010) Effects of individual segmental trisomies of human chromosome 21 syntenic regions on hippocampal long-term potentiation and cognitive behaviors in mice. *Brain Res* 1366:162-171.
213. Yuen EY, Jiang Q, Chen P, Gu Z, Feng J, Yan Z (2005) Serotonin 5-HT_{1A} receptors regulate NMDA receptor channels through a microtubule-dependent mechanism. *J Neurosci* 25:5488-5501.
214. Zeng H, Chattarji S, Barbarosie M, Rondi-Reig L, Philpot BD, Miyakawa T, Bear MF, Tonegawa S (2001) Forebrain-specific calcineurin knockout selectively impairs bidirectional synaptic plasticity and working/episodic-like memory. *Cell* 107:617-629.
215. Zhao C, Teng EM, Summers RG, Jr., Ming GL, Gage FH (2006) Distinct morphological stages of dentate granule neuron maturation in the adult mouse hippocampus. *J Neurosci* 26:3-11.